عنوان البحث

دراسة نظرية للاهتزاز الحر للقشريات المتناظرة المحور المتطاولة ذات الخواص المتشابهة نحيفة الجدران

أطروحة

مقدمة إلى كلية الهندسة في جامعة بابل

كجزء

من متطلبات نيل درجة ماجستير علوم في الهندسة الميكانيكية

أعدت من قبل

محمد جواد عبيد

٢٠٠٦

الخلاصة

تناولت هذة الأطروحة دراسة نظرية للاهتزاز الحر للقشريات المتناظرة المحور المتطاولة ذات الخواص المتشابهة نحيفة الجدران, وقد افترض إن سمك الجدار متغير. وقد تم إتباع أسلوبين في التحليل, هما طريقة (Rayleigh-Ritz) وطريقة (Boundary Matching).

وقد اعتمدت هاتين الطرقتين من اجل إيجاد الذبذبات الطبيعة وأشكال النسق للقشريات الكروية المتطاولة. وقد اجري التحليل وذلك بافتراض إن القشريات مكونة من جزئين كرويين مثبتين على طول خط الاتصال بالاعتماد على نظرية القشريات الغير مفلطحة و النظرية الخطية القشريات.

ولقد تم استخدام طريقة العناصر المحددة لدعم النتائج المستحصلة بالتحليل المذكور أعلاه. وقد وجد إن النتائج المستحصلة في هذا العمل متوافقة بشكل مناسب وتلك التي تم الحصول عليها باستخدام برنامج (ANSYS)

وجد بان التردد الطبيعي للقشرة المقوسة المتطاولة يمتلك سلوك تجاه زيادة سمك القشرة واللامركزية, حيث يزداد بزيادة كل من السمك واللامركزية.

ووجد بان التثبيت بملزم يمتلك اكبر قيمة للتردد من أي نوع أخر وذلك بسبب زيادة في جساءة القشرة وذلك يسبب زيادة في طاقة الانفعال للنظام.

Republic of Iraq

Ministry of Higher Education

and Scientific Research

Babylon University

College of Engineering

A Theoretical Investigation of The Axisymetrical Free Vibration Characteristic of an Isotropic Thin Prolate Spheroidal Shell

A Thesis

Submitted to the Engineering College University

of Babylon in a a Partial Fulfillment of Requirements

for the Degree of Master of Science in

Mechanical Engineering

(Applied Mechanics)

*By***MOHAMMED JAWAD AL- ROBAI**

(B.Sc.)

١٤٢٧ ٢٠٠٦

ABSTRACT

This thesis includes a theoretical investigation of the axisymmetric free vibration characteristics of an isotropic thin prolate spheroidal shell. The thickness of the shell is assumed to be variable and the material is isotropic. Two approaches are followed in the analysis, which are the Rayleigh –Ritz's method and the Boundary Matching method.

The capability of these techniques was investigated in this work to predict the natural frequencies and mode shape of prolate spheroidal shell. The analysis based on considering the prolate spheroidal as a continuous system constructed from two spherical shell elements matched at the continuous boundaries. The non –shallow shell theory, Rayleigh-Ritz method, Boundary Matching method and linear shell theory is used for the analysis.

In order to certify the analysis the ANSYS package is used to find the natural frequencies of the shell. The results produced from the ANSYS agree with the results obtained by the above two approaches.

It was found that the natural frequencies of prolate shell have a behavior against increasing the shell thickness and eccentricity. The natural frequency increases with increasing both the eccentricity and thickness ratio.

The effect of different boundary conditions such as (clamped – clamped, clamped –free and pinned –pinned) of the prolate spheroidal shell at the region of matched at the continuous boundaries is investigated. It is found that the clamped- clamped prolate spheroidal shell has the higher values of natural frequency than shells with other types of boundary conditions because the increase the stiffness of the shell it is case to increase the strain energy of the system.

بسم الله الرحمن الرحيم

اقرأ باسم ربك الذي خلق ﴿١﴾ خلق الإنسان من علق ﴿٢﴾ اقرأ

وربك الأكرم ﴿٣﴾ الذي علم بالقلم ﴿٤﴾ علم الإنسان ما لم يعلم

﴿٥﴾

صدق الله العظيم

سورة العلق

الآيات (١-٥)

CERTIFICATION

We certify that we have read this thesis entitled **"Theoretical Investigation of The Axisymmetric free vibration Characteristic of an Isotropic Thin Prolate Spheroidal Shell"** was prepared under our supervision at the Department of Mechanical Engineering, college of Engineering/ University of Babylon.

Signature:

Name: Asst. Prof.

Dr. Ahmed A. Al - Rajihy

(Supervisor)

Date: / / ٢٠٠٦

Signature:

Name: Asst. Prof.

Dr. Ala M. H. Al - Jesany

(Supervisor)

Date: / / ٢٠٠٦

ACKNOWLEDGMENTS

*"Praise be to **ALLAH**, lord of the whole creation"*

*I would like to thank sincerely and wholeheartedly **Dr. Ahmed A. Al – Rajihy** and **Dr. Ala M. H. Al – Jesany** for their guidance and kindness throughout this work. Their patience as advisors, boundless energy while teaching, promptness while reviewing all my writing, and a passion for research is to be commended and worth emulating. I am indebted to them for cajoling me into achieving the research work and thus opening a whole new exciting world for me.*

Most importantly, I would like to thank my parents, for their unconditional support, love, and affection. Their encouragement and endless kindness made everything easier to achieve.

Mohammed Jawad Al - Robai

٢٠٠٦

NOTATIONS

Symbol	Meaning	Units
A_i	Arbitrary constants.	…
a	Major semi – axis of a prolate spheroidal shell.	m
B_i	Arbitrary constants.	….
b	Manor semi – axis of a prolate spheroidal shell.	m
$C_{i,j}$	Element of the boundary conditions matrix.	….
D_b	The flexural rigidity of the shell.	N.m
E	Young's modulus of elasticity	GPa
e	Eccentricity ratio $(\sqrt{1-b^2/a^2})$.	….
h	Shell thickness.	mm
M_Φ, M_θ	Moments per unit length.	N.m/m
N_Φ, N_θ	Membrane forces per unit length.	N/m
$P_n(x)$	Legendre functions of the first kind.	….
$P_n'(x)$	First derivative of the Legendre function of the first kind.	….
$P_n''(x)$	Second derivative of the Legendre function of the first kind.	….
$Q_n(x)$	Legendre functions of the second kind.	….
$Q_n'(x)$	First derivative of the Legendre function of the second kind.	….
Q_Φ	Transverse shearing force per unit length.	N/m

R_Φ, R_θ	Principal radii of curvatures of a prolate spheroidal surface.	m
u_Φ	Tangential displacement.	m
w	Transverse or radial displacement	m
U	Potential energy.	KJ
$U_{\max}$	Maximum potential energy.	KJ
K	Kinetic energy.	KJ
$K^*_{\max}$	Maximum Kinetic energy.	Kj
R_r	Radius of shell.	mm
β_i	Roots of the non – shallow shell cubic equation.	….
$\varepsilon_\Phi, \varepsilon_\theta$	Strains.	mm/mm
Φ	Inclination angle of a prolate spheroid.	rad
Φ_o	Opening angle of a spherical shell model.	rad
λ	Non – dimensional frequency parameter $(\sqrt{\rho/E}\omega a)$ (used for prolate spheroid shells).	….
θ	Angle of rotation in the meridian direction.	rad
ρ	Density.	kg/m^3
Ω	Non – dimensional frequency parameter $(\sqrt{\rho/E}\omega R)$ (used for spherical shells).	….
ω	Circular frequency.	rad/sec
ν	Poisson ratio.	….
$\sigma_\Phi, \sigma_\theta$	Stress resultants.	N/m^2

Note:-

Other symbols are defined during the text.

List of Contents

APPENDIX

INTRODUCTION

Derivation of the differential equations of motion of a prolate spheroidal shell is conducted in terms of a curvilinear coordinate system based upon the radii, R_Φ, R_θ, which expresses the principal curvatures of the surface as a function of the angle of inclination (Φ). This appendix is provided for the purpose of deriving R_Φ and R_θ as function of (Φ) by transformation from the prolate spheroidal coordinate system, and, for deriving the equations of motion of a prolate spheroidal shell including the effect of bending resistance.

Finally all forces and moments are derived as functions of displacements.

APPENDIX A. ١

DERIVATION OF RADII OF CURVATURES

١ – PROLATE SPHEROIDAL COORDINATES

Consider the prolate spheroidal coordinate system: ***[٣٤]***

$x = p \cosh\alpha \cos\beta \cos\theta$ (A.١.١)

$y = p \cosh\alpha \cos\beta \sin\theta$ (A.١.٢)

$z = p \sinh\alpha \sin\beta$ (A.١.٣)

where,

$p = a\ e$ (A.١.٤)

For the equation of prolate spheroid, however, α must be constant, thin it can be written as:

$\cosh\alpha = c$ (A١.٥)

$$e = \frac{1}{\cosh\alpha} = \frac{1}{c}$$ (A.١.٦)

In view of this consideration, the equations of the prolate spheroidal shell can be written in the following form,

$x = p\ c \cos\beta \cos\theta = a \cos\beta \cos\theta$ (A.١.٧)

$y = p\ c \cos\beta \sin\theta = a \cos\beta \sin\theta$ (A.١.٨)

$z = p \sqrt{c^2 - 1} \sin\beta = a \sqrt{1 - e^2} \sin\beta$ (A.١.٩)

٢ – VECTORIAL REPRESENTATION OF THE SURFCE

Let the position vector of the ellipsoid be represented in the following form:

$r = xi + yj + zk = a\cos\beta\cos\theta i + a\cos\beta\sin\theta j + a\sqrt{1-e^2}\sin\beta k$

(A.١.١٠)

now a rotational ellipsoid can be represented by the equation

$$\frac{\zeta^2}{a^2}+\frac{z^2}{a^2\tanh^2\alpha}=1 \qquad \text{(A.١.١١)}$$

where, $\zeta^2 = x^2 + y^2$

this represented a prolate spheroidal surface

٣ – PROPERTIES OF THE SURFACE

The first fundamental form of an element of the arc of ellipsoid can be expressed as:

$ds^2 = E\,d\beta^2 + 2F\,d\beta\,d\theta + G\,d\theta^2$ (A.١.١٢)

where, $r_\beta = \frac{\delta r}{\delta \beta}$

$E = r_\beta r_\beta = a^2(1 - e^2\cos^2\beta)$ (A.١.١٣)

$F = r_\beta r_\theta = 0$ (A.١.١٤)

$G = r_\theta r_\theta = a^2 \cos^2\beta$ (A.١.١٥)

The discriminate is

$$\sqrt{EG - F^2} = a^2 \cos\beta \sqrt{1 - e^2 \cos^2\beta} \quad \text{(A.١.١٦)}$$

The normal unit vector of the prolate spheroid is

$$N = \frac{(r_\theta \; r_\beta)}{\sqrt{EG - F^2}} \quad \text{(A.١.١٧)}$$

$$= \frac{1}{\sqrt{1 - e^2 \cos^2\beta}} (\sqrt{1-e^2}\cos\beta\cos\theta\, i + \sqrt{1-e^2}\cos\beta\cos\theta\, j + \sin\beta\; k$$

(A.١.١٨)

or

$N = N_1 i + N_2 j + N_3 k$ (A.١.١٩)

Where i, j, k are the unit vectors of the coordinate system. Now it can easily be calculate that.

$$\cos\Phi = \frac{N_3}{|N|} = \frac{\sin\beta}{\sqrt{1 - e^2\cos^2\beta}}$$

(A.١.٢٠)

where (Φ) is the angle in the space between the vertical axis and the normal vector.

The terms of the second fundamental form of the surface are:-

$$e^{\bullet} = \frac{r_{\beta\beta} \; r_\beta \; r_\theta}{\sqrt{EG - F^2}} = \sqrt{\frac{1-e^2}{1 - e^2\cos^2\beta}} \quad \text{(A.١.٢١)}$$

$$r_{\beta\beta} = \frac{\delta^2 r}{\delta \beta^2}$$

$$r_{\theta\theta} = \frac{\delta^2 r}{\delta \theta^2}$$

(A.١.٢٢)

$$g = \frac{(r_{\theta\theta}\, r_\beta\, r_\theta)}{\sqrt{EG - F^2}} = \frac{a\sqrt{1-e^2}\cos^2\beta}{\sqrt{1-e^2\cos^2\beta}} \qquad \text{(A.١.٢٣)}$$

The normal curvatures of the surface x_1 and x_2, in the two principle directions are

$$x_1 = \frac{1}{R_\Phi} = \frac{e^{\bullet}}{E} = \frac{\sqrt{1-e^2}}{a(1-e^2\cos^2\beta)^{3/2}} \qquad \text{(A.١.٢٤)}$$

$$x_2 = \frac{1}{R_\theta} = \frac{g}{G} = \frac{\sqrt{1-e^2}}{a(1-e^2\cos^2\beta)} \qquad \text{(A.١.٢٥)}$$

The two principal radii of the surface can be then written as;

$$R_\Phi = \frac{a(1-e^2\cos^2\beta)^{3/2}}{\sqrt{1-e^2}} = \frac{(1-e^2)\, R_\theta^3}{a^2} \qquad \text{(A.١.٢٦)}$$

$$R_\theta = \frac{a\sqrt{1-e^2\cos^2\beta}}{\sqrt{1-e^2}} \qquad \text{(A.١.٢٧)}$$

Now the radii can be expressed as a function of the variable (Φ) alone in the following form:

$$R_\Phi = \frac{a(1-e^2)}{(1-e^2\cos^2\Phi)^{3/2}} \qquad \text{(A.١.٢٨)}$$

$$R_\theta = \frac{a}{(1-e^2\cos^2\Phi)} \qquad (A.١.٢٩)$$

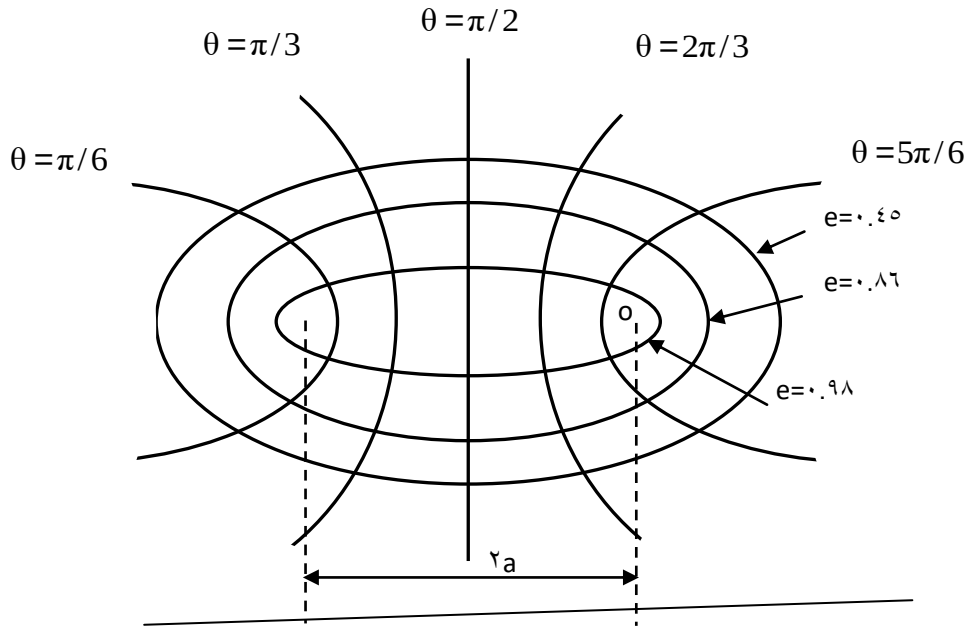

Fig. (A١): Prolate Spheroidal Coordinates

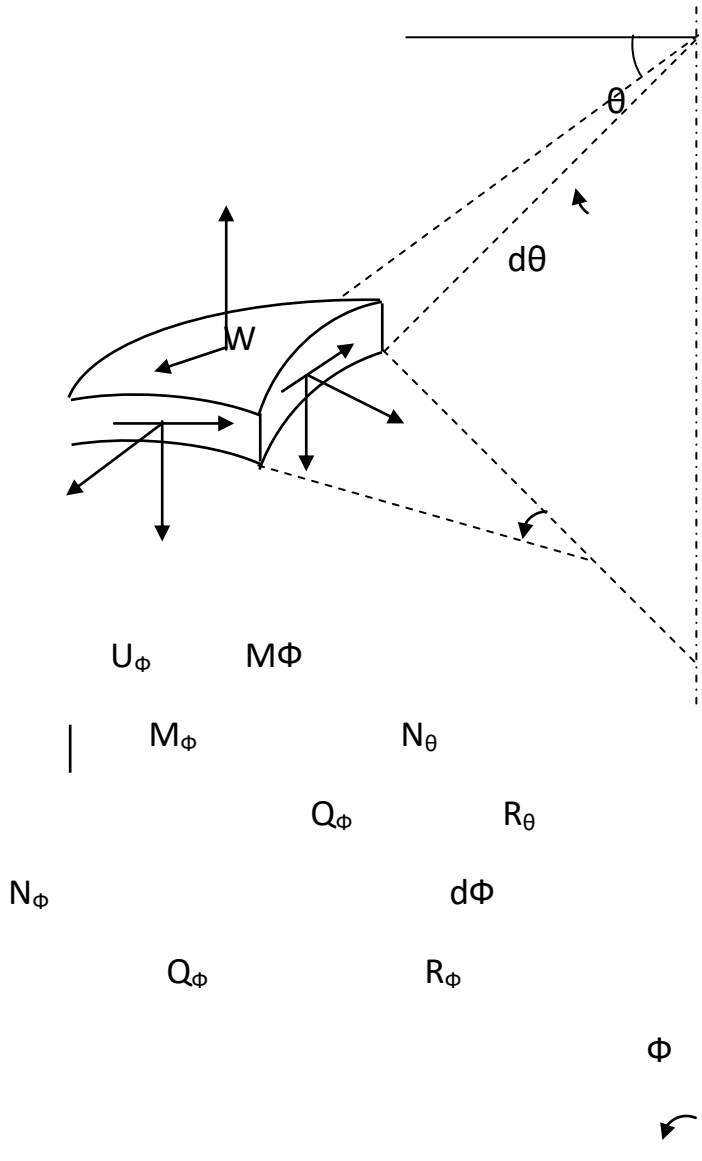

Fig. (A٢): Prolate Spheroidal Shell Element

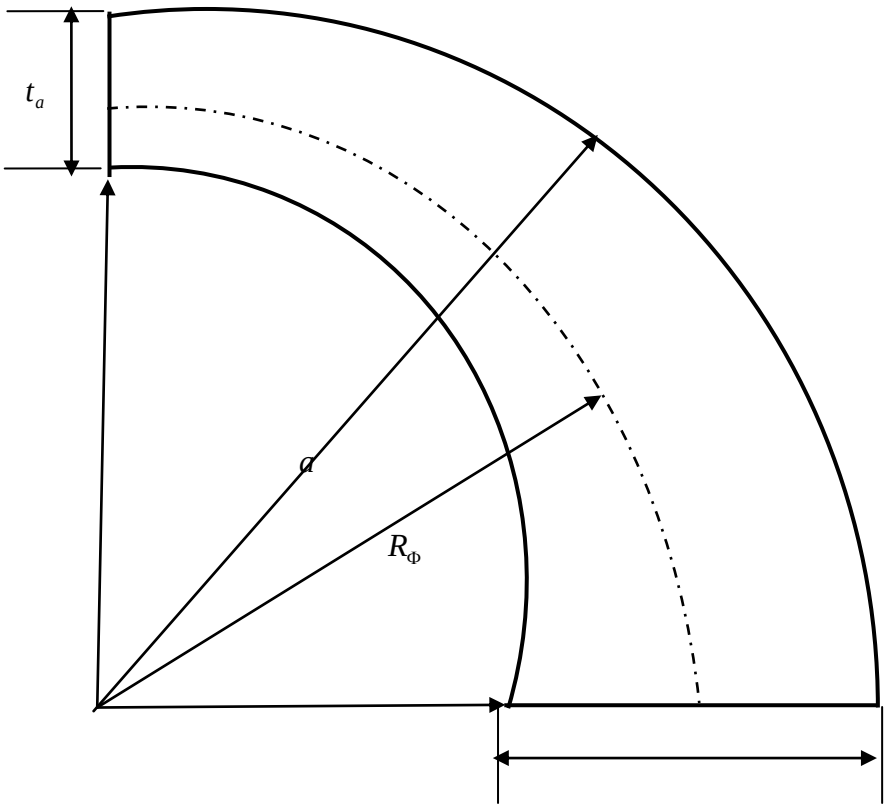

t_b

Fig. (A٣): Prolate Spheroidal Shell with Variable Thickness Ratio

APPENDIX A. ٢

DERIVATION THE EQUATIONS OF MOTION

The vectors N_Φ and N_θ represent forces per unit length of the section corresponding to the stresses σ_Φ and σ_θ respectively.

The victors M_Φ and M_θ are the moment per unit length of the section corresponding to the stress couples. Finally the Q vector is the transverse shearing stress resultant, as represented in Fig. A٢. The equations of motion may be derived by using Loves' which are;

That if the shell is thin it can be assumed that the displacements in the θ and Φ directions vary linearly through the shell thickness while the displacements are independent of thickness. Moreover, if we assume that we may neglect shear deflections which implies that the normal shear strains are zero and neglecting the rotary inertia one can get:-

$$\frac{\partial N_1 A_2}{\partial \alpha_1}+\frac{\partial N_{21} A_1}{\partial \alpha_2}+N_{12}\frac{\partial A_2}{\partial \alpha_2}-N_2\frac{\partial A_2}{\partial \alpha_1}+A_1A_2\frac{Q_1}{R_1}=A_1A_2\rho\, h\frac{\partial^2 u_1}{\partial t}$$

(A.٢.١)

$$\frac{\partial N_{12} A_2}{\partial \alpha_1}+\frac{\partial N_2 A_1}{\partial \alpha_2}+N_{21}\frac{\partial A_2}{\partial \alpha_1}-N_1\frac{\partial A_1}{\partial \alpha_{21}}+A_1A_2\frac{Q_2}{R_2}=A_1A_2\rho\, h\frac{\partial^2 u_2}{\partial t}$$

(A.٢.٢)

$$\frac{\partial Q_1 A_2}{\partial \alpha_1} + \frac{\partial Q_2 A_1}{\partial \alpha_2} - \left(\frac{N_1}{R_1} + \frac{N_2}{R_2} \right) A_1 A_2 = A_1 A_2 \rho \frac{\partial^2 w}{\partial t} \qquad \text{(A.٢.٣)}$$

$$\frac{\partial M_1 A_2}{\partial \alpha_1} + \frac{\partial M_{21} A_1}{\partial \alpha_2} + M_{12} \frac{\partial A_1}{\partial \alpha_2} - M_2 \frac{\partial A_2}{\partial \alpha_1} - Q_1 A_1 A_2 = 0 \qquad \text{(A.٢.٤)}$$

$$\frac{\partial M_{12} A_2}{\partial \alpha_1} + \frac{\partial M_2 A_1}{\partial \alpha_2} + M_{21} \frac{\partial A_2}{\partial \alpha_1} - M_1 \frac{\partial A_1}{\partial \alpha_2} - Q_2 A_1 A_2 = 0 \qquad \text{(A.٢.٥)}$$

Now for the case under consideration the following terms are applied;

$R_1 = R_\Phi$ (A.٢.٦)

$R_2 = R_\theta$ (A.٢.٧)

$\alpha_2 = \theta$

$A_1 = R_\Phi$ (A.٢.٨)

$A_2 = R_\theta \sin\Phi$ (A.٢.٩)

$N_1 = N_\Phi$, $N^2 = N_\theta$, $M^1 = M_\Phi$, $M_2 = M_\theta$, $N_{12} = N_{\Phi\theta}$, $M_{12} = M_{\Phi\theta}$

(A.٢.١٠)

Moreover assuming axisymmetric motion where all derivatives with respect to θ are zero and

$N_{\Phi\theta} = M_{\Phi\theta} = Q_\theta = u_2 = 0$ (A.٢.١١)

Then, the following equations are drawn;

$$\frac{\partial}{\partial \Phi}(N_{\Phi} R_{\theta} \sin \Phi) - N_{\theta} R_{\Phi} \cos\Phi + Q_{\Phi} R_{\theta} \sin \Phi = \rho\, h R_{\Phi} R_{\theta} \sin \Phi \frac{\partial^2 u}{\partial t^2}$$

(A .٢.١٢)

$$\frac{\partial}{\partial \Phi}(Q R_{\theta} \sin \Phi) - \left(\frac{N_{\Phi}}{R_{\Phi}} + \frac{N_{\theta}}{R_{\theta}} \right) R_{\Phi} R_{\theta} \sin \Phi = \rho\, h R_{\Phi} R_{\theta} \sin \Phi \frac{\partial^2 w}{\partial t^2}$$

(A.٢.١٣)

$$\frac{\partial}{\partial \Phi}(M_{\Phi} R_{\theta} \sin \Phi) - M_{\theta} R_{\Phi} \cos\Phi - Q R_{\Phi} R_{\theta} \sin \Phi = 0 \qquad \text{(A.٢.١٤)}$$

The strains, expressed in terms of displacements, can be written as:

$$\varepsilon_{\Phi}^{0} = \frac{1}{R_{\Phi}} \left[\frac{\partial u_{\Phi}}{\partial \Phi} + w \right] \qquad \text{(A.٢.١٥)}$$

$$\varepsilon_{\theta}^{0} = \frac{1}{R_{\theta} \sin \Phi} \left[u_{\Phi} \cos\Phi + w \sin \Phi \right] = \frac{1}{R_{\Phi}} \left[u_{\Phi} \cot\Phi + w \right] \qquad \text{(A.٢.١٦)}$$

$$k_{\Phi} = \frac{1}{R_{\Phi}} \frac{\partial}{\partial \Phi} \left[\frac{1}{R_{\Phi}} \left(u_{\Phi} - \frac{\partial w}{\partial \Phi} \right) \right] \qquad \text{(A.٢.١٧)}$$

$$k_{\theta} = \frac{1}{R_{\Phi} \sin \Phi} \left[\frac{\cos\Phi}{R_{\Phi}} \left(u_{\Phi} - \frac{\partial w}{\partial \Phi} \right) \right] \qquad \text{(A.٢.١٨)}$$

If E, υ are as in nomenclature then, the forces, moments and the shearing forces per unit length will be

$$N_{\Phi} = \frac{E\ h}{1-\nu^2}\left[\varepsilon_{\Phi}^{0} + \varepsilon_{\theta}^{0}\right] \qquad \text{(A.٢.١٩)}$$

$$N_{\theta} = \frac{E\ h}{1-\nu^2}\left[\varepsilon_{\theta}^{\circ} + \nu\,\varepsilon_{\Phi}^{\circ}\right] \qquad \text{(A.٢.٢٠)}$$

$$M_{\Phi} = \frac{E\ h^3}{12(1-\nu^2)}\left[k_{\Phi} + \nu\ k_{\theta}\right] \qquad \text{(A.٢.٢١)}$$

$$M_{\theta} = \frac{E\ h^3}{12(1-\nu^2)}\left[k_{\theta} + \nu\ k_{\Phi}\right] \qquad \text{(A.٢.٢٢)}$$

Substituting the relevant expressions we get:-

$$N_{\Phi} = \frac{E\ h}{1-\nu^2}\left[\frac{1}{R_{\Phi}}\left(\frac{\partial u_{\Phi}}{\partial \Phi} + w\right) + \frac{\nu}{R_{\Phi}}\left(u_{\Phi}\cot\Phi + w\right)\right] \qquad \text{(A.٢.٢٣)}$$

$$N_{\theta} = \frac{E\ h}{1-\nu^2}\left[\frac{1}{R_{\theta}}\left(u_{\Phi}\cot\Phi + w\right) + \frac{\nu}{R_{\Phi}}\left(\frac{\partial u_{\Phi}}{\partial \Phi} + w\right)\right] \qquad \text{(A.٢.٢٤)}$$

$$M_{\Phi} = \frac{E\ h^3}{12(1-\nu^2)}\left[\frac{1}{R_{\Phi}}\frac{\partial}{\partial \Phi}\frac{1}{R_{\theta}}\left(u_{\Phi} - \frac{\partial w}{\partial \Phi}\right) + \frac{\nu\cos\Phi}{R_{\Phi}R_{\theta}\sin\Phi}\left(u_{\Phi} - \frac{\partial w}{\partial \Phi}\right)\right]$$

(A.٢.٢٥)

$$M_{\theta} = \frac{E\ h^3}{12(1-\nu^2)}\left[\frac{\cos\Phi}{R_{\Phi}R_{\theta}\sin\Phi}\left(u_{\Phi} - \frac{\partial w}{\partial \Phi}\right) + \frac{\nu}{R_{\Phi}}\frac{\partial}{\partial \Phi}\left(\frac{1}{R_{\theta}}\left(u_{\Phi} - \frac{\partial w}{\partial \Phi}\right)\right)\right]$$

(A.٢.٢٦)

APPENDIX

DERIVATION OF THE RAYLEIGH – RITZ'S ENERGY METHOD FOR NON – SHALLOW SPHEROIDAL SHELL:

From an expression for maximum potential energy ($U_{\max}$) ***[٣٤]***

$$
\begin{aligned}
U_{\max} = \frac{E\,h}{2(1-\nu^2)} \int_0^{2\pi}\int_0^{2\pi} \frac{h^2}{12} \Bigg[& \frac{1}{R_\Phi^2}\left[\frac{\partial}{\partial\Phi}\left[\frac{U_\Phi}{R_\Phi} - \frac{\partial W}{R_\Phi\,\partial\Phi}\right]\right]^2 \\
& + \frac{\cos^2\Phi}{R_\Phi^2\,R_\theta^2\sin^2\Phi}\left[U_\Phi - \frac{\partial W}{\partial\Phi}\right]^2 + 2\,\upsilon\,\frac{\cos\Phi}{R_\theta\,R_\Phi^2\,\sin\Phi}\left[U_\Phi - \frac{\partial W}{\partial\Phi}\right] \\
& \frac{\partial}{\partial\Phi}\left[\frac{U_\Phi}{R_\Phi} - \frac{\partial W}{R_\Phi\partial\Phi}\right]\Bigg] + \frac{1}{R_\Phi^2}\left[\frac{\partial U_\Phi}{\partial\Phi} + W\right]^2 \\
& + \frac{1}{(R_\theta\,\sin\Phi)^2}\,(U_\Phi\,\cos\Phi + W\,\sin\Phi)^2 \\
& + \frac{2\,\nu}{R_\theta\,R_\Phi\sin\Phi}\left[\frac{\partial U_\Phi}{\partial\Phi} + W\right](U_\Phi\cos\Phi + W\,\sin\Phi) \\
& R_\Phi\,R_\theta\sin\Phi d\Phi\,d\theta
\end{aligned}
$$

(B.١)

But

$$W(\Phi) = \sum_{i=1}^{n} a_i\,W_i(\Phi) \quad , \quad U_\Phi(\Phi) = \sum_{i=1}^{n} b_i\,U_{\Phi i}(\Phi)$$

$$\frac{\partial W(\Phi)}{\partial\Phi} = \sum_{i=1}^{n} a_i\,\frac{\partial W_i(\Phi)}{\partial\Phi} \quad , \quad \frac{\partial U_\Phi(\Phi)}{\partial\Phi} = \sum_{i=1}^{n} b_i\,\frac{\partial U_{\Phi i}(\Phi)}{\partial\Phi}$$

(B.٢)

After substituting Eq. (B.٢) into Eq. (B.١) yield the following expression:

$$
\begin{aligned}
U_{\max} = \frac{E\,h}{2(1-\nu^2)} \int_0^{2\pi}\int_0^{2\pi} \frac{h^2}{12}\Bigg[& \frac{1}{R_\Phi^2}\left[\frac{\partial}{\partial\Phi}\left[\frac{\sum_{i=1}^{n} b_i\ U_{\Phi i}(\Phi)}{R_\Phi} - \sum_{i=1}^{n} a_i \frac{\partial W_i(\Phi)}{R_\Phi\,\partial\Phi}\right]\right]^2 \\
& + \frac{\cos^2\Phi}{R_\Phi^2\ R_\theta^2\ \sin\ \Phi}\left[\sum_{i=1}^{n} b_i\ U_{\Phi i}(\Phi) - \sum_{i=1}^{n} a_i \frac{\partial W_i(\Phi)}{\partial\Phi}\right]^2 \\
& + 2\,\nu \frac{\cos\Phi}{R_\theta\ R_\Phi^2 \sin\Phi}\left[\sum_{i=1}^{n} b_i\ U_{\Phi i}(\Phi) - \sum_{i=1}^{n} a_i \frac{\partial W_i(\Phi)}{\partial\Phi}\right] \\
& \frac{\partial}{\partial\Phi}\left[\frac{\sum_{i=1}^{n} b_i U_{\Phi i}(\Phi)}{R_\Phi} - \sum_{i=1}^{n} a_i \frac{\partial W_i(\Phi)}{R_\Phi\,\partial\Phi}\right]\Bigg] \\
& + \frac{1}{R_\Phi^2}\left[\sum_{i=1}^{n} b_i \frac{\partial U_{\Phi i}(\Phi)}{\partial\Phi} + \sum_{i=1}^{n} a_i\ W_i(\Phi)\right]^2 \\
& + \frac{1}{(R_\theta\ \sin\Phi\ )^2}\left(\sum_{i=1}^{n} b_i U_{\Phi i}(\Phi)\cos\Phi + \sum_{i=1}^{n} a_i W_i(\Phi)\sin\Phi\right)^2 \\
& + \frac{2\ \nu}{R_\theta\ R_\Phi \sin\Phi}\left[\sum_{i=1}^{n} b_i \frac{\partial U_{\Phi i}(\Phi)}{\partial\Phi} + \sum_{i=1}^{n} a_i\ W_i(\Phi)\right] \\
& \left(\sum_{i=1}^{n} b_i U_{\Phi i}(\Phi)\cos\Phi + \sum_{i=1}^{n} a_i W_i(\Phi)\sin\Phi\right) \\
& R_\Phi\ R_\theta\ \sin\Phi d\Phi\ d\theta
\end{aligned}
\qquad \text{(B.٣)}
$$

After algebraic simplifications for Eq. (B.٣) yield the following expression:

$$U_{\max} = \frac{E\,h}{2(1-\nu^{2})}\int_{0}^{2\pi}\int_{0}^{2\pi}\frac{h^{2}}{12}\left[\frac{1}{R_{\Phi}^{2}}\left[\left[\frac{1}{R_{\Phi}}\left(\sum_{i=1}^{n} b_{i}\,\frac{\partial U_{\Phi i}(\Phi)}{\partial\Phi}-\sum_{i=1}^{n} a\,\frac{\partial^{2} W_{i}(\Phi)}{R_{\Phi}\,\partial\Phi^{2}}\right)\right]\right]^{2}\right.$$

$$+\frac{\cos^{2}\Phi}{R_{\Phi}^{2}\;R_{\theta}^{2}\sin^{2}\Phi}\left[\sum_{i=1}^{n} b_{i}U_{\Phi i}(\Phi)-\sum_{i=1}^{n} a_{i}\,\frac{\partial W_{i}(\Phi)}{\partial\Phi}\right]^{2}$$

$$+\;2\,\nu\,\frac{\cos}{R_{\theta}\;R_{\Phi}^{2}\sin\Phi}\left[\sum_{i=1}^{n} b_{i}\,U_{\Phi i}(\Phi)-\sum_{i=1}^{n} a_{i}\,\frac{\partial W_{i}(\Phi)}{\partial\Phi}\right].$$

$$\left[\frac{1}{R_{\Phi}}\left(\sum_{i=1}^{n} b_{i}\,\frac{\partial U_{\Phi i}(\Phi)}{\partial\Phi}-\sum_{i=1}^{n} a_{i}\,\frac{\partial^{2} W_{i}(\Phi)}{R_{\Phi}\,\partial\Phi^{2}}\right)\right]\Bigg]$$

$$+\frac{1}{R_{\Phi}^{2}}\left[\sum_{i=1}^{n} b_{i}\,\frac{\partial U_{\Phi i}(\Phi)}{\partial\Phi}+\sum_{i=1}^{n} a_{i}\,W_{i}(\Phi)\right]^{2}$$

$$+\frac{1}{(R_{\theta}\sin\Phi)^{2}}\left(\sum_{i=1}^{n} b_{i}\,U_{\Phi i}(\Phi)\cos\Phi+\sum_{i=1}^{n} a_{i}W_{i}(\Phi)\sin\Phi\right)^{2}$$

$$+\frac{2\,\nu}{R_{\theta}\,R_{\Phi}\sin\Phi}\left[\sum_{i=1}^{n} b_{i}\,\frac{\partial U_{\Phi i}(\Phi)}{\partial\Phi}+\sum_{i=1}^{n} a_{i}W_{i}(\Phi)\right]$$

$$\left(\sum_{i=1}^{n} b_{i}\;U_{\Phi i}(\Phi)\cos\Phi+\sum_{i=1}^{n} a_{i}W_{i}(\Phi)\sin\Phi\right)$$

$$R_{\Phi}\,R_{\theta}\sin\Phi\,d\Phi\;d\theta$$

$$U_{max} = \frac{E\,h}{2(1-\nu^{2})}\int_{0}^{2\pi}\int_{0}^{2\pi}\frac{h^{2}}{12}\left[\frac{1}{R_{\Phi}^{2}}\left[\frac{1}{R_{\Phi}^{2}}\left\{\left(\sum_{i=1}^{n} b_i\,\frac{\partial U_{\Phi i}(\Phi)}{\partial\Phi}\right)^{2} - 2\sum_{i=1}^{n} b_i\,\frac{\partial U_{\Phi i}(\Phi)}{\partial\Phi}\right.\right.\right.$$

$$\left.\left.\left. .\sum_{i=1}^{n} a_i\,\frac{\partial^{2} W_i(\Phi)}{R_{\Phi}\,\partial\Phi^{2}} + \left(\sum_{i=1}^{n} a_i\,\frac{\partial^{2} W_i(\Phi)}{R_{\Phi}\,\partial\Phi^{2}}\right)^{2}\right\}\right]$$

$$+\frac{\cos^{2}\Phi}{R_{\Phi}^{2}\,R_{\theta}^{2}\,\sin^{2}\Phi}\left[\left(\sum_{i=1}^{n} b_i\,U_{\Phi i}(\Phi)\right)^{2} - 2\sum_{i=1}^{n} b_i\,U_{\Phi i}(\Phi)\sum_{i=1}^{n} a_i\,\frac{\partial W_i(\Phi)}{\partial\Phi}\right.$$

$$\left.+\left(\sum_{i=1}^{n} a_i\,\frac{\partial W_i(\Phi)}{\partial\Phi}\right)^{2}\right]$$

$$+\ 2\,\nu\,\frac{\cos\Phi}{R_{\theta}\,R_{\Phi}^{3}\,\sin\Phi}\left[\sum_{i=1}^{n} b_i U_{\Phi i}(\Phi)\sum_{i=1}^{n} b_i\,\frac{\partial U_{\Phi i}(\Phi')}{\partial\Phi} - \sum_{i=1}^{n} b_i U_{\Phi i}(\Phi)\,.\right.$$

$$.\sum_{i=1}^{n} a_i\,\frac{\partial W_i^{2}(\Phi)}{\partial\Phi^{2}} - \sum_{i=1}^{n} a_i\,\frac{\partial W_i(\Phi)}{\partial\Phi}\ \sum_{i=1}^{n} b_i\,\frac{\partial U_{\Phi i}(\Phi)}{\partial\Phi}$$

$$\left.+\sum_{i=1}^{n} a_i\,\frac{\partial W_i(\Phi)}{\partial\Phi}\ \sum_{i=1}^{n} a_i\,\frac{\partial W_i^{2}(\Phi)}{\partial\Phi^{2}}\right]\Bigg]$$

$$+\frac{1}{R_{\Phi}^{2}}\left[\left(\sum_{i=1}^{n} b_i\,\frac{\partial U_{\Phi i}(\Phi)}{\partial\Phi}\right)^{2} + 2\sum_{i=1}^{n} b_i\,\frac{\partial U_{\Phi i}(\Phi)}{\partial\Phi}\sum_{i=1}^{n} a_i\,W_i(\Phi)\right.$$

$$\left.+\left(\sum_{i=1}^{n} a_i W_i(\Phi)\right)^{2}\right]$$

$$+\frac{1}{(R_{\theta}\,\sin\Phi)^{2}}\left[\left(\sum_{i=1}^{n} b_i\,U_{\Phi i}(\Phi)\cos\Phi\right)^{2} + 2\sum_{i=1}^{n} b_i\,U_{\Phi i}(\Phi)\cos\Phi\right.$$

$$\left.. \sum_{i=1}^{n} a_i\,W_i(\Phi)\sin\Phi + \left(\sum_{i=1}^{n} a_i\,W_i(\Phi)\sin\Phi\right)^{2}\right]$$

$$+\frac{2\,\nu}{R_{\theta}\,R_{\Phi}\sin\Phi}\left[\left(\sum_{i=1}^{n} b_i\,\frac{\partial U_{\Phi i}(\Phi)}{\partial\Phi}\ \sum_{i=1}^{n} b_i\,U_{\Phi i}(\Phi)\cos\Phi\right)\right.$$

$$+\left(\sum_{i=1}^{n} b_i\,\frac{\partial U_{\Phi i}(\Phi)}{\partial\Phi}\sum_{i=1}^{n} a_i\,W_i(\Phi)\sin\Phi\right)$$

$$+\left(\sum_{i=1}^{n} a_i\,W_i(\Phi)\sum_{i=1}^{n} b_i U_{\Phi i}(\Phi)\cos\Phi\right)$$

$$\left.+\left(\sum_{i=1}^{n} a_i\,W_i(\Phi)\sum_{i=1}^{n} a_i W_i(\Phi)\sin\Phi)\right)\right]\ R_{\Phi}\,R_{\theta}\,\sin\Phi d\Phi\,d\theta \qquad (B.4)$$

but

$$\left.\begin{aligned}\left(\sum_{i=1}^{n} a_i\ W_i(\Phi)\right)^2 &= \sum_{i=1}^{n}\sum_{j=1}^{n} a_i\, a_j\ W_i(\Phi)\ W_j(\Phi)\\ \left(\sum_{i=1}^{n} b_i\ U_{\Phi i}(\Phi)\right)^2 &= \sum_{i=1}^{n}\sum_{j=1}^{n} b_i b_j U_{\Phi i}(\Phi)\, U_{\Phi j}(\Phi)\end{aligned}\right\} \qquad \text{(B.٥)}$$

hence

$$
\begin{aligned}
U_{\max} = \frac{E\,h}{2(1-\nu^2)}\Bigg[\frac{h^2}{12}\Bigg\{\frac{1}{R_\Phi^4}\Bigg[&\sum_{i=1}^{n}\sum_{j=i}^{n} b_i b_j \int_0^{2\pi}\int_0^{2\pi} \frac{\partial U_{\Phi i}}{\partial \Phi}\,\frac{\partial U_{\Phi j}}{\partial \Phi} \\
&- 2\sum_{i=1}^{n} b_i \sum_{j=i}^{n} a_i \int_0^{2\pi}\int_0^{2\pi} \frac{\partial U_{\Phi i}}{\partial \Phi}\,\frac{\partial^2 W_i}{\partial \Phi^2} \\
&+ \sum_{i=1}^{n}\sum_{j=1}^{n} a_i a_j \int_0^{2\pi}\int_0^{2\pi} \frac{\partial^2 W_i}{\partial \Phi^2}\,\frac{\partial^2 W_j}{\partial \Phi^2}\Bigg] \\
&+ \frac{\cos^2\Phi}{R_\Phi^2\; R_\theta^2\; \sin^2\Phi}\Bigg[\sum_{i=1}^{n}\sum_{j=1}^{n} b_i b_j \int_0^{2\pi}\int_0^{2\pi} U_{\Phi i}\,U_{\Phi j} - 2\sum_{i=1}^{n} b_i \sum_{i=1}^{n} a_i \int_0^{2\pi}\int_0^{2\pi} U_{\Phi i}\,\frac{\partial W_i}{\partial \Phi} \\
&+ \sum_{i=1}^{n}\sum_{j=1}^{n} a_i a_j \int_0^{2\pi}\int_0^{2\pi} \frac{\partial W_i}{\partial \Phi}\,\frac{\partial W_j}{\partial \Phi}\Bigg] \\
&+ 2\,\nu\,\frac{\cos\Phi}{R_\theta\; R_\Phi^3\; \sin\Phi}\Bigg[\sum_{i=1}^{n} b_i \sum_{i=1}^{n} b_i \int_0^{2\pi}\int_0^{2\pi} U_{\Phi i}\,\frac{\partial U_{\Phi i}}{\partial \Phi} - \sum_{i=1}^{n} b_i \sum_{i=1}^{n} a_i \int_0^{2\pi}\int_0^{2\pi} U_{\Phi i}\,\frac{\partial W_i^{\,2}}{\partial \Phi^2} \\
&- \sum_{i=1}^{n} a_i \sum_{i=1}^{n} b_i \int_0^{2\pi}\int_0^{2\pi} \frac{\partial W_i}{\partial \Phi}\,\frac{\partial U_{\Phi i}}{\partial \Phi} + \sum_{i=1}^{n} a_i \sum_{i=1}^{n} a_i \int_0^{2\pi}\int_0^{2\pi} \frac{\partial W_i}{\partial \Phi}\,\frac{\partial W_i^{\,2}}{\partial \Phi^2} \\
&+ \sum_{i=1}^{n} a_i \sum_{i=1}^{n} a_i \int_0^{2\pi}\int_0^{2\pi} \frac{\partial W_i\,(\Phi)}{\partial \Phi}\,\frac{\partial W_i^{\,2}(\Phi)}{\partial \Phi^2}\Bigg]\Bigg\} \\
&+ \frac{1}{R_\Phi^2}\Bigg[\sum_{i=1}^{n}\sum_{i=1}^{n} b\; b_j \int_0^{2\pi}\int_0^{2\pi} \frac{\partial U_{\Phi i}}{\partial \Phi}\,\frac{\partial U_{\Phi j}}{\partial \Phi} + 2\sum_{i=1}^{n} b_i \sum_{i=1}^{n} a_i \int_0^{2\pi}\int_0^{2\pi} \frac{\partial U_{\Phi i}}{\partial \Phi}\; W_i \\
&+ \sum_{i=1}^{n}\sum_{ji=1}^{n} a_i . a_j \int_0^{2\pi}\int_0^{2\pi} W_i\; W_j\Bigg] \\
&+ \frac{1}{(R_\theta\,\sin\Phi\,)^2}\Bigg[\sum_{i=1}^{n}\sum_{j=1}^{n} b_i b_j \int_0^{2\pi}\int_0^{2\pi} U_{\Phi i}\cos\Phi\; U_{\Phi j}\cos\Phi \\
&+ 2\sum_{i=1}^{n} b_i \sum_{i=1}^{n} a_i \int_0^{2\pi}\int_0^{2\pi} U_{\Phi i}\cos\Phi\; W_i\,\sin\Phi \\
&+ \sum_{i=1}^{n}\sum_{j=1}^{n} a_i\, a_j \int_0^{2\pi}\int_0^{2\pi} W_i\,\sin\Phi\; W_j\,\sin\Phi\Bigg]
\end{aligned}
$$

$$+\frac{2\nu}{R_\theta\ R_\Phi \sin\Phi}\left[\sum_{i=1}^{n} b_i \sum_{i=1}^{n} b_i \int_0^{2\pi}\int_0^{2\pi} \frac{\partial U_{\Phi i}}{\partial \Phi}\ U_{\Phi i}\ \cos\Phi \right.$$
$$+\sum_{i=1}^{n} b_i \sum_{i=1}^{n} a_i \int_0^{2\pi}\int_0^{2\pi} \frac{\partial U_{\Phi i}}{\partial \Phi}\ W_i\ \sin\Phi$$
$$+\sum_{i=1}^{n} a_i \sum_{i=1}^{n} b_i \int_0^{2\pi}\int_0^{2\pi} W_i\ U_{\Phi i}\ \cos\Phi$$
$$\left.+\sum_{i=1}^{n} a_i \sum_{i=1}^{n} a_i \int_0^{2\pi}\int_0^{2\pi} W_i\ W_i(\Phi)\sin\Phi\ )\right]\ R_\Phi\ R_\theta \sin\Phi d\Phi\, d\theta$$

(B.٦)

After simplifying Eq. (B.٦) and making some arrangements, the following expression

yields:-

$$U_{\max} = \sum_{i=1}^{n}\sum_{j=1}^{n} c_i\, c_j\, \frac{E\,h\,\pi}{(1-\nu^2)} \int_0^{2\pi} \frac{h^2}{12\,R_\Phi^4}\left[U'_{\Phi i}\,U'_{\Phi j} - 2U'_{\Phi i}\ W_i'' + W_i'' W_j''\right]\sin\Phi$$
$$+\frac{\nu\ h^2}{6\,R_\theta\ R_\Phi^3}\left[U_{\Phi i}\,U'_{\Phi i} - U_{\Phi i}\,W_i'' - U'_{\Phi i}\,W_i' + W_i'\,W_i''\right]\cos\Phi$$
$$+\frac{h^2}{12\,R_\Phi^2\ R_\theta^2}\left[U_{\Phi i}U_{\Phi j} - 2U_{\Phi i}\,W_i' + W_i'\,W_j'\right]\frac{\cos^2\Phi}{\sin\Phi}$$
$$+\frac{1}{R_\Phi^2}\left[U_{\Phi i}'\,U_{\Phi j}' + 2U_{\Phi i}'\,W_i + W_i\,W_j\right]\sin\Phi$$
$$+\frac{1}{R_\theta^2}\left[U_{\Phi i}\,U_{\Phi j}\,\frac{\cos^2\Phi}{\sin\Phi} + 2U_{\Phi i}\ W_i\cos\Phi + W_i\,W_j\sin\Phi\right]$$
$$+\frac{2\nu}{R_\Phi\ R_\theta}\left[U_{\Phi i}\,U'_{\Phi i}\cos\Phi + U'_{\Phi i}\,W_i\sin\Phi + U_{\Phi i}\,W_i\cos\Phi + W_i\,W_i\sin\Phi\right]$$
$$R_\Phi\ R_\theta\, d\Phi$$

(B.٧)

where,

$$U_{\max} = \sum_{i=1}^{n}\sum_{j=1}^{n} c_i\, c_j\, \frac{E\,h\,\pi}{(1-\nu^2)} \int_0^{2\pi} K_{ij} \qquad \text{(B.٨)}$$

Hence

$$K_{ij} = \frac{E\,h\,\pi}{(1-\upsilon^2)} \int_0^{2\pi} \frac{h^2}{12\,R_\Phi^4}\left[U'_{\Phi i}\,U'_{\Phi j} - 2U'_{\Phi i}\,W_i'' + W_i''W_j''\right]\sin\Phi$$
$$+ \frac{\upsilon\,h^2}{6\,R_\theta\,R_\Phi^3}\left[U_{\Phi i}\,U'_{\Phi i} - U_{\Phi i}\,W_i'' - U'_{\Phi i}\,W_i'' + W_i'\,W_i''\right]\cos\Phi$$
$$+ \frac{h^2}{12\,R_\Phi^2\,R_\theta^2}\left[U_{\Phi i}U_{\Phi j} - 2U_{\Phi i}\,W_i' + W_i'\,W_j'\right]\frac{\cos^2\Phi}{\sin\Phi}$$
$$+ \frac{1}{R_\Phi^2}\left[U'_{\Phi i}\;U'_{\Phi j} + 2U'_{\Phi i}\;W_i + W_i\,W_j\right]\sin\Phi$$
$$+ \frac{1}{R_\theta^2}\left[\,U_{\Phi i}\,U_{\Phi j}\;\frac{\cos^2\Phi}{\sin\Phi} + 2U_{\Phi i}\;W_i\cos\Phi + W_i\,W_j\sin\Phi\right]$$
$$+ \frac{2\upsilon}{R_\Phi\,R_\theta}\left[U_{\Phi i}\,U'_{\Phi i}\cos\Phi + U'_{\Phi i}\;W_i\sin\Phi + U_{\Phi i}\,W_i\cos\Phi + W_i\,W_i\sin\Phi\,\right]$$
$$R_\Phi\,R_\theta\,d\Phi$$

(B.٩)

where,

K_{ij} is the tow dimensional stiffness matrix of spheroidal shell.

In order to find the mass matrix of spheroidal shell it can be started from the maximum kinetic energy as:-

$$K_{\max} = \frac{\omega^2\rho h}{2}\int_0^{2\pi}\int_0^{2\pi}(U_\Phi^2 + W^2)R_\Phi R_\theta \sin\Phi d\Phi d\theta$$

(B.١٠)

Following the same procedure used in the maximum potential energy and after some simplifications arrangements the maximum kinetic energy can be written as:

$$K_{\max} = \sum_{i=1}^{n} \sum_{j=1}^{n} c_i c_j \int_0^{2\pi} \rho h \pi \left[U_i U_j + W_i W_j \right] R_\Phi R_\theta \sin\Phi \, d\Phi$$

(B.١١)

where,

$$K_{\max} = \sum_{i=1}^{n} \sum_{j=1}^{n} c_i c_j \int_0^{2\pi} m_{ij} \qquad \text{(B.١٢)}$$

hence

$$m_{ij} = \int_0^{2\pi} \rho h \pi \left[U_i U_j + W_i W_j \right] R_\Phi R_\theta \sin\Phi \, d\Phi$$

(B.١٣)

where, m_{ij} is a two dimensional mass matrix of spheroidal shell.

CHAPTER ONE

INTRODUCTION

١.١ General and Background

A shell is a sheet of elastic material which conforms to a curved surface. A shell can be curved about one axis like a cylindrical storage tank or about multiple axes like some types of glass. A shell can be one like a curved roof or closed like a hallow ball. In other words, a shell is a continuum which is bounded by two curved surfaces separated by thickness. Several theoretical and experimental methods relevant to the plates and shells solutions are available. Analysis for the natural frequencies and mode shapes of shell is generally much more complex than analysis of beams and plate***s.***

The static and structural dynamic analysis has great importance in the design and development of new structures. The requirements are to quantify

the structural response by using signal analysis techniques (modal analysis) or any other approach.

The results forces When a large structure such as aircrafts, bridges, ships, vehicles and tall building can introduce vibrations which may lead to structural failure. An essential requirement of an engineering structure is to sustain the applied load to it during service life without failure. To obtain an optimum design of structure, depending on the type of problem, a variety of characteristics of structure must be established in both sides of static and dynamic analysis. The dynamic characteristic of any structure are governed by its stiffness and mass properties. The most important dynamic characteristic of the structure is the natural frequency which is a function of material constants or properties, geometry and dimensions of investigated structure.

There are variety of methods that can be used to determine the free and force vibrational characteristics of structural components and systems. These methods can be classified broadly as analytical (exact or called closed solution), approximate approaches and experimental method.

Typical framed structures are beams, rods, plane and space trusses, plane and space frame. The large and complicated structures may be constructed from combination of beams, plates and shells. These structures are analyzed as subjected to a combination of axial, bending, torsion phenomena. It is of importance to the designer being able to predict the vibration characteristic of a whether in the context of frequency, amplitude and dynamic stresses as well as static analysis.

It is worthy to indicate the industrial applications and importance of plates and shells structure. This interest was appreciated today in aerospace

and sea vehicles industry. The plates and shells vibration problems increased in a practical importance, if they are used alone or as sandwich structures. The ease or difficulty in obtaining the solution for plates and shells problem is dependent on the geometry, loading and boundary conditions. Continuous geometry, smooth loading and idealized boundary conditions are generally required to obtain analytical solutions.

The vibration analysis of shell is considerably more complicated than their counterparts for beams or plates. Primarily this is caused by the effects of the curvature on the dynamic behavior, for beams and plates it is possibly to consider separately the flexural and extensional vibrations. These two effects are necessary to combined for complex problems; for shells membrane and flexural deformations are coupled, and any theory must consider these coupled effects simultaneously.

For flexural vibrations of beams and plates there are well established theories. For shells, because of the coupling, mutually perpendicular components of displacement must be considered and thus an equilibrium equation in terms of these displacement components should be derived. However, there is no universally accepted set of equations; in fact, many sets of slightly different equations are exist. The differences depend upon the assumptions made in the derivation.

١. ٢ Prolate and Oblate Spheroidal Shells

A shell of revolution is produced by a rotation of a plane curve about a common axis. One of the commonly used types of elastic thin shell which has appreciated interest in this work is spheroidal shell.

According to the geometry, the shells may be classified as prolate and oblate shells. A prolate spheroidal shell is a shell of revolution with elliptical intersection curves with respect to perpendicular axis. It is the locus surface which is produced by rotating an ellipse around the major axis. On the other hand, an oblate spheroidal shell is defined as the locus surface resulting from rotating an ellipse about minor axis.

The two types have many practical applications. The structure of the fuel tanks of rocket can be considered as a prolate shell. Which the second type has several applications among these applications; the liquid oxygen tanks used in several upper stages of space vehicles have the shape of an oblate spheroidal shell.

١.٣ Theories of Shells

The most common shell theories are based on linear elasticity concepts. Linear shell theories adequately predict stresses and deformations. For shells exhibiting small elastic deformation that is deformation for which the equilibrium – equation condition of deformed elements are the same as if they were not deformed and Hooks law applies.

The nonlinear theory of elastic forms the basis for the finite – deflection and stability theories of shells. Large –deflection theories are often required when dealing shallow shells, highly elastic membranes and buckling problems. The nonlinear shell equations are considerably more difficult to solve.

Practical difficulties in both theory and experiment have to led the development and application of applied engineering method for the analysis of shells. While these methods are approximate and valid only under specific

conditions, they are generally very useful and give a good accuracy for the analysis of the practical engineering shell structures.

Theory of small deflections of thin elastic shells is based upon the equations of the mathematical theory of linear elasticity. The consideration of the complete elasticity equations leads to expressions and equations which are so complicated that it becomes impossible to obtain solutions for shell problems of practical interest. Linear theory of shells can be classified into: -

١- Bending shell theory.

٢- Membrane shell theory.

Bending shell theory:

This theory included the bending resistance of shell and predicts accurate stresses whenever bending is involved. It is more general and exact than the membrane shell theory because it permits the use of all possible boundary conditions.

This method is much more elaborate. However, in certain instances, this theory can be simplified when applied to rotationally symmetric geometries subjected to rotationally symmetric loads. Theoretically, if one of the bending theories is used, any shell with any boundary condition may be solved. Unfortunately, because of the complexity of such analysis, the process in more cases is very difficult. It requires the solution of the systems of differential equations which is a complicated problem in itself. Solutions can be obtained only for certain loadings and geometries. The bending modes vary with thickness, therefore, when the bending theory is employed, and then the

frequency interval of modes extends to infinity for every value of thickness which is greater then zero.

Membrane shell theory:

The membrane theory studies the equilibrium of a shell, it assumes that the basic resistance of the shell to loads by inplane tension, compression, and shear. The membrane theory is applicable only if the boundary conditions are compatible with conditions of equilibrium such as tress all joints are pinned (each member of the truss is stressed only axially). If under external applied loads, bending of the shell is negligible, the middle surface of the shell can be assumed to suffer only extension, then a pure membrane state of stress.

١.٤ Geometry of Shells

The geometry of a shell is entirely defined by specifying the form of the middle surface and the thickness of a thin shell at each point. To describe the form of the middle surface, it is necessary to present some of the important geometrical properties of the surface.

In the engineering applications of thin shells, a shell whose reference surface is in the form of a surface of revolution has extensive usage. A surface of revolution is obtained by rotation of a plane curve about an axis lying in the plane of the curve. This curve is called the meridian and its plane is the meridian plane. The intersection of the surface with planes perpendicular to the axis of rotation are parallel circles. For such a shell the lines of principal curvature are its meridians and parallels.

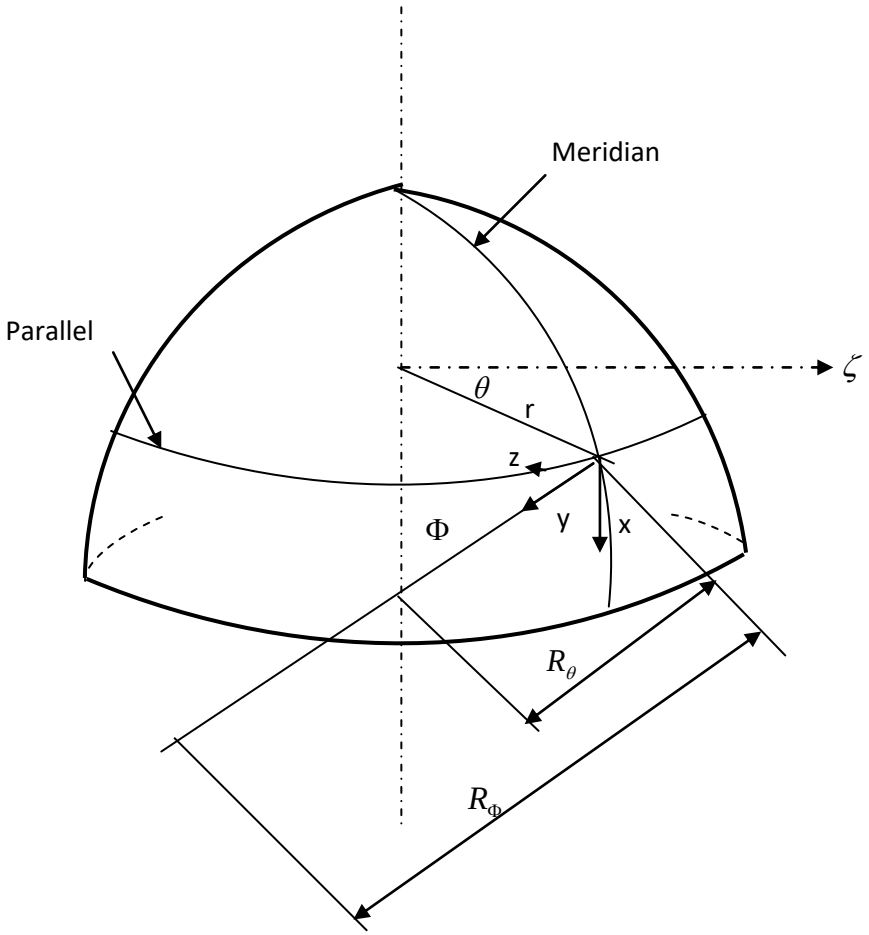

Fig.: (١-١) Shell of revolution

١.٥ Work Objectives

The main objectives of this work may be summarized as follows:

١- An analysis formulation of the problem of the dynamic analysis will be attempted. The investigation was carried out on the prolate shell structure. The Rayleigh – Ritz's method and Boundary Matching method must be considered as a tool for the analysis of structure.

٢- Using the method of matching the boundary conditions and Rayleigh-Ritz's method to obtain the vibration characteristics of non-shallow spheroidal shell for various eccentricity ratios.

٣- Studying the effect of radius to thickness ratio of shell on the natural frequency.

٤- Investigating the effect of the variable thickness between the head and the base of the shell at region of matching on the natural frequency.

٥- Study the effect of the different types of the boundary conditions at region of matching such as (Clamped – free, Clamped –clamped and Pinned – pinned).

Sphere

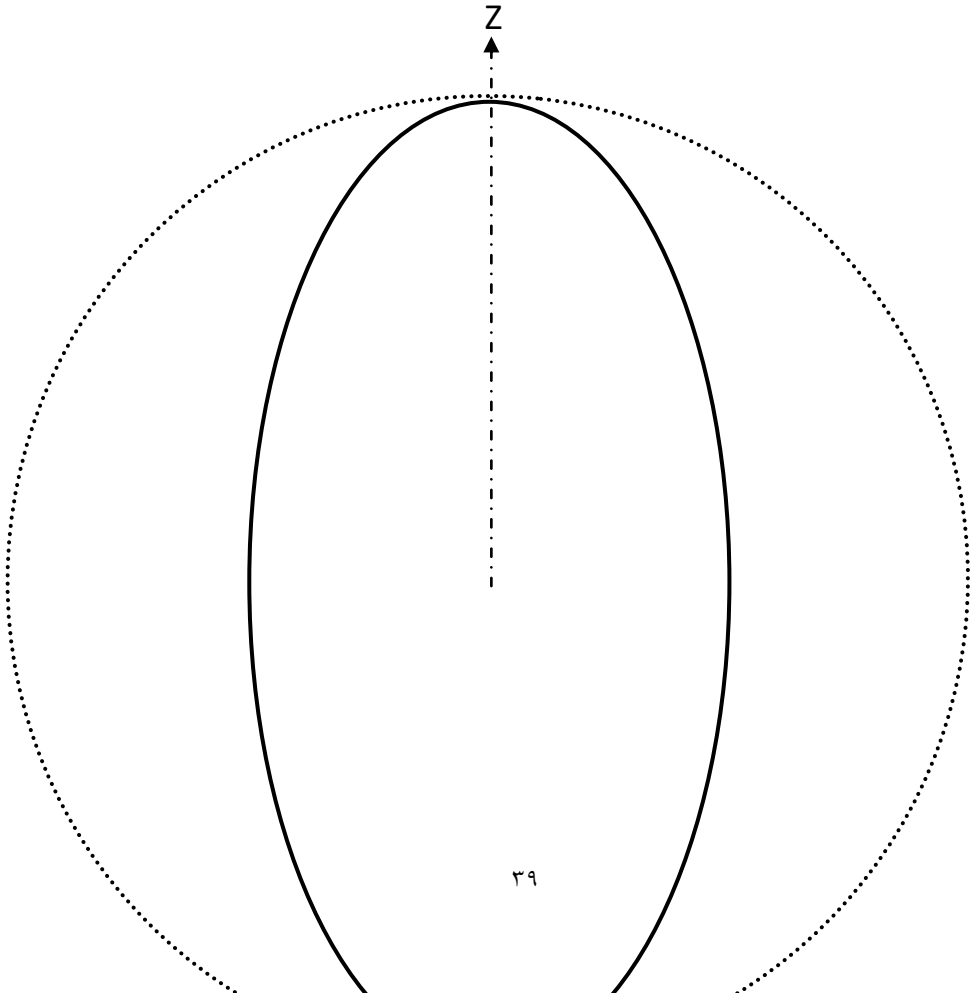

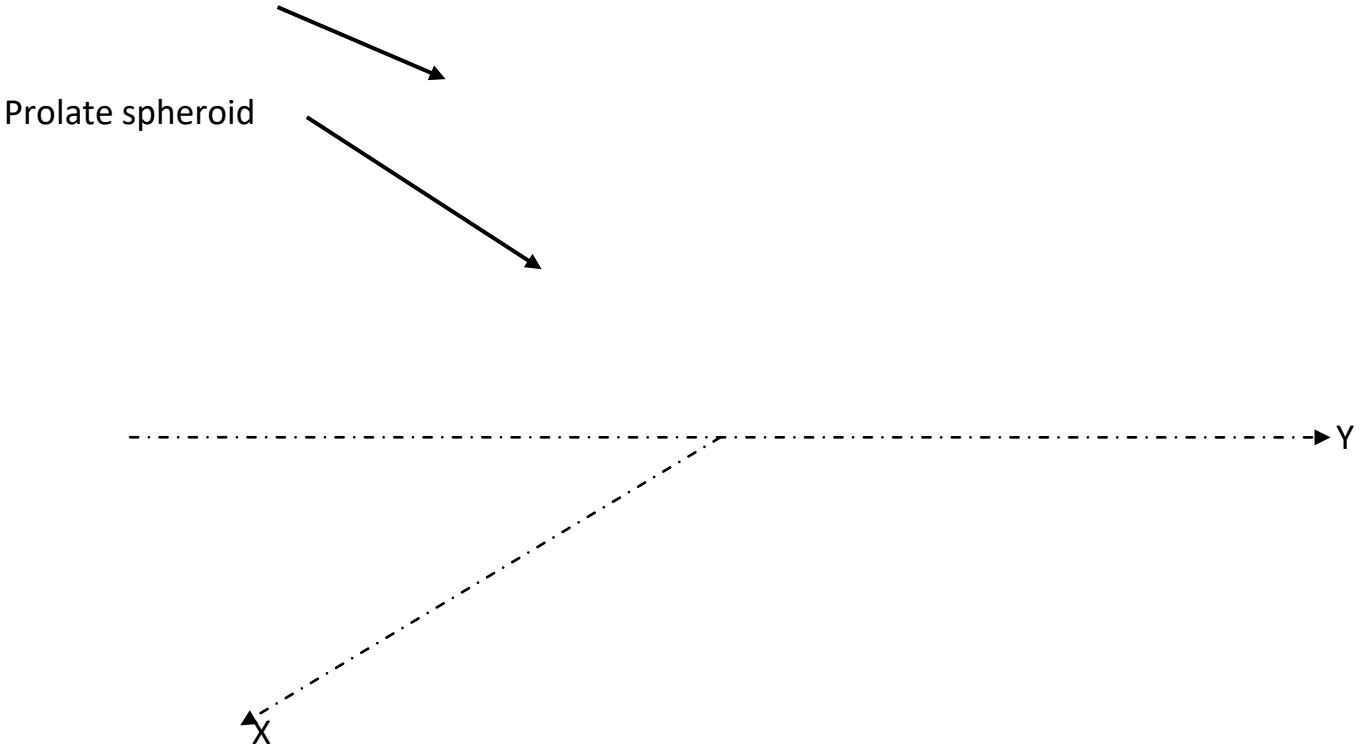

Fig. : (٢-١) A Prolate Spheroid Shell

CHAPTER TWO

LITRATURE REVIEW

٢. ١ Literature Review

The study of the static and dynamic analysis of shells has been treaded by many investigators using different methods, only few papers are published in non classified (according to the author's knowledge) dealing with the free vibration of ellipsoidal shells. There is a sufficient lack in numerical results. Due

to the complexity of the problem it appears that a closed form analytical solution does not exist. Several investigators, using a variety of mathematical techniques, have obtained approximate solution for the natural frequencies of axisymmetric vibrations of thin prolate spheroid shells.

Sitzungsber [١] numerical solutions of the frequency equations of the complete free- vibration problem began to appear in this paper for spherical shells. With the appearance of these publications, it was recognized that the approximate treatment of shell vibration, by considering either only the extensional or only the flexural strain energy, could provide useful information in some special cases (spherical shell), but that covered only a small part of the possible vibration modes.

The treatment of transverse vibration of a shallow spherical shell has been previously given by ***Reissner [٢] and by Johnson and Reissner [٣],*** which for transverse vibration, the longitudinal inertia terms can be neglected. Starting with this assumption, Reissnere was able to formulate.

The problem in a sampler way and obtained exact solutions. Analysis for the coupled longitudinal (torsion less) and transverse with axial symmetry was given by ***Kalnins A. and Naghbi P. M. [٤].***

Dimaggio and Silbeger [٥] obtained solutions of differential equation for the mode shapes for the torsional vibration of a prolate spheroidal shell by the application of Hamilton's principle, was found by a single prolate spheroid angle function of the first kind and the transcendental frequency equation is readily solved with the aid of tabular eigenvalues. Numerical and graphical non- dimensional results are presented for the first eight modes. The same authors in ***[٦]*** used the membrane shell theory, in which the effects of bending

resistance were ignored, and the Raleigh –Ritz's variation method was used to obtain approximate solutions for the non-torsional mode shape and natural frequencies.

Wilfred E. Baker [٧] presented a detailed study of the theory of free, axisymmetric vibration of thin elastic spherical shell and demonstrates by experiment that the normal modes of vibration predicted do exist. Theory predicts the existence of two infinite sets of normal modes, one of which is bounded in frequency and the other is unbounded. The first four modes in each set are identified by experiments on a small steel shell. The author was determined the vibration modes of a thin spherical shell, and was showed by experiment that these modes Physically exist.

Shiraishi and Dimaggio [٨] obtained perturbation solutions for the modes and frequencies of extensional axisymmetric vibration of thin elastic prolate spheroidal shells with displacements in the meridian planes. These solutions, which are in the form of infinite series in powers of the square of the eccentricity having as their first term the solution for a spherical shell, converge rapidly for small rations of major to minor axis. The smaller the eccentricity making these series the more convergent.

The same problem given in ***[٢, ٣]*** was reconsidered by ***Kalnins [٩]*** with all the inertia terms included. The complete frequency equation was solved and found an additional set of modes that was not considered by Reissner. After the examination of their mode shapes, the additional modes were shown to have tangential displacements larger than the transverse displacement. The results of this paper show that the complete frequency spectrum of a shallow spherical shell consists of two infinite sets of modes with separate increasing nodes counts in the displacement. They also show that

when curvature is diminished indefinitely these two sets of modes reduces to the purely longitudinal and purely transverse modes of a circular plate. The longitudinal modes contain mostly extensional strain energy, while the transverse modes contain mostly flexural strain energy.

Kalnins [١٠] concerned with the vibration analysis of spherical shells, closed at one pole and open at any other, by means of the linear classical bending theory of shells. Frequency equations are derived in terms of Legendre function with complex indices, and for axisymmetric vibration the natural frequencies and mode shapes are deduced for opening angles ranging from a shallow to a closed spherical shell. It was found that for all opening angles the frequency spectrum consists of two coupled infinite sets of modes that can be labeled as bending (or flexural) and membrane modes. It was also found that the membrane modes are practically independent of thickness, whereas the bending modes vary with the thickness. The same author concerned with a theoretical investigation of the free vibration of arbitrary shells of revolution by means of the classical bending theory of shell. A method is developed that is applicable to rotationally symmetric shells with meridian variations (including discontinuities) in Young's modulus, poison's ratio, radii of curvature, and thickness. The natural frequencies and the corresponding mode shapes of axisymmetric free vibration of rotationally symmetric shell can be obtained without any limitation on the length of the meridian of the shell. The results of the free vibration of spherical and conical shell obtained earlier by means of the bending theory. In addition, parapoloidal shells and sphere- cone shell combination are considered, which have been previously analyzed by means of the inextentional theory of shell, and natural frequencies and mode shapes predicated by the bending theory are given.

Nemergut and Brand [١١] determined the lower axisymmetric modes of prolate spheroid shell with five values of eccentricity. Their work was distinguished by applying their solution to constant thickness membrane shell by means of numerically integrating the equations of motion while all the others such as ***[٥, ٦, and ٨]*** have considered prolate spheroid shells with varying thickness. It is found that the frequencies associated with higher modes are strongly dependent on the eccentricity.

As for the oblate spheroid shells , ***Penzes and Burgin [١٢]*** were solve the problem of free vibrations of thin isotropic oblate spheroid shells by Galerkin's method .Membrane theory and harmonic axisymmetric motion were assumed in order to derive the differential equations of motion . It was shown that Galerkin's method of solution for the oblate spheroid shell yields the exact solution for the closed spherical shell as the eccentricity of the oblate spheroid shell approaches zero. The characteristic mode shapes for spherical shell are described by associated Legendre functions according to the improved theory of shell.

Kallins and Wilkinson [١٣] included the effects of transverse shear and rotary inertia. The natural frequencies of closed spherical shell may be obtained from their analysis. It was shown that the five branches appear in the frequency spectrum, whereas only three are known to be predicated by the classical bending theory of shells.

Dimaggio and Rand [١٤] applied the finite differences method to obtain approximate solution to determination the modes and frequencies for the same problem for two different geometries of middle surface of shell. The first is of constant length of major axis and varying ratio of major axis to minor axis by changed the length of minor axis, the second of constant length of minor

axis and varying ratio of major axis to minor axis by changed the length of major axis.

Yen and Dimaggio [١٥] extended the work of reference ***[١٤]*** to include the influence of fluid loading and an axisymmetric harmonic forcing function. A finite difference method was applied to obtain approximate solutions for radial displacement of the shell surface and the pressure in the fluid both at the shell surface and in the for field .for different frequencies of the harmonic forcing function, numerical results were given for a shell with an eccentricity of ٠.٩٨٦.

Fluid filled prolate spheroid shells were further studied by ***Rand and Dimaggio [١٦]*** determine the upper branch of the spectrum is below the lowest branch where a scheme for the problem was developed and extensive numerical results in the form of frequency spectra and mode shapes were displayed.

Penzes L. [١٧] extended the solution of reference ***[١٣]*** to include thin orthotropic oblate spheroid shells. He used the same assumptions and equations of motion of the latter reference except that the principle direction of the elastic compliances was assumed to be along parallels of latitude and along meridians. Both of the spheroid and spherical shells were investigated with various orthotropic constants. However, the isotropic case was taken as the limit of the orthotropic problem, and applying the former case to the orthotropic theory yielded the previously published results of the isotropic oblate spheroid shell. The discussion restricted to the axially symmetric less motion of the shells, and entirely neglects calculation concerning torsion motion. The stiffness being constant through the thickness of the shell.

A series solution for the response of an empty submerged spherical shell excited by a plane step-exponential wave was first presented by ***Huang H. et al. [١٨].*** He concluded that the response which was obtained by summing the first eight modes (N=٧) was taken as the measured response. This study represents numerical results for steel spherical shells submerged in water that are either empty or filled with water.

Hayek and Dimaggio [١٩] added peretubation terms to the solution for a spherical shell to determine approximate solutions for the resonance frequencies for submerged prolate spheroidal shell. Numerical results for the first flexural resonance mode were presented for steel shell in water.

Bedrsoian and Dimaggio [٢١] used techniques similar to those used by ***Yen and Dimaggio [١٥]*** , to obtain the response of as prolate spheroidal shell to transient, uniform forcing function. Numerical results for the radial response are given for steel shell with an eccentricity of .٩٨٦ that was submerged in sea water.

Berger B.S. [٢٢] used sanders, shell theory to treat a fluid-loaded prolate spheroidal shell of constant thickness subjected to an arbitrary dynamic loading. The infinite region outside the shell was transformed into a finite region before applying a finite difference method to obtain approximate solution. Numerical results were presented for the acoustic pressure in the response to the application of a spatially uniform ramp-shaped transient forcing function. In all the works cited, except Berger's, the effects of bending resistance were ignored. In Berger's work the effects of transverse shear and rotary inertia are not included.

Burtough C.B. and Magrab E. B. [٢٤] derived the displacement equilibrium equations for the non-symmetric dynamic motion of a prolate shell of constant thickness. They included the effect of bending resistance, transverse shear, rotary inertia and a generalized normal loading applied to the middle shell surface. Galirkin's method was then used to obtain the natural frequencies of the shell for various combinations of physical and geometric parameters.

Concerning related topics, ***Irie T., Yamada G., and Marumoto Y. [٢٥]*** analyzed the free vibration of an elastically or rigidly point supported spherical shell. The deflection displacements of the shell were written in a series of the Legendre functions and the trigonometric functions. The dynamical energies of the shell were evaluated and the frequency equation was derived by Ritz method. The natural frequencies and mode shapes were calculated numerically for a closed spherical shell supported at equi-spaced four points located along a parallel of latitude.

Tavakoli M.S. and Singh R. [٢٦] used a substructure synthesis method based on state space mathematics for the eigen-solution of axisymmetric joined/hermitic shell structures. In the state space method (SSM), a system of differential equations of order eight is solved for each shell substructures using the padre approximation for matrix exponentiation. The substructures are then joined by matching all of the displacement and force boundary variables. The authors applied the state space method to the cylindrical, conical, spherical, and toroidal shell. They compared their results to the results for the same shells by applying the finite element method. The state space method has strengths lies primarily in its ability to join substructures and match the boundery variables comprehensively.

Okazaki, A., Urata, Y. and Tatemichi, A. [٢٧] damping properties of three-layered shallow spherical shells have been studied in this paper. Expressing the in-plane displacements in terms of auxiliary functions, the general solution of the equations of motion for non-axiymmetric modes was given in terms of Bessel's functions. Different shell and plate theories can be used to analyze the sandwich structures.

Zhang P. and Geer T.L. [٢٨] employed convergence-enhancement techniques to obtain series solutions for the response of a fluid-filled or empty submerged spherical shell excited by a plane step-wave; these techniques are partial series closure at early time. Partial series closure consists of separating the early- time response into a closed-form portion and a complementary mode-sum portion. The closed- form portion invokes the plane-wave approximation for the fluid-structure interaction and neglects stiffness effects in the shell.

Zhu F. [٢٩] based upon a general thin shell theory and basic equations of fluid-mechanics; the Rayleigh-Ritz's method for coupled fluid-structure free vibrations is developed for arbitrary fully or partially filled in viscid, irrigational and compressible or incompressible fluid, by means of the generalized orthogonality relations of wet modes and the associated Rayleigh quotients.

Hatim R. Wasmi [٣٠] finite element and modal analysis techniques, where applied to the static and dynamic investigation of oblate spheroidal dishes, prolate and the relevant structures. Different types of elements were considered in one dimension (bar and beam), two dimension (plate) and three dimensions (shell). For framed structures, Euler Bernouilli theory, Tiomshenko theory, integrated Tiomshenko and improved Tiomshenko theories were applied. While for plates and shells, Kirchhoff's, Zienkiewicz and Mindlin

theories were applied. The capability of these trenchancies was investigated in this work to predict the natural frequencies and mode shapes, as well as the static analysis of framed structures and spheroidal dishes. It was found that the natural frequencies of oblate and prolate shells have two types of behavior against increasing the shell thickness and eccentricity, which are the membrane and bending modes. The membrane modes natural frequencies tend to increase with increasing the eccentricity of oblate while the bending mode natural frequencies decrease with increasing the value of eccentricity till they reached the optimum eccentricity.

Michael, Spague and Thomas [٣١] concluded that fluid – structure interaction, underwater shock, Doubly-Asymptotic approximations, Benchmark solutions the title problem is solved through extension of a method previously formulated for plane step-wave excitation, which employs generalized Fourier series augmented by partial closure of those series at early time. The extension encompasses both plane and spherical incident waves with step exponential pressure profiles. The effects of incident-wave curvature and profile decay rate on response behavior are examined. A method previously developed for assessing the discrepancy between calculated and measured response histories is employed to evaluate the convergence of the truncated series solutions. Also then studied the performance of doubly-asymptotic approximations. The documented computer program that produced the numerical results has been published in this paper.

Aleksandr Korjanik et al. [٣٢] investigated the free damped vibrations of sandwich shells of revolution. As special cases the vibration analysis under consideration of damping for cylindrical, conical and spherical sandwich shells is performed. A specific sandwich shell finite element with ٥٤ degrees of

freedom is employed. Starting from the energy method the damping model is developed. Numerical examples for the free vibration analysis with damping based on the proposed finite element approach are discussed. Results for sandwich shells show a satisfactory agreement with various references solutions.

Antoine Chaign et. Al. [٣٣] liner and nonlinear vibrations of shallow spherical shells with free edge are investigated experimentally and numerically and compared to previous studies on percussion instruments such as gongs. The preliminary bases of a suitable analytical model are given. The prime objective of the work is to take advantage of the specific geometry of perfectly isotropic and homogeneous spherical shells in order to isolate the influence of curvature from other possible causes of nonlinearities. Hence, combination resonances due to quadratic nonlinearities are especially studied, for a harmonic forcing of the shell. Identification of excited modes is achieved through systematic comparisons between spatial numerical results obtained from a finite element modeling, and spectral information derived from experiments.

Nawal [٣٤] investigation of the axisymmetric free vibration of an isotropic thin oblate spheroid shells. The analysis depends on two approaches which are the Rayleigh–Ritz's Method and the Boundary Matching Method. Both of the shallow shells and non – shallow shells theories are used for the analysis. Some experiments, which were taken from the literature, are used to improve the theoretical work. The experimental model satisfies the same requirements and conditions of this thesis. Throughout the results, it is shown that when the eccentricity ratio reaches zero, an exact thin sphere solution emerges and when the

eccentricity ratio approaches one an exact thin circular plate solution emerges. Therefore, the eccentricity ratio of an oblate shell at medium value lies between these two values.

The Rayleigh Method is found to be suitable for eccentricities less than ٠.٦, while for the Rayleigh–Ritz's Method and Boundary Matching Method are suitable for all eccentricities.

From the above survey of the available literature related to the vibration characteristics of prolate spheroid shells, it can be concluded that none of the references deals directly with the generality of the problem. Furthermore, only certain approaches are attempted to solve special purpose problems. For the sake of generality of the problem as well as for a special purpose investigation, the following three points (which are not found in the literature) are examined;

١- The Rayleigh - Ritz's method is used to show its validity for such shells.

٢- The effects of variable thickness of the prolate spheroid shells on the free vibration characteristics.

٣- The effect of different boundary conditions at the region of matching such as (clamped –clamped, clamped –free and pinned –pinned) of the prolate spheroidal shell on the free vibration characteristics.

The free vibration characteristics of a thin elastic prolate spheroid shell will be comprehensively examined. Two theoretical approaches will be attempted in this work. The first approach is boundary matching method and the second approach is Rayleigh – Ritz method.

CHAPTER THREE

THORETICAL ANALYSIS

٣. ١ Introduction

The review of literature reveals that even though the differential equations of motion for general shell of revolution are well spelt out, nevertheless, the formulation of these equations for prolate spheroidal shells are available. Therefore, the derivation of these equations will be presented in appendix (A). However, the exact solutions of these equations are unobtainable. Hence, an approximate energy approach will be presented in this chapter.

Furthermore, an exact solution will be tried based on modeling the system under consideration as a structure composed of two open profile spherical shells by matching the continuous boundary conditions. Evidently, the exact solutions for open non – shallow spheroidal shells are available. This will allow a closed form formulation of the undergoing problem as presented in sections (٣.٣) and (٣.٤).

٣. ٢ The Rayleigh – Ritz's Method

Because of the complexity encountered in solving the governing equations of motion given in appendix (A) in a closed form solution, for the problem of prolate spheroidal shell, an approximate energy approach based on Rayleigh – Ritz's Method is used in this section. Rayleigh – Ritz's method can be used for more complex elastic bodies, such as plates and shells. It will be shown that with these methods, elastic bodies which posses an infinite number of degrees of freedom are replaced effectively by an approximate multi – degree of freedom system. This method helps to determine the natural frequencies and their associated mode shapes with general boundary conditions in approximate forms. The continuous systems lend to eigenvalue problems that do not lend themselves to closed form solution, owing to non uniform mass or stiffness distributions. Hence, quite often one is forced to seek approximate solution of the eigenvalue problem. The Rayleigh – Ritz's method may be viewed as an extension of Rayliegh's quotient and used to obtain more accurate estimate. Therefore, Rayleigh quotient, and its extension, the Rayleigh – Ritz procedure, are essentially statements on the ratio of potential energy to the kinetic energy. Physically, it makes sense that this ratio is related to the frequency of oscillation, at the natural frequency (ω), and assuming separation of

variables, the shell displacement may be written in the following forms ***[٢٣]:-***

$$\left.\begin{array}{l} w(\Phi, t) = W(\Phi) \, . \, e^{i\omega t} \\ \text{and} \\ u_{\Phi}(\Phi, t) = U_{\Phi}(\Phi) \, . \, e^{i\omega t} \end{array}\right\} \qquad (٣.٢.١)$$

Substituting these displacements in the strain energy expression gives:

$$U = \int_{-h/2}^{h/2} \int_{0}^{2\pi} \int_{0}^{2\pi} \frac{1}{2} [\sigma_{\Phi} \varepsilon'_{\Phi} + \sigma_{\theta} \varepsilon'_{\theta}] \, R_{\Phi} \, R_{\theta} \sin \Phi \, d\Phi \, d\theta \, dz \qquad (٣.٢.٢)$$

where, the stresses can be written in terms of strains as:

$$\left.\begin{array}{l} \sigma_{\Phi} = \dfrac{E}{(1-\nu^2)} [\varepsilon'_{\Phi} + \nu \, \varepsilon'_{\theta}] \, , \; \sigma_{\theta} = \dfrac{E}{(1-\nu^2)} [\varepsilon'_{\theta} + \nu \, \varepsilon'_{\Phi}] \\ \text{and} \\ \varepsilon'_{\Phi} = \varepsilon^{\circ}_{\Phi} + z k_{\Phi} \quad , \quad \varepsilon'_{\theta} = \varepsilon^{\circ}_{\theta} + z k_{\theta} \end{array}\right\} \qquad (٣.٢.٣)$$

The maximum potential energy $[U_{\max}]$ may be obtained upon taking $e^{i\omega t}$ to be unity and applying the appropriate expressions for $б_{\Phi}$, $б_{\theta}$, ε'_{Φ} and ε'_{θ} as derived in appendix (A), the maximum Potential energy can be written as :

$$U_{max} = \frac{E\,h}{2(1-\nu^2)} \int_0^{2\pi} \int_0^{2\pi} \Big\{ \frac{h^2}{12} \Big[\frac{1}{R_\Phi^2} \Big[\frac{\partial}{\partial\Phi} \Big[\frac{U_\Phi}{R_\Phi} - \frac{\partial W}{R_\Phi\,\partial\Phi} \Big] \Big]$$
$$+ \frac{\cos^2\Phi}{R_\Phi^2\,R_\theta^2\,\sin^2\Phi} \Big[U_\Phi - \frac{\partial W}{\partial\Phi} \Big]^2 + 2\,\nu\,\frac{\cos\Phi}{R_\theta\,R_\Phi^2\,\sin\Phi} \Big[U_\Phi - \frac{\partial W}{\partial\Phi} \Big]$$
$$\frac{\partial}{\partial\Phi} \Big[\frac{U_\Phi}{R_\Phi} - \frac{\partial W}{R_\Phi\,\partial\Phi} \Big] \Big] + \frac{1}{R_\Phi^2} \Big[\frac{\partial U_\Phi}{\partial\Phi} + W \Big]^2$$
$$+ \frac{1}{(R_\theta\,\sin\Phi)^2} (U_\Phi\,\cos\Phi + W\,\sin\Phi)^2$$
$$+ \frac{2\,\nu}{R_\theta\,R_\Phi\sin\Phi} \Big[\frac{\partial U_\Phi}{\partial\Phi} + W \Big] (U_\Phi\cos\Phi + W\,\sin\Phi) \Big\}$$
$$R_\Phi\,R_\theta\,\sin\Phi\,d\Phi\,d\theta$$

(٣.٢.٤)

The kinetic energy is given by;

$$K = \int_{-h/2}^{h/2} \int_0^{2\pi} \int_0^{2\pi} \frac{1}{2}\,\rho \Big[\Big[\frac{\partial U_\Phi}{\partial t} \Big]^2 + \Big[\frac{\partial W}{\partial t} \Big]^2 \Big] R_\Phi\,R_\theta \sin\Phi\,d\Phi d\theta\,dz \qquad (٣.٣.٥)$$

After integrating with respect to (z) and substituting for the appropriate expressions, the maximum kinetic energy will take the form:

$$K_{max} = \frac{\omega^2\rho\,h}{2} \int_0^{2\pi} \int_0^{2\pi} (U_\Phi^2 + W^2) R_\Phi R_\theta \sin\Phi d\Phi d\theta \qquad (٣.٢.٦)$$

the kinetic energy for ω=١ rad/sec is customarily defined as K^*_{max}, and, therefore,

$K_{max} = \omega^٢\ K^*_{max}$

For a system with no dissipation losses, such as those due to friction or damping, the maximum potential energy equals the maximum kinetic energy,

$U_{max} = \omega^٢\ K^*_{max}$

For conservative system, it is obviously known that the maximum kinetic energy is equal to the maximum potential energy. Hence the expression for the natural frequency may be written as:

$$\omega_r^2 = \frac{U_{\max}}{K^*_{\max}} = \frac{N}{D} \qquad r = ١, ٢, ٣, ..., n \qquad (٣.٢.٧)$$

where N and D represent the equations in the numerator and denominator, respectively. Following the procedure of Rayleigh–Ritz's Method, the radial (or transverse) and tangential displacements can be written in power series form as:

$$W(\Phi) = \sum_{i=1}^{n} a_i . W_i(\Phi) \quad , \quad U_\Phi(\Phi) = \sum_{i=1}^{n} b_i . U_{\Phi i}(\Phi) \qquad (٣.٢.٨)$$

where a_i's and b_i's are coefficients to be determined. The functions $W_i(\Phi)$ and $U_\Phi(\Phi)$ satisfy all the geometry boundary conditions of the system. Equation (٣.٢.٧) is an exact expression for the frequency according to Rayleigh quotient. In order to use the procedure of Rayleigh–Ritz's method, equation (٣.٢.٨) is substituted into equation (٣.٢.٤), and (٣.٢.٦), and then the result is used in equation (٣.٢.٧).

Now substituting equation (٣.٢.٨) into equations (٣.٢.٤) and (٣.٢.٦), and after some mathematical manipulations, the following equation will result [appendix B]:

$$\omega_r^2 = \frac{\alpha}{\Psi} \qquad r = ١, ٢, ٣, n \qquad (٣.٢.٩)$$

where,

$$\alpha = \sum_{i=1}^{n}\sum_{j=1}^{n} c_i c_j \frac{E h \pi}{(1-\nu^2)} \int_0^{2\pi} \Big\{ \frac{h^2}{12 R_\Phi^4}\Big[U_{\Phi i} U_{\Phi j} - 2U_{\Phi i} W_i'' + W_i'' W_j''\Big]\sin\Phi$$
$$+ \frac{\nu h^2}{6 R_\theta R_\Phi^3}\Big[U_{\Phi i} U_{\Phi i} - U_{\Phi i} W_i'' - U_{\Phi i} W_i' + W_i W_i''\Big]\cos\Phi$$
$$+ \frac{h^2}{12 R_\Phi^2 R_\theta^2}\Big[U_{\Phi i} U_{\Phi j} - 2U_{\Phi i} W_i + W_i' W_j'\Big]\frac{\cos^2\Phi}{\sin\Phi}$$
$$+ \frac{1}{R_\Phi^2}\Big[U_{\Phi i} U_{\Phi j} + 2U_{\Phi i} W_i + W_i W_j\Big]\sin\Phi$$
$$+ \frac{1}{R_\theta^2}\left[U_{\Phi i} U_{\Phi j}\frac{\cos^2\Phi}{\sin\Phi} + 2U_{\Phi i} W_i \cos\Phi + W_i W_j \sin\Phi\right]$$
$$+ \frac{2\nu}{R_\Phi R_\theta}\Big[U_{\Phi i} U_{\Phi i}\cos\Phi + U_{\Phi i} W_i \sin\Phi + U_{\Phi i} W_i \cos\Phi + W_i W_j \sin\Phi\Big] \Big\}$$
$$R_\Phi R_\theta d\Phi$$

(۳.۲.۹a)

and

$$\Psi = \sum_{i=1}^{n}\sum_{j=1}^{n} c_i c_j \int_0^{2\pi} \rho h \pi \left[U_i U_j + W_i W_j\right] R_\Phi R_\theta \sin\Phi \, d\Phi \qquad (۳.۲.۹b)$$

An n – term finite sum leads to the estimation of the first frequencies. Equations (۳.۲.۹a) and (۳.۲.۹b) give the physical properties of the shell from the stiffness and mass distribution point of view.

The stiffness and mass of the shell are given by the following two equations respectively:

$$k_{ij} = \frac{E\,h\,\pi}{(1-\nu^2)}\int_0^{2\pi}\Big\{\ \frac{h^2}{12\,R_\Phi^4}\Big[U_{\Phi i}U_{\Phi j}-2U_{\Phi i}\,W_i''+W_i''\,W_j''\Big]\sin\Phi$$
$$+\frac{\nu\ h^2}{6\,R_\theta\ R_\Phi^3}\Big[U_{\Phi i}U_{\Phi i}-U_{\Phi i}W_i''-U_{\Phi i}\,W_i\ +W_i'\,W_j''\Big]\cos\Phi$$
$$+\frac{h^2}{12\,R_\theta^2\ R_\Phi^2}\Big[U_{\Phi i}\,U_{\Phi j}-2U_{\Phi i}\,W_i'+\,W_i'W_j'\Big]\frac{\cos^2\Phi}{\sin\Phi}$$
$$+\frac{1}{R_\Phi^2}\Big[U_{\Phi i}\,U_{\Phi j}+2U_{\Phi i}\ W_j+W_i\ W_j\Big]\sin\Phi$$
$$+\frac{1}{R_\theta^2}\left[\ U_{\Phi i}\,U_{\Phi j}\,\frac{\cos^2\Phi}{\sin\Phi}+2U_{\Phi i}\,W_i\cos\Phi+W_iW_j\sin\Phi\right]$$
$$+\frac{2\nu}{R_\Phi\ R_\theta}\Big[U_{\Phi i}\,U_{\Phi i}\cos\Phi+U_{\Phi i}W_i\sin\Phi+U_{\Phi i}W_i\cos\Phi+W_iW_j\sin\Phi\ \Big]\ \Big\}.$$
$$.R_{\ \Phi}R_\theta\,d\Phi$$

(٣.٢.١٠)

and

$$m_{ij}=\int_0^{2\pi}\rho\,h\pi\left[U_iU_j+W_iW_j\ \right]R_\Phi R_\theta\sin\Phi\,d\Phi \qquad (٣.٢.١١)$$

Hence,

$$\omega_r^{\ 2}=\frac{N}{D}=\frac{\sum_{i=1}^{n}\sum_{j=1}^{n}c_i\,c_j\ \ k_{ij}}{\sum_{i=1}^{n}\sum_{j=1}^{n}c_i\,c_j\,m_{ij}} \qquad (٣.٢.١٢)$$

The exact frequency is always smaller than the approximate value. In order to minimize the approximate value, which is given by equation (٣. ٢.١٢), it should be differentiated with respect to c_i and equating the resulting expression to zero, that is:

$$\frac{\partial}{\partial c_i}\left(\frac{N}{D}\right)=\frac{D\,\partial N/\partial c_i\ -\ N\ \partial D/\partial c_i}{D^2}=0 \quad \text{i = ١, ٢, ٣, ..., n} \qquad (٣.٢.١٣)$$

This equation can be satisfied if and only if the numerator equals zero, since D is never equal to zero. The numerator can be written in a more useful form as:

$$\frac{\partial N}{\partial c_i} - \frac{N}{D}\frac{\partial D}{\partial c_i} = 0 \qquad \text{i = ١, ٢. . . n} \qquad (٣.٢.١٤)$$

It is as given by equation (٣. ٢.٧), $\omega_r^{٢}$ = N / D, and n is the number of terms in the approximate solution. The infinite degrees of freedom system has been replaced by an n degree of freedom system. Therefore, Equation (٣.٢.١٣) for i = ١, ٢, can be written in matrix form as:

$$\begin{bmatrix} k_{11}-\omega^2 m_{11} \\ k_{12}-\omega^2 m_{12} \end{bmatrix}$$

$$\begin{bmatrix} k_{12}-\omega^2 m_{12} \\ k_{22}-\omega^2 m_{22} \end{bmatrix} \begin{Bmatrix} c_1 \\ c_2 \end{Bmatrix} = \begin{Bmatrix} 0 \\ 0 \end{Bmatrix} \qquad (٣.٢.١٥)$$

or in general matrix notation as :

$$\left[\{K\}-\omega^2\{M\}\right]\{c\}=\{0\} \qquad (٣.٢.١٦)$$

The evaluation of this determinant of the matrix in eq(٣.٢.١٥) provides the estimation of the first two natural frequencies $\omega_{١}^{٢}$ and $\omega_{٢}^{٢}$. Since two–term approximate solution has been used, it results in a two degree of freedom approximation system ***[٢٣]***.

٣. ٣ Mathematical Modeling (Non – Shallow Shell Theory)

٣. ٣. ١ Formulation of the problem:

The problem of vibration of prolate spheroid shells will be treated in an engineering modeling approach where the prolate spheroid shell is modeled as a structure composed of two spherical shells joined rigidly at their ends. Centers of curvature of the two spherical shell elements fall along the major axis of the proposed prolate spheroid Fig. (٣–١).

Such approximation is not far from reality, as the oblate spheroidal tanks are produced by joining, either by welding or riveting, two spherical shell elements through a toroidal shell element.

The effective radius (R_r) of the spherical shell model represents the radius of curvature at the apex of the shell. This radius can be obtained from the geometrical relation.***[٢٠]***

$$R_{\Phi} = \frac{a(1-e^2)}{(1-e^2\cos^2\Phi)^{3/2}} \qquad (٣.٣.١)$$

Setting (Φ) to zero results the radius of the shell at the apex as:

$$R_r = \frac{a}{(1-e^2)^{1/2}} \qquad (٣.٣.٢)$$

where,

e = ٠ for sphere.

e = ١ for plate.

An approximate opening angle (Φ_0) may be obtained by using the following formula:

$$\Phi_o = \cos^{-1}\frac{R_r - b}{R_r} \qquad (٣.٣.٣)$$

Closer approximate is expected for the exact spheroid and the model at small values of eccentricities. The separable homogeneous solutions to the axisymmetric vibration problem of thin elastic spherical shells including the effects of bending can be obtained from the equations derived in appendix (A) for a prolate spheroid shell by setting the eccentricity ratio to zero. Dividing equations (A.٢.١٢ – A.٢.١٤) by R_r sin Φ results the following equations of motion. $\frac{\partial N_\Phi}{\partial \Phi} + \left(N_\Phi - N_\theta \cot \Phi + Q_\Phi \right) = R_r \rho h \frac{\partial^2 U_\Phi}{\partial t^2}$

(٣.٣.٤)

$$\frac{\partial Q_\Phi}{\partial \Phi} + Q_\Phi \cot \Phi - \left(N_\Phi + N_\vartheta \right) = R_r \rho h \frac{\partial^2 W}{\partial t^2} \qquad (٣.٣.٥)$$

$$\frac{\partial M_\Phi}{\partial \Phi} + \left(M_\Phi - M_\theta \right) \cot \Phi - R_r Q_\Phi = 0 \qquad (٣.٣.٦)$$

(In this case $R_\Phi = R_\theta = R_r$)

The same equations were derived by Naghdi and Kalnins ***[٤],*** as the equations of motion of spherical shells.

Assuming that the temporal and spatial dependence of the free vibration are separable, the displacements may be assumed as ***[٣٤]***:

$$\left.\begin{aligned} u_\Phi (\Phi , t) &= U (\Phi) \cos \omega t \\ w (\Phi , t) &= W (\Phi) \cos \omega t \end{aligned}\right\} \qquad (٣.٣.٧)$$

Where (ω) denotes the circular frequency, t: time and Φ denotes the angle measured from the (vertical axis).

The stress resultants and couples are related to the displacements of the reference surface by the same expressions derived in appendix A of the thesis with the eccentricity set equals to zero.

The free vibration of spherical shells was solved analytically as in ***[١٠].*** In this work considering the actual Φ – dependent coefficient of the variable as those derived in the latter reference which are :

$$W=\sum_{i=1}^{3}\ \left[A_i\ P_{ni}\ (x)+B_i\ Q_{ni}\ (x)\right] \qquad (٣.٣.٨a)$$

$$U_{\Phi}=\sum_{i=1}^{3}\ -(1+\nu)C_i\ \left[A_i\ P'_{ni}\ (x)+B_i\ Q'_{ni}\ (x)\right] \qquad (٣.٣.٨b)$$

$$N_{\Phi}=\frac{E.h}{(1-\nu)R_r}\sum_{i=1}^{3}\ \{\ (1+C_i\ \beta_i).\ \left[A_i\ P_{ni}\ (x)+B_i\ Q_{ni}\ (x)\right]$$

$$+\ (1-\nu)C_i\ \cot\Phi\ \left[A_i\ P'_{ni}\ (x)+B_i\ Q'_{ni}\ (x)\right] \qquad (٣.٣.٨c)$$

$$N_{\theta}=\frac{E.h}{(1-\nu)R_r}\sum_{i=1}^{3}\ \{\ (1+\nu\ C_i\ \beta_i).\ \left[A_i\ P_{ni}\ (x)+B_i\ Q_{ni}\ (x)\right]$$

$$-\ (1-\nu)C_i\ \cot\Phi\ \left[A_i\ P'_{ni}\ (x)+B_i\ Q'_{ni}\ (x)\right] \qquad (٣.٣.٨d)$$

$$M_{\Phi}=\frac{D_b}{R_r{}^2}\sum_{i=1}^{3}\ \left[\ 1+(1+\nu)C_i\ \right]\{\ \beta_i\ \left[A_i\ P_{ni}\ (x)+B_i\ Q_{ni}\ (x)\right]\ +(1-\nu)C_i\ \cot\Phi$$

$$\left[A_i\ P'_{ni}\ (x)+B_i\ Q'_{ni}\ (x)\right] \qquad (٣.٣.٨e)$$

$$M_{\theta}=\frac{D_b}{R_r{}^2}\sum_{i=1}^{3}\ \left[\ 1+(1+\upsilon)C_i\ \right]\{\ \nu\ \beta_i\ \left[A_i\ P_{ni}\ (x)+B_i\ Q_{ni}\ (x)\right]\ -(1-\nu)\cot\Phi$$

$$\left[A_i\ P'_{ni}\ (x)+B_i\ Q'_{ni}\ (x)\ \right]\ \} \qquad (٣.٣.٨f)$$

$$Q_{\Phi} = \frac{D_b}{R_r^{\,2}} \sum_{i=1}^{3} \left[\, 1 + (1+\nu) C_i \,\right] (\nu + \beta_i - 1) \left[A_i \, P'_{ni}\,(x) + B_i \, Q'_{ni}\,(x) \right]$$

(٣.٣.٨g)

where,

$$C_i = \frac{1 + (\beta_i - 2) / \left[(1+\nu)(1+\xi\,) \right]}{1 - \nu - \beta_i + \xi \left(1-\nu^2\right) \Omega^2 / \left(1+\xi^{\,2}\right)}$$

$$\xi = 12 R_r^{\,2} / h^{\,2}$$

$$n_i = -\tfrac{1}{2} + \sqrt{1/4 + \beta_i}$$

x=cos Φ

The parameters β_i's are the three roots of the cubic equation ***[١٠]:-***

$$\beta^{\,3} - \left[4 + (1-\nu^2)\Omega^2 \right] \beta^{\,2} + \left[4 + (1-\nu)\left(1-\nu^{\,2}\right)\Omega^{\,2} + (1+\xi)\left(1-\theta^{\,2}\right) \right]$$

$$\left(1-\Omega^{\,2}\right)\beta + (1-\nu)\left(1-\nu^{\,2}\right)\left[\Omega^{\,2} - \frac{2}{1-\nu} \right] \left[1 + (1+\nu) \left[\Omega^{\,2} - \frac{1}{1+\nu} \right] \right] = 0$$

(٣.٣.٩)

and

$$\Omega^2 = \frac{\rho\, \omega^{\,2} R_r^2}{E}$$

$$D_b = \frac{E\, h^3}{12\ (\,1 - \nu^{\,2}\,)}$$

$P(x), Q_n(x)$ are Legendre functions of the first and the second kinds, respectively $P_n'(x), Q_n'(x)$ are the derivatives with respect to (Φ) of the Legendre functions of the first and the second kinds, respectively. A_i & B_i are arbitrary constants.

The above solutions can be applied to study the free vibration of an elastic spherical shell bounded in general by any two concentric openings. As we are dealing with shells closed at the apex (Φ = ٠), and since the Legendre function of the second kind is singular at that point, then the arbitrary constants (B_i's) are set equals to zero. For this reason, in the remainder of this section all terms involving $Q_n(x)$ is omitted.

The character of the solution given by equations (٣.٣.٨) is strongly dependent on the character of the three indices n ١, n ٢, and n ٣. For the purpose of illustration of the various combinations of complex and real values that the indices may assume, figure (٣–٢) which is extracted from reference ***[١٠]*** shows a plot of n_i (i =١, ٢, ٣) vs. Ω for a given constant value of υ and h / a, the character of n_i varies little with the latter two parameters.

The variation of the characters $n_١$, $n_٢$, and $n_٣$ are given by ***[٤]***:

Zone I

$$n_1 = b_1$$
$$n_2 = b_2 + i b_3$$
$$n_3 = b_2 - i b_3$$

$$n_1 = b_1$$

Zone II $$n_2 = -\tfrac{1}{2} + i b_3$$

$$n_3 = -\tfrac{1}{2} - i b_2$$

$$n_1 = b_1$$

Zone III $$n_2 = b_2$$

$$n_3 = -\tfrac{1}{2} + i b_3$$

Here b_1, b_2, and b_3 are real numbers.

It is clear that for zone I it is appropriate to observe that a pair of Legendre functions have indices which are complex conjugates; they can be written in the form;

$$P_{a\pm b}(\cos\Phi) = R_e\left[P_{a+ib}(\cos\Phi)\right] \pm \mathrm{Im}\left[P_{a+ib}(\cos\Phi)\right]$$

Now, according to the fact that the deflections (W) and (U_Φ) must be real quantities, we must insure that the right side of equation (٣.٣.٨a and b) will also be real. This is accomplished by defining the arbitrary constants according to the scheme.

$A_2 + A^3 = C^2$, $i\,(A_2 - A_3) = C^3$

Hence, the solution takes the form:

$$W = \sum_{i=1}^{3} C_1 P_{b1}(\cos\Phi) + C_2 [\mathrm{Re}\, P_{b2+ib3}(\cos\Phi)] + C_3 [\mathrm{I_m}\, P_{b2-ib3}(\cos\Phi)] \quad (٣.٣.١٠)$$

In this way, the solution in zone I can be expressed in terms of real functions. As for zones II and III it is appropriate to recall that the Legendre functions of the index -١/٢ + ib are called conical functions which are always real quantities.

Also the corresponding values of β_2 and β_3 are real, thus the solution given in the form of equation (٣.٣.٨a and b) is directly applicable.

٣.٣.٢ The Frequency Equation

As stated before the two spherical shell elements are assumed to be rigidly connected along their edge $\Phi=\Phi_o$. To guarantee that the continuity of all deflections, slopes, moments and forces along the function is insured, (selecting the coordinates of the top shell as the reference coordinates) the boundary conditions at the junctions may be written as follows (Fig.(٣ – ١)) ***[٣٤]***:

١ – Kinematics:

$$W_1 - U_{\Phi 2}\sin 2\Phi_0 + W_2\cos 2\Phi_0 = 0 \quad (٣.٣.١١)$$

$$U_{\Phi 1} - U_{\Phi 2}\cos 2\Phi_0 - W_2\sin 2\Phi_0 = 0 \quad (٣.٣.١٢)$$

$$\frac{\partial W_1}{\partial \Phi_1} + \frac{\partial W_2}{\partial \Phi_2} = 0 \quad (٣.٣.١٣)$$

٢ - Equilibrium:

$$- Q_1 - Q_2 \cos 2\Phi_0 - N_{\Phi 2} \sin 2\Phi_0 = 0 \qquad (٣.٣.١٤)$$

$$N_{\Phi 1} - Q_2 \sin 2\Phi_0 - N_{\Phi 2} \cos 2\Phi_0 = 0 \qquad (٣.٣.١٥)$$

$$M_{\Phi} - M_{\theta} = 0 \qquad (٣.٣.١٦)$$

Substituting the terms of equations.(٣.٣.٨a–g) into the boundary conditions results in six homogenous simultaneous equations in terms of the constants which can be written as follows : -

$$\sum_{i=1}^{6} C_{i,K}\,(\Omega).A_{i.k} = 0 \qquad , \qquad k=١,\ldots ٦ \qquad (٣.٣.١٧)$$

where the elements $C_{i,k}$ are functions of Ω. For non trivial solution of the simultaneous equations, the determinant of the coefficients $C_{i,k}$ must vanish, thus

$$\begin{vmatrix} C_{11} & & C_{16} \\ & & \\ C_{61} & & C_{66} \end{vmatrix} = ٠ \qquad (٣.٣.١٨)$$

The resulting determinant equation is the intended frequency equation.

The calculation of the natural frequency is carried out by specifying an initial guessed value (٠.٠١) then evaluating the determinant $\left| C_{i,j} \right|$. Increasing the frequency by small increments and repeating the same procedure until the value of the determinant changes its sign. This

indicates that a natural frequency is expected in the new value. The frequency increment is then minimized and the operation is repeated until the desired accuracy (10^{-5}) of the natural frequency is obtained when the determinant is vanished. The mode shape associated with any natural frequency is then derived by substituting the value of the natural frequency obtained above in equation. (٣.٣.١٨) and normalizing the $[A]$ coefficients to evaluate determining the eigenvectors.

٣. ٤ Computational Procedure

The main purpose of this section is to present the computer programs used in this thesis to obtain the natural frequencies. The programs are written in Quick Basic Language.

١. Matching Boundary Conditions of Two Non – Shallow Spherical Shells:

In this section the main program for finding the natural frequencies of a prolate spheroidal shell is presented and as shown in flow chart fig.(٣-٣).

Input data to the program includes starting the non – dimensional frequency parameter (λst), by which the iterations will start at number of decimal digits of the natural frequency to be found. The eccentricity ratio, major axis, thickness and poison ratio of the material represent the inputs parameters.

The first step is to calculate the effective radius and opening angle of the relative spherical shells model. Then, the non – dimensional frequency

parameter (λ_{st}) is changed to (Ω_{st}) parameter to be used in the process of calculations. The iteration then starts with the starting value of (Ω_{st}) that corresponds to the input parameter (λ_{st}) in the following procedure:-

١. The coefficients of the indicial third order polynomial which are functions of the non dimensional frequency parameter Ω, the poisson's ratio υ, the effective radius R_r, and the thickness h, are first computed eq. (٣.٣.٩).

٢. Calling Siljak subprogram, the real and imaginary roots of the polynomial are calculated. Once, these roots are found, the real and imaginary parts of the Legendre functions indices are calculated eq. (٣.٣.١٠).

٣. Introducing the values of the real and the imaginary parts of the index, along with the value of the opening angle, into the Legendre and the derivative Legendre subprograms, the Legendre function of the first kind and its derivative with respect to the angle (Φ) are calculated using the definition ***[٣٤]***.

$$P_n(\cos\Phi) = F(-n, n+1, 1, \sin^2\Phi/2) \qquad (٣.٤.١)$$

where, F(. . .) is the hypergeometric function, which is evaluated by the following expression: -

$$F(a, b, c, z) = \frac{\Gamma(c)}{\Gamma(a)\Gamma(b)} \sum_{k=0}^{\infty} \frac{\Gamma(a+k)\,\Gamma(b+k)}{\Gamma(c+k)} \frac{z^k}{k!} \qquad (٣.٤.٢)$$

Here Γ (. . .) denotes the Gamma function. The derivative of the Legendre function is determined by differentiating (٣.٤.١) with respect to (Φ).

٤. The displacements, slopes, forces and moments are then determined at the edge ($\Phi=\Phi_o$) of the spherical shells using eq. (٣.٣.٨).

٥. The values equated in (٤) above are then substituted in the following determinant of the boundary matched conditions:-

$$\begin{vmatrix} C_{1,1} & .. & .. & . -C_{2,1}\sin 2\Phi_0 + C_{1,1}\cos 2\Phi_0 & .. & .. \\ C_{2,1} & .. & .. & . -C_{2,1}\cos 2\Phi_0 - C_{1,1}\sin 2\Phi_0 & .. & .. \\ C_{3,1} & .. & .. & . \ C_{3,1} & .. & .. \\ C_{4,1} & .. & .. & . -C_{4,1}\cos 2\Phi_0 - C_{5,1}\sin 2\Phi_0 & .. & .. \\ -C_{5,1} & .. & .. & . \ C_{4,1}\sin 2\Phi_0 - C_{5,1}\cos 2\Phi_0 & .. & .. \\ C_{6,1} & .. & .. & . -C_{6,1} & & \end{vmatrix}$$

where,

C(١ , i) = $P_{nI}\ (\cos\Phi)$

C(٢ , i) = - (١ + ν) C$_I$ $P'_{nI}\ (\cos\Phi)$

C(٣ , i) = $P'_{nI}\ (\cos\Phi)$

C(٤ , i) = $\frac{h^3}{12(1-\nu^2).R_r^3}\left[1+\left((1+\nu)C_I\right).(\nu+\beta_I-1).\left(P'_{nI}\ (\cos\Phi)\right)\right]$

C(٥ , i) = $\frac{h}{(1-\nu).R_r}\left[\left(1+C_I\ .\beta_I\right).P_{nI}\left(\cos\Phi_o\right)+(1-\nu).\cot\Phi.C_I\right.$

$\left.\ .P'_{nI}(\cos\Phi)\right]$

C(٦ , i) = $\frac{h^3}{12(1-\nu^2).R_r^2}\left(1+(1+\nu)C_I\right)\ \left[\beta_I\ \left(P_{nI}\ (\cos\Phi)\right)\right.$

$\left.+(1-\nu).\cot\Phi_o\ .P'_{nI}\ (\cos\Phi_o)\right]$

where,

All the above symbols are the same as mentioned in section (٣. ٣), I= ١, ٢, ٣ [***١٠].***

٦. The value of the determinant in (٥) is then evaluated, and recorded by using the hardware of the computer. Then the computations are repeated for the next value of (Ω) and the value of the determinant is compared to the value of the previous run. If, however, the sign of the value changes i.e., from positive to negative sign, a natural frequency is expected to occur between the two successive values of (Ω). Thus, the step of iteration is divided by ten and the operation is repeated until the non dimensional natural frequency with the needed accuracy is found.

٢. The Rayleigh Ritz's Energy Method of Two Non – Shallow Spherical Shells:

The computation process in this section is nearly identical to the section (١); the calculation here follows the solution presented section in (٣.٢).

The stiffness and mass are then determined at the edge ($\Phi=\Phi_o$) of the spherical shells using (Eqs. ٣.٢.١٠, ٣.٢.١١) respectively.

The values equated in the above equations are then substituted in the following determinant:

$$\begin{vmatrix} k_{11}-\Omega^2 m_{11} & k_{12}-\Omega^2 m_{12} & k_{13}-\Omega^2 m_{13} \\ k_{21}-\Omega^2 m_{21} & k_{22}-\Omega^2 m_{22} & k_{23}-\Omega^2 m_{23} \\ k_{31}-\Omega^2 m_{31} & k_{32}-\Omega^2 m_{32} & k_{33}-\Omega^2 m_{33} \end{vmatrix} = ٠$$

The same procedure of point (٦) in the section (٣.٤.٢) is repeated until a natural frequency is found

٣.٥ Finite Element Method

The finite element method is a tool with which the perform stress and vibration analysis of mechanical system and structures. Can be performed a typical finite element analysis requires the following information for analysis:-

١-Nodal point.
٢-Structural elements that connect the nodal points, representing the stiffness of the structure.
٣-Mass properties of the structure.
٤-Boundary conditions or structure restraints.
٥-Static or dynamic load specification.
٦-Analysis options.

The finite element method has been used to solve complex aerospace, automatic, civil, and mechanical systems and strictures.

In finite element method, mechanical system and structure are discrtized. They are represented by discrete grid or node points connected by structural element.

In actuality, however, such system or structures are continuous entities, without physically defined grid boundaries.

The finite element method is a discrete representation of a continuous physical system made in order to simulate its structural

behavior. In the present work the finite element method used to obtain of results for frequency as Ansys package.

The representation is in the form of a mathematical model consisting of discrete element connecting discrete nodal points. Coefficients of the mathematical model are automatically computed based on the geometric dimensions and physical properties of the system being represented.

There is a rule generally applied to discreization"the more node points, the more accurate the solution". Many texts have shown that a more exact answer for simple problems is achieved through the use of more mode points. If the aim of the analyst is detailed stress analysis, then nodal density must be increased in region of large stress gradients. If the aim of the analyst is deflection analysis only, then fewer nodes may be used than would other wise be required for stress analysis. Normal mode problems have discreization requirements similar to those of deflection analysis.

Normal mode analysis:-

The principal advantage of the finite element method is its generality. It can be used to determine the natural frequency and mode shapes of any linear, elastic structure. It is limited only by the size of the computer available and the desired accuracy.

Normal mode analysis has several users first, the modes are used to solve for the transient response for system and structures. Secondly normal mode analysis yields insight into the dynamic behavior of the system and structure, under any type of dynamic loading. Knowing the

lowest few resonant frequencies and mode shapes can often aid in spotting potential are as for redesign to better with stand dynamic loading.

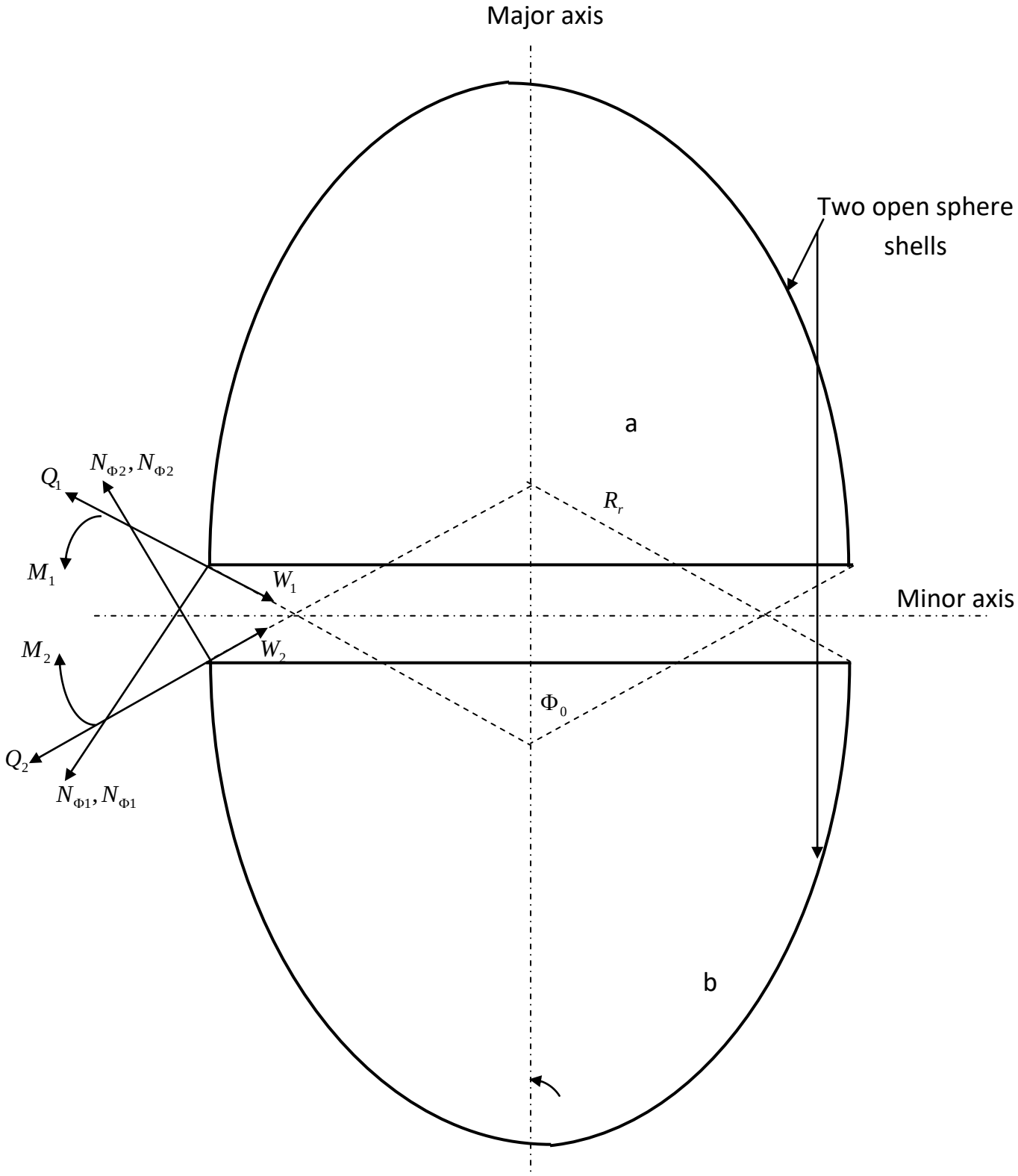

Fig. (٣-١): Matching Boundary Conditions of Two Non-Sallow Spherical Shells Elements

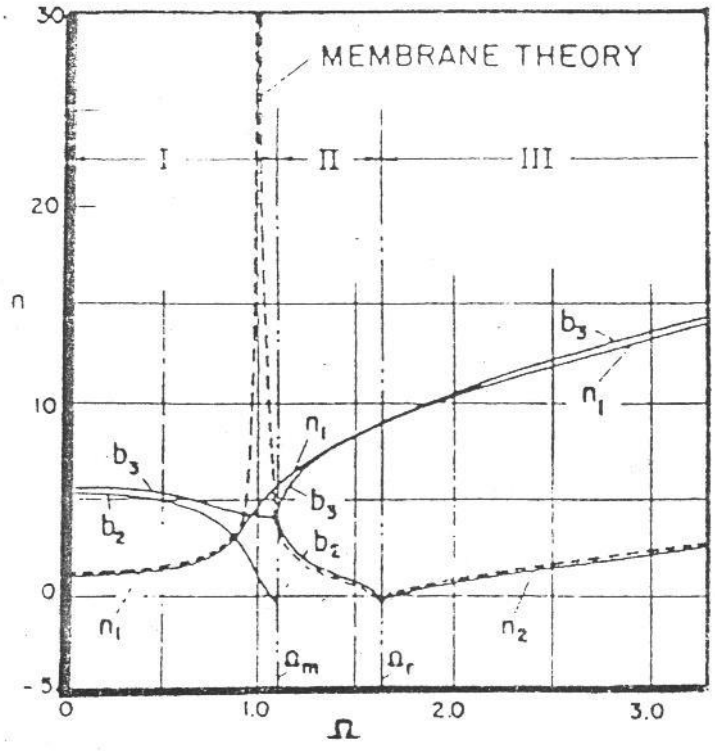
MEMBRANE THEORY
I
II
III
30
20
10
0
-5
n
0
1.0
2.0
3.0
Ω
b_3
b_2
n_1
n_2
Ω_m
Ω_r

Fig. (٣-٤) [illegible]

(Ω)

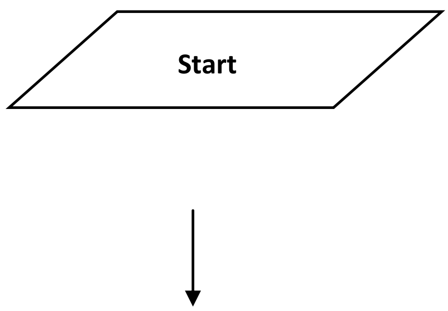

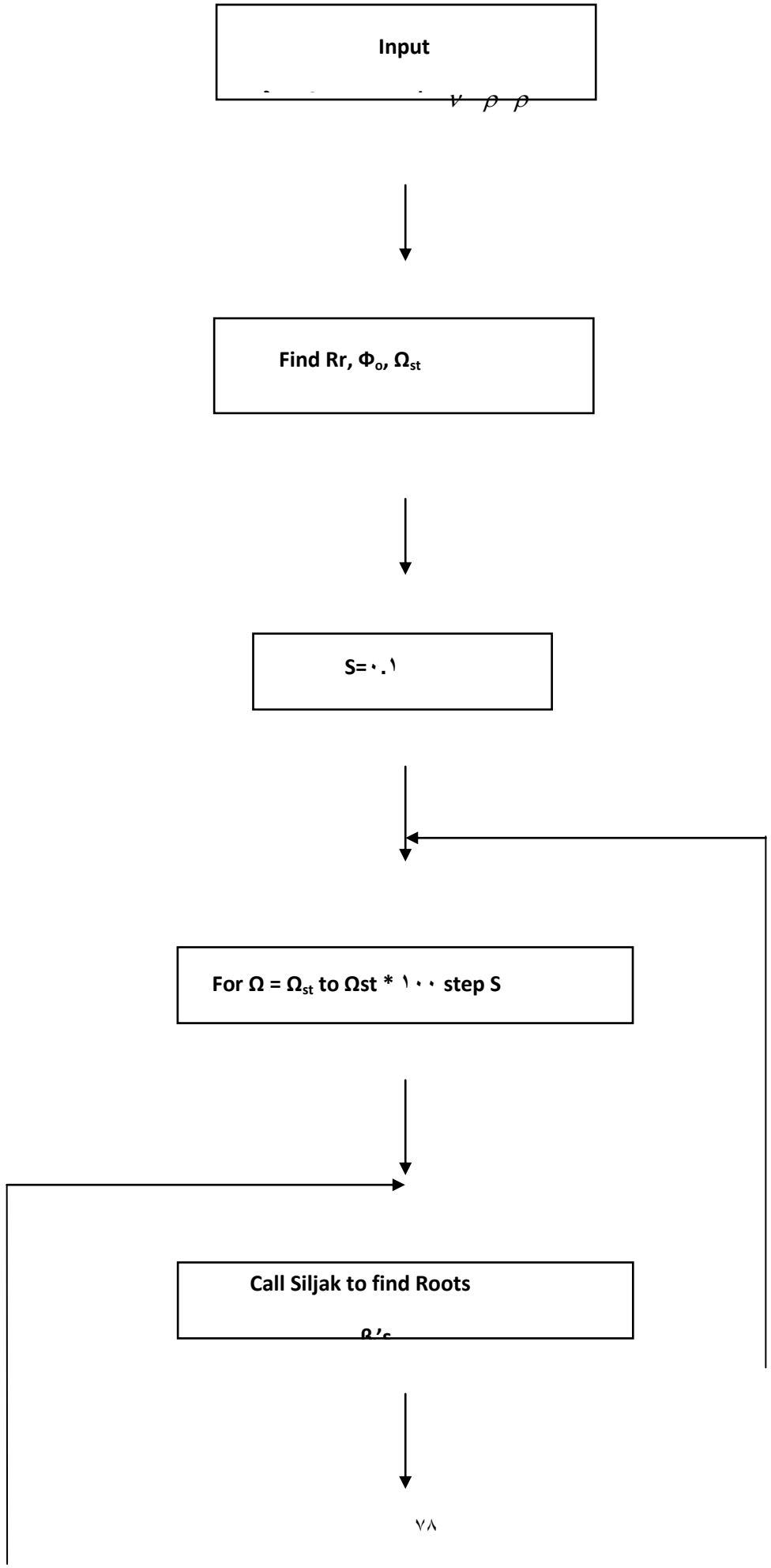
Input
Find Rr, Φo, Ωst
S=٠.١
For Ω = Ωst to Ωst * ١٠٠ step S
Call Siljak to find Roots

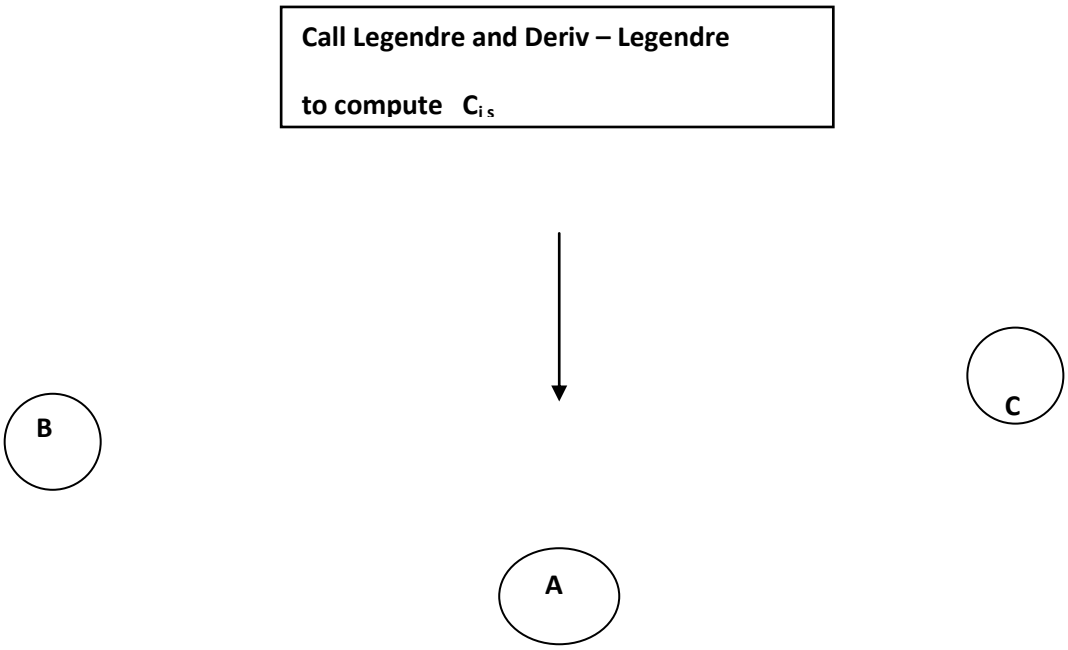

Fig.(٣–٣): Flow chart of non – shallow spheroidal shell. . . . Continue

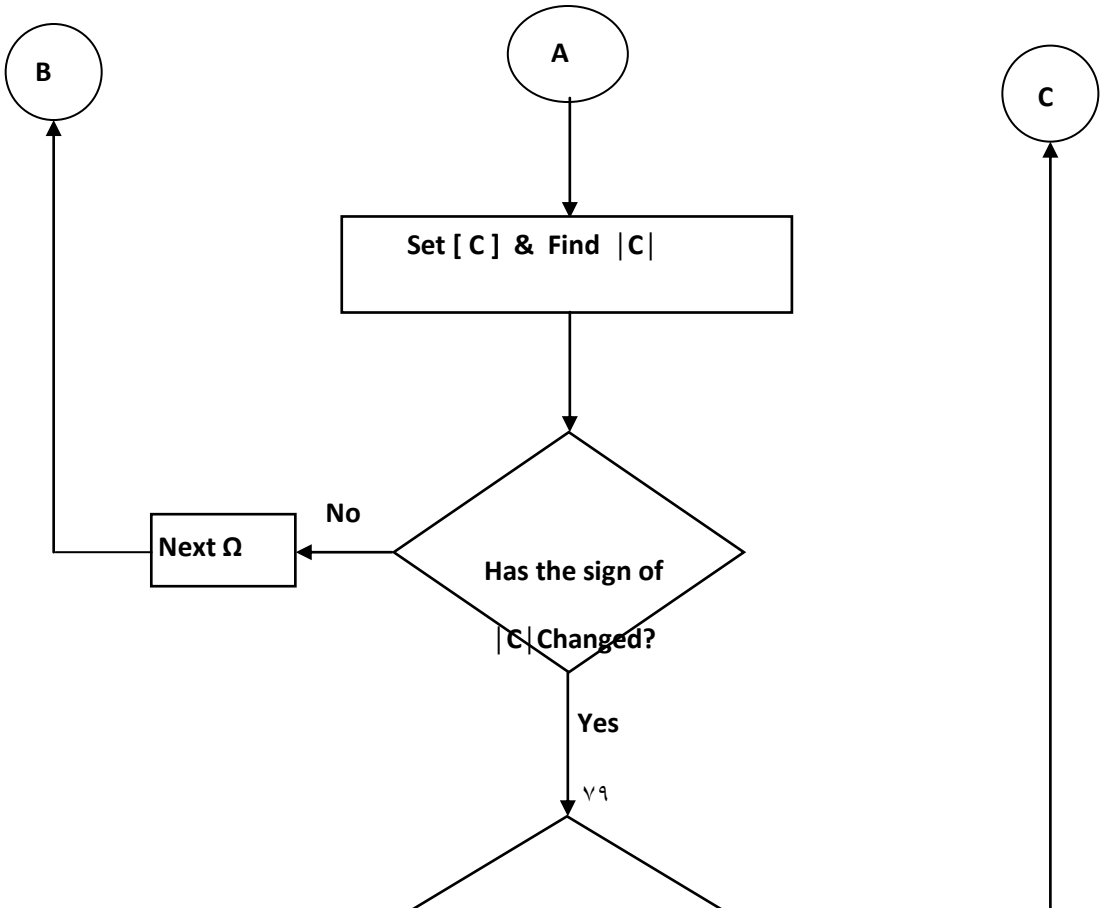

Is

The natural frequency within accuracy?

No

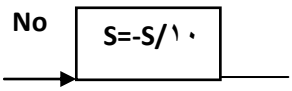

Compute λ

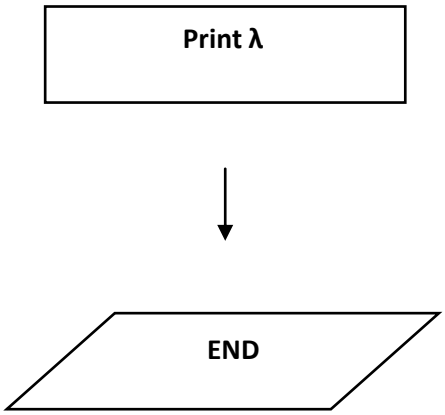

CHAPTER FOUR

RESULTS AND DISCUSSION

٤. ١ Introduction

In this work a comprehensive study of a dynamic analysis on a prolate spheroidal shell with various eccentricity ratios (٠- ٠.٩).

In this chapter the results obtained from the solution of the governing equations presented in chapter three are discussed and compared with that published in literatures.

The aim of this study is to determine active a general methods for dealing with the dynamic problem of a prolate shell under various boundary conditions and to investigate the effect of variable thickness ratio on the dynamic analysis of a prolate shell.

٤. ٢ Validity of The Employed Methods

The lack of numerical results in the literature and complexity of obtaining a closed form solution for the free vibrational characteristics of a prolate spheroid oblige us to seek alternative approaches for justifying the feasibility of the theoretical methods used in this thesis such as Rayleigh-Ritz method and Boundary matching method.

Eventually, these methods are general and may be used for any physical and geometrical parameters of the prolate spheroid. Therefore, the natural frequency for a thin sphere which is considered as an ultimate shape of the prolate spheroid may be determined by using these methods and the results are compared with the available literature.

Table (٤-١) shows the natural frequency of the first three axisymmetric modes of a full sphere of (٠.١١٤٣m) radius and (٠.٠٠٥٧) m thickness with material properties of E=٢٠٧ GPa, ρ = ٧٨٠٠ kg/m^{٣} and ν = ٠.٣.

These frequencies were obtained from applying the finite element method (FEM) where fourty elements axisymetrical models were used *[٧]*, and that obtained from the Raleigh-Ritz method (RRM) and the boundary matching method (BMM).

The results corresponding to zero eccentricity ratio in equation (٣.٣.١) and the boundary matching method were applied to two hemispherical shell elements.

From this table, it can be perceived that the (RRM) and (BMM) give the natural frequencies within the computational error of the used computers.

Also it can be seen that the Raleigh – Ritz's method predicts frequencies higher than the other methods given in the table. This fact is inherited to this method for its higher bounds prediction, however, it may be stated from this table that the two methods of solution presented in this work are dependable and may

be used for other shell geometrical and physical parameters because can used this methods for plate or any type of shells.

Table (٤-٣) shows the natural frequency of the first three modes of a prolate spheroid with variable values of eccentricity have dimensions and properties specification in table (٤-٢).

From this table it can be perceived that the RRM and BMM give natural frequencies with in the computational error of the used computers.

Also it can be seen that the finite element give results between the two methods and it was closed to the BMM but to governed on the batter method the approximate results predict that from the using methods.

Figure (٤-١) shows that the non-dimensional frequencies of the first three modes of vibration as a function of the eccentricity obtained by RRM for prolate of eccentricities (٠-٠.٣).

Figures (٤-٢, ٤-٣ and ٤-٤) show the natural frequency increase with increasing the eccentricity. Also it is indicated that the curve obtained by RRM, adjoin to that obtained by ANSYS for eccentricity is less than ٠.٢, but for large than that difference is increased because the difference is become (٠.١٩) percent for eccentricity (٠.٤) this indicated that the error large at increase the eccentricity for this reason and from this results obtained from this work this method give the accuracy results at eccentricity for sphere or shape closed to sphere (e < ٠.٣).

٤.٣ Comparison between RRM and BMM

Figure (٤-٥) shows the non-dimensional natural frequencies $(\lambda = \sqrt{\rho / E}\omega a)$ of the first three modes of vibration as functions of the eccentricity obtained by the Raleigh - Ritz's method and the boundary matching method using the non – shallow shell theory. This figure shows clearly that the natural frequency increased with increasing the eccentricity. Also it is indicated that the curve obtained by the Raleigh – Ritz's method, adjoin to that obtained by the boundary matching method, although with slightly higher value for all values of eccentricity.

This behavior could be explained by the fact that the mode shapes of a closed spherical shell would resemble those of a prolate spheroid up to certain eccentricity. As the eccentricity increase the bending stresses increased and the potential energy increase. Another reason that the geometry of the prolate shape becomes stiffer than the spherical shape.

٤.٤ Effect of Radius to The Thickness Ratio of Shell on The Natural Frequency

In prolate spheroidal shells the radius to the thickness ratio is defined as the shell thickness (h) to the major semi axis length (a). Figures (٤-٦) and (٤-٧) give the first few natural frequencies as function of the thickness ratio for a prolate spheroid with (e=٠) obtained by the BMM and RRM respectively. However, Fig. (٤-٨) shows the results given by Kalnins *[١٠]* for complete

sphere. The three figures are in a good agreement and justify very well the validity of the method used in this thesis.

Figures (٤-٩, ٤-١٠, ٤-١١ and ٤-١٢) show the first few natural frequencies as a functions of radius to the thickness ratio with (e=٠.٣) and (e=٠.٧) respectively and (ν =٠.٣). They figures show the bending as well as the membrane modes using the non-shallow shell theory. It can be noted that the variation of the natural frequency of the bending modes increases with increasing the thickness and with the mode number. This phenomenon can be elaborated due to the fact that the strain energy increased with increasing the thickness ratio. Also, for larger eccentricities, the variations are more pronounced than that for smaller eccentricities. Since the membrane modes occur at relatively higher values of the non – dimensional frequency parameter value (λ) in comparison with the first bending modes, the variation of only few of the membrane modes with the thickness ratio are investigated.

It can be concluded that the membrane modes have small variation – if no variation at all – with thickness ratio. This can be further explained by considering the strain energy expression of the two spherical shell elements.

If the strain energy due to the stretching of the middle surface of the shell is represented by u_m and due to the bending of the shell by u_b where, ***[١٠]***

$$u_m = \frac{E\,h\,\pi\,R_\Phi^2}{1-\nu^2}\int_0^{\Phi_0}\left(\varepsilon_\Phi^2 + 2\nu\,\varepsilon_\Phi\,\varepsilon_\theta + \varepsilon_\theta^2\right)\sin\Phi\;d\Phi \qquad (٤.٤.١)$$

$$u_b = \frac{E\,h^3\,\pi\,R_\Phi^2}{1-\nu^2}\int_0^{\Phi_0}\left(k_\Phi^2 + 2\nu\,k_\Phi\,k_\theta + k_\theta^2\right)\sin\Phi\;d\Phi \qquad (٤.٤.٢)$$

For membrane modes, the stretching effect strain energy is dominant as given by equation (٣.٢.٧) while for bending modes; the bending effect on strain energy is dominant.

To get some quantitative feeling of this fact consider a complete sphere (a prolate spheroid with zero eccentricity) with thickness ratio of (٠.٠٥).

Let $(\eta = u_b/(u_b + u_m))$ which represents the ratio of the bending strain energy to the total strain energy, the numerical values of (η) for the first and second bending modes and for the first membrane mode are:

First bending mode = ٠.٠١٥

Second bending mode = ٠.٢٨٣

First membrane mode =٠.٠٠٠

Eventually, these values elaborate the preceding explanation, for further illustration of the effect of thickness on the bending modes.

٤.٥ The Effect of Eccentricity on Natural Frequencies

One of the main indices of a prolate spheroid is its eccentricity (e), which is defined as:

$$e = \left[1 - \frac{b^2}{a^2}\right]^{1/2} \qquad (٤.٥.١)$$

Where,

a and b represent the major axis and minor axis respectively.

To study the effect of the eccentricity on natural frequencies, the two classified modes, namely the bending model (in which the bending strain energy is dominant) and the membrane model (in which the stretching strain energy is dominant), will be referred to. Taking this into consideration, Figs (٤-١٣, ٤-١٤ and ٤-١٥) illustrate the boundaries of the first three bending modes and the first membrane mode respectively as functions of eccentricity (e). It may be observed from figures (٤-١٣) and (٤-١٤) that as the eccentricity increased, the bending stress increased and the potential energy increased. On the other hand Fig (٤-١٥) shows the effect of eccentricity on the first membrane mode obtained by the RRM and BMM. It is seen that the natural frequency increase with increasing the eccentricity. The eccentricity effects on the natural frequency hardly at the lower range, while this effect decreased where the eccentricity beyond ٠.٨. .

Figures (٤-١٦ through ٤-٢١) explain the ratio of the maximum values of transverse and longitudinal displacements of the bending modes for the prolate spheroidal shell has eccentricity ratio (e=.٧٠٧). These results obtained by two method (RRM and BMM), from this figures it can be seen that, the first mode increases with the increase of the angle (Φ), and for the second mode the displacements (w and u) move to the left were decreased with increasing the angle (Φ) for the third mode, where the first node for the second mode at 27^0 but first node for the third mode at 18^0.

٤.٦ The Effect of The Thickness Variation on Natural Frequency

The thickness variation is given by;

$$h = t_b\left[1-\alpha(R_\Phi / b)\right] \quad , \quad \alpha = 1-(t_a / t_b) \qquad (٤.٦.١)$$

where,

t_a : thickness of shall at $\Phi = 90$

t_b : thickness of shall at $\Phi = 0$, Fig.(A٣)

Figures (٤-٢٢ and ٤-٢٣), show the non-dimensional frequencies of the prolate shell as a function of the ratio (t_a / t_b) according to the RRM. It is show that when the ratio (t_a / t_b) increased the natural frequency increased because the increasing in thickness cause the increase in strain energy.

Figure (٤-٢٤) shows the effect of thickness ratio (t_a / t_b) on the value of the non-dimensional natural frequency for eccentricity (e=٠.٧). It is seen that the ratio of thickness (t_a / t_b) has lifting the natural frequencies to higher value. This behavior can be elaborated as follows; as the thickness at the $\Phi = 90$ increased the bending is increased and the shell becomes stiffer as the natural frequency proportional the bending therefore, the natural frequency will increased.

Figures (٤-٢٥, ٤-٢٦ and ٤-٢٧) show the mode shapes for the prolate spheroidal shell with the thickness variation $(t_a / t_b = 2)$, for eccentricity =٠.٧.

Figures (٤-٢٨, ٤-٢٩ and ٤-٣٠) show the comparesions of mode shape for different thickness ratio this figures indicated that the deformation directed to the region for lower stiffer when increase in thickness ratio cause increase the strain energy i.e. increase the stress in this region.

٤.٧ The Effect of Boundary Conditions on Natural Frequencies

Figures (٤-٣١, ٤-٣٢ and ٤-٣٣) show the non-dimensional natural frequencies $(\lambda = \sqrt{\rho / E}\omega a)$ of the first three modes of vibration as functions of

the eccentricity obtained by using the matching of boundary method for various boundary conditions.

It is well indicated that the three figures obey the previous observation of the effect of eccentricity on bending modes. However, it is further observed that the curve of clamped-clamped boundary conditions in the three figures predicts higher values than the other two curves for other boundary conditions. This is attributed to the fact that the structure for clamped-clamped of boundary conditions are in general stiffer than the structure for the other two boundary conditions due to the consideration at the clamps because when the region is clamped tend to the increase the stiffness in this region this cause increase in strain energy .

Figures (٤-٣٤, ٤-٣٥ and ٤-٣٦) show the mode shapes for clamped – free boundary conditions with eccentricity =٠.٧ when compare this figures with figures (٤-١٦, ٤-١٧ and ٤-١٨)it is show that the curve of the radian displacement (W) direct to the right i.e. the deformed direct to the region lower stiffer .

Table (٤-١): Natural frequencies (Hz) of the first three axisymmetric modes of thin sphere.

R=٠.١١٣ m, h =٠.٠٠٥٧ m, E = ٢٠٧ GPa, ρ = ٧٨٠٠ kg/m^{٣}, υ = ٠.٣

n	FEM[١]	RRM[٢]	BMM[٣]	$\delta_{١}$%	$\delta_{٢}$%
٢	٥٣٨٣	٥٣١٥	٥٢٨٦	٠.٠١	٠.٠١
٣	٦٣١٩	٦٥١٣	٦٣١٩	٠.٠٣	٠

٤	٦٨٧٥	٦٩٥٠	٦٨٨٣	٠.٠١	≈ ٠.٠

(١) Finite element method [٣٠] .

(٢)Raleigh – Ritz method [present work].

(٣) Boundary matching method [present work].

δ_1 = (FEM – RRM)/FEM*١٠٠

δ_2 = (FEM – BMM)/FEM*١٠٠

Table (٤-٢): Specifications of the tested models

Parameter	Symbol	Value	Units
Major semi axis	a	٠.٣	m
Minor semi axis	b	٠.٢١٢١	m
Eccentricity	e	٠.٧٠٧	N.D
Normal thickness	h	١.٥*١٠$^{-٣}$	m
Poisson ratio	υ	٠.٣	N.D
Modulus of Elasticity	E	٦٨	GPa
Density	ρ	٢٧٢٠	kg/m^{٣}

Table (٤-٣): Theoretical natural frequency (Hz) compared with Ansys results

a\ Prolate spheroidal shell have (e=٠)

	RRM	BMM	ANSYS	δ_1%	δ_2%
W١	١٢٥٠	١١٥٠	١١٧٨	.٠٥	.٠٣
W٢	١٥٠٠	١٣٨٣.٣	١٤٥٤.٧	.٠٣	.٠٤
W٣	١٨٣٣.٣	١٦٩٣.٣	١٨١٧.٨	.٠٠٨	.٠٨

b\ Prolate spheroidal shell have (e=٠.١)

	RRM	BMM	ANSYS	δ_1%	δ_2%
W١	١٣٣٣.٤	١٢٦٦.٧	١٢٩٩	.٠٢	.٠٢
W٢	١٨٣٣.٣	١٦٦٦.٧	١٧٦٧.٥	.٠٣	.٠٥
W٣	٢٠٠٠	١٨٥٠	١٩٢٩.١	.٠٣	.٠٤

c\ Prolate spheroidal shell have (e=٠.٢)

	RRM	BMM	ANSYS	δ_1%	δ_2%
W١	١٥٠٠	١٣٦٦.٧	١٤٢٨.٧	.٠٤	.٠٤

W٢	١٩٨٣.٤	١٨٦٦.٧	١٨٩٧.٨	.٠٤	.٠١
W٣	٢٣٣٣.٤	٢٠٨٣.٤	٢١٨٨.٦	.٠٦	.٠٤

d\ Prolate spheroidal shell have (e=٠.٣)

	RRM	BMM	ANSYS	δ_1%	δ_2%
W١	٢٦٦٦.٧	٢٥٦٦.٧	٢٤٦٩.١٧	.٠٨	.٠٤
W٢	٥٠٠٠	٤٨٨٣.٤	٤٥٨٧.١	.٠٩	.٠٦
W٣	٦١٦٦.٦	٥٩٦٦.٦	٥٥٥٥.٥	.١١	.٠٧

e\ Prolate spheroidal shell have (e=٠.٣٥)

	RRM	BMM	ANSYS	δ_1%	δ_2%
W١	٣٥٠٠	٣٣٣٣.٣	٣٢١١	.٠٩	.٠٤
W٢	٥٨٣٣.٣	٥٧٥٠	٥١٦٢.٢	.١٣	.١١
W٣	٧١٦٦.٦	٦٩١٧.٧	٦٢٣١.٨	.١٥	.١١

f\ Prolate spheroidal shell have (e=٠.٤)

	RRM	BMM	ANSYS	δ_1%	δ_2%
W١	٤٣٣٣.٣	٤١٦٦.٧	٣٨٠١.٢	.١٤	.١
W٢	٦٨٣٣.٤	٦٦٦٦.٧	٥٨٩٠.٤	.١٦	.١٣
W٣	٨٠٠٠	٧٨٣٣.٤	٦٧٢٢.٧	.١٩	.١٦

δ_1= (ANSYS-RRM)/ANSYS*١٠٠

δ_1= (ANSYS-BMM)/ANSYS*١٠٠

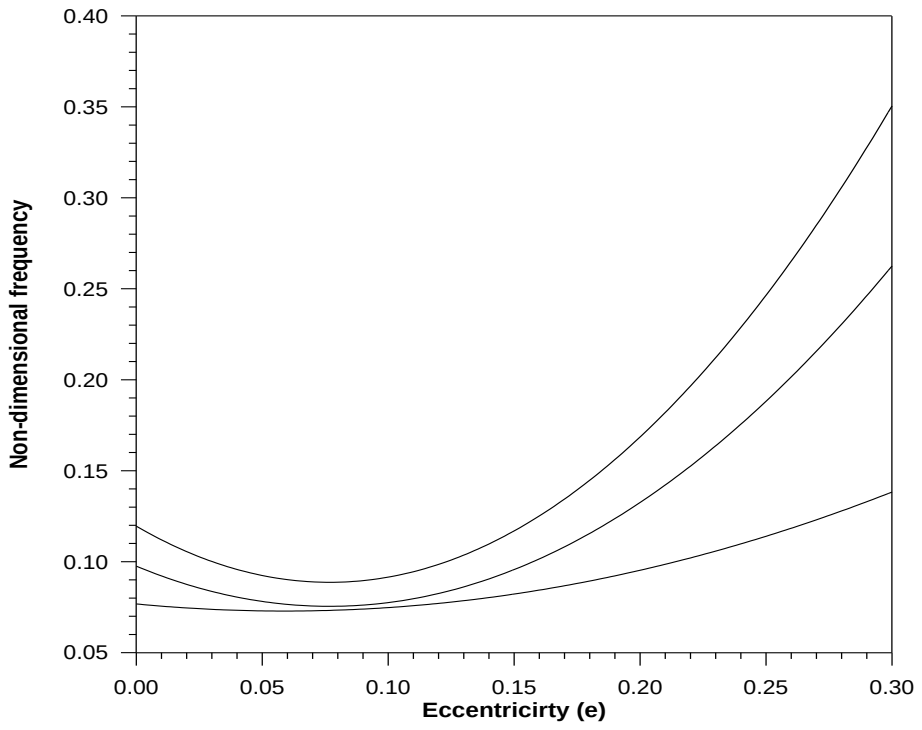

Fig. (٤-١): Effect of eccentricity ratio on the first three bending modes of vibration for prolate closed to sphere.

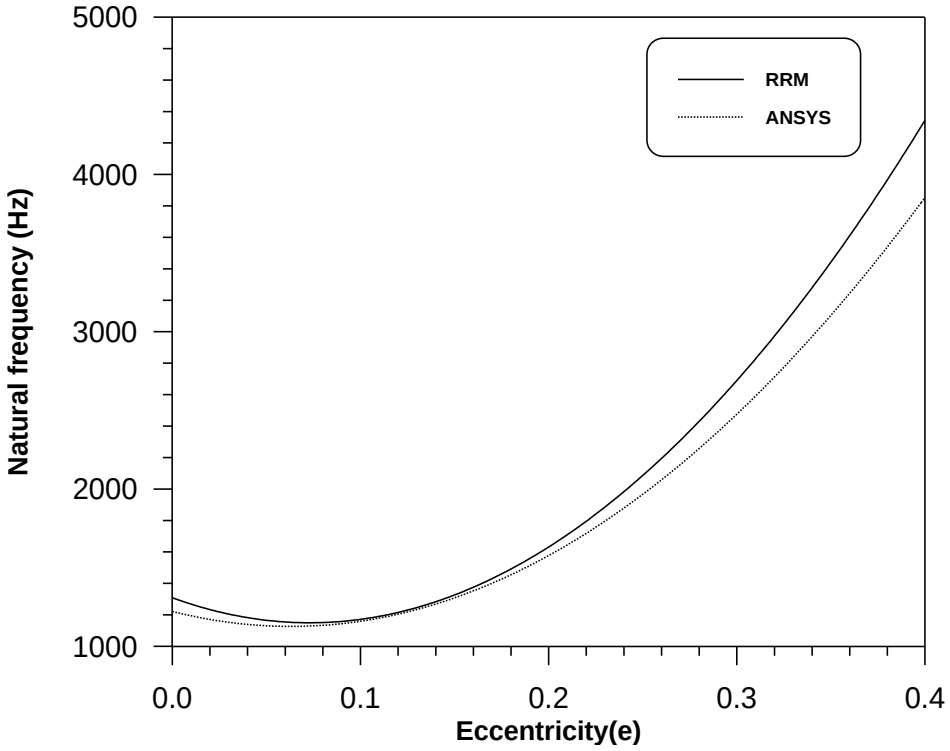

Fig.(٤-٢): Effect the eccentricity on the first model

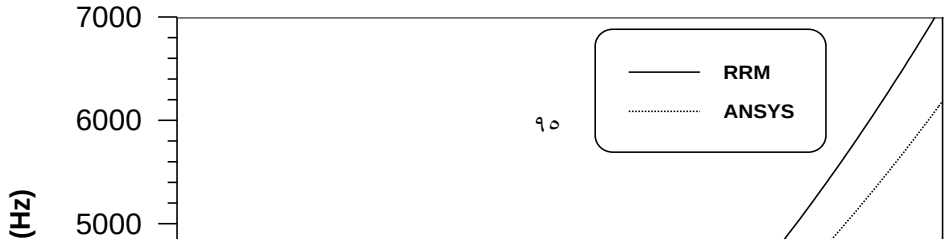

Fig.(٤-٣): Effect the eccentricity on the second mode

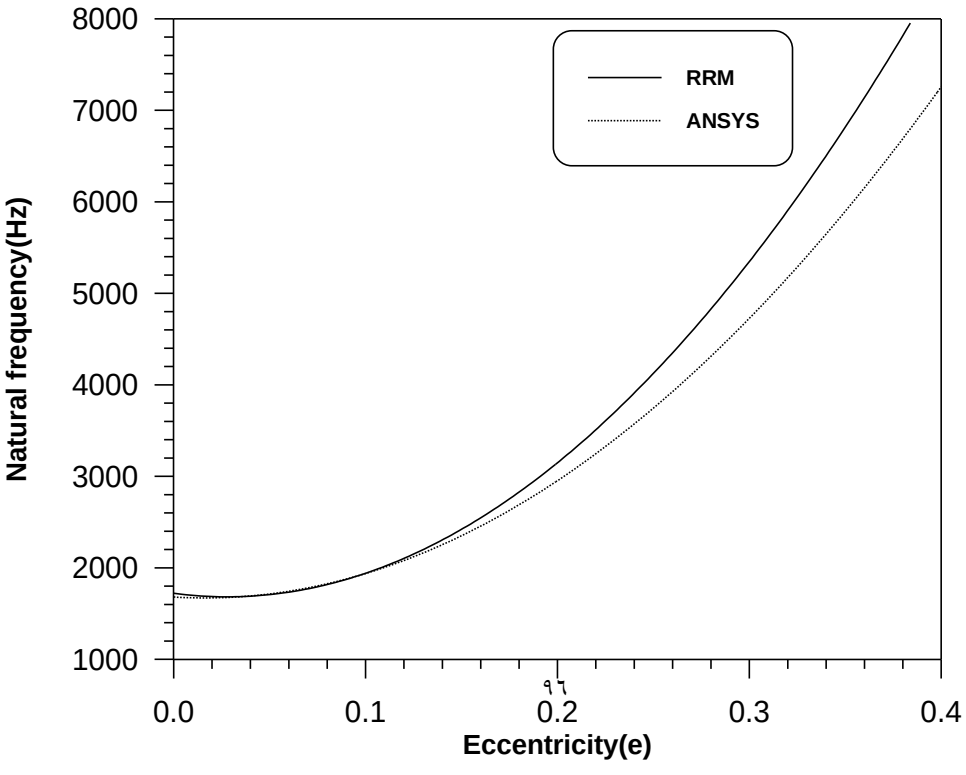

Fig.(٤-٤): Effect the eccentricity on the third mode

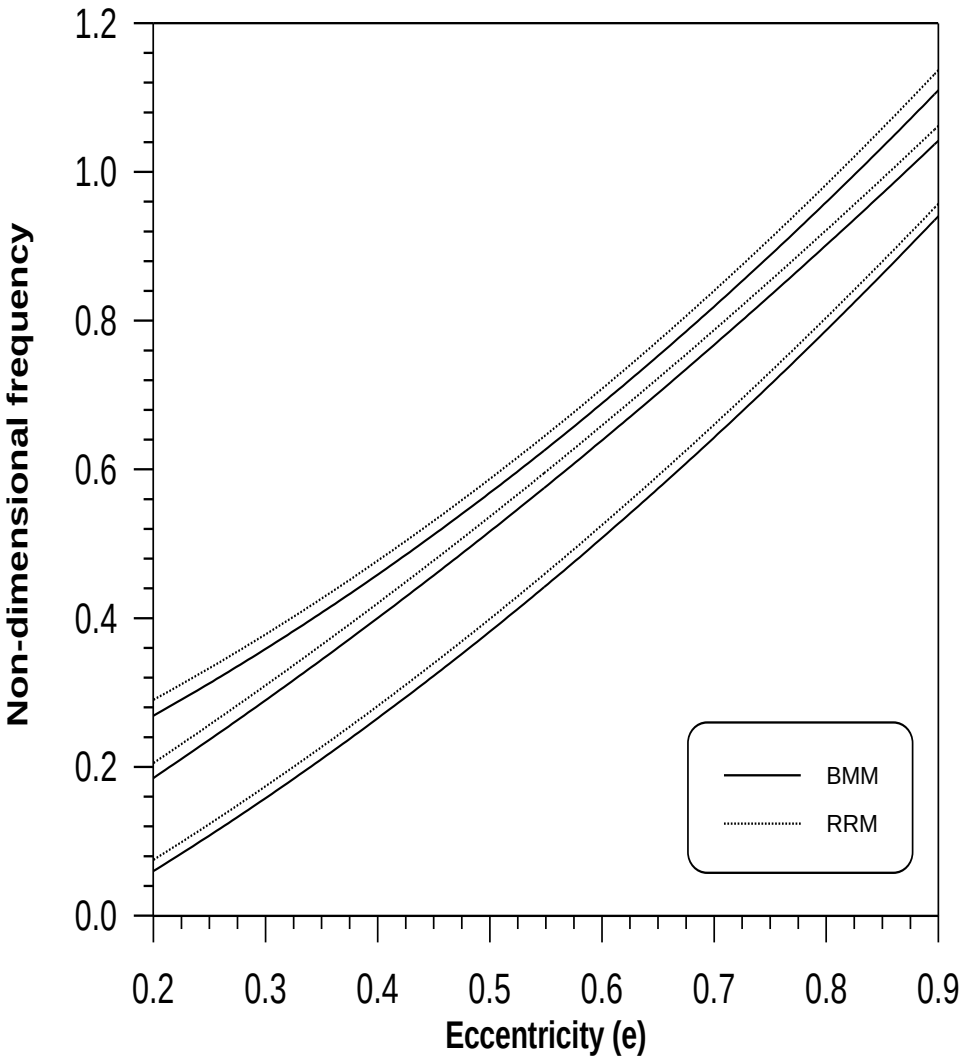

Fig. (٤-٥): Effect of eccentricity ratio on the first three bending modes of vibration

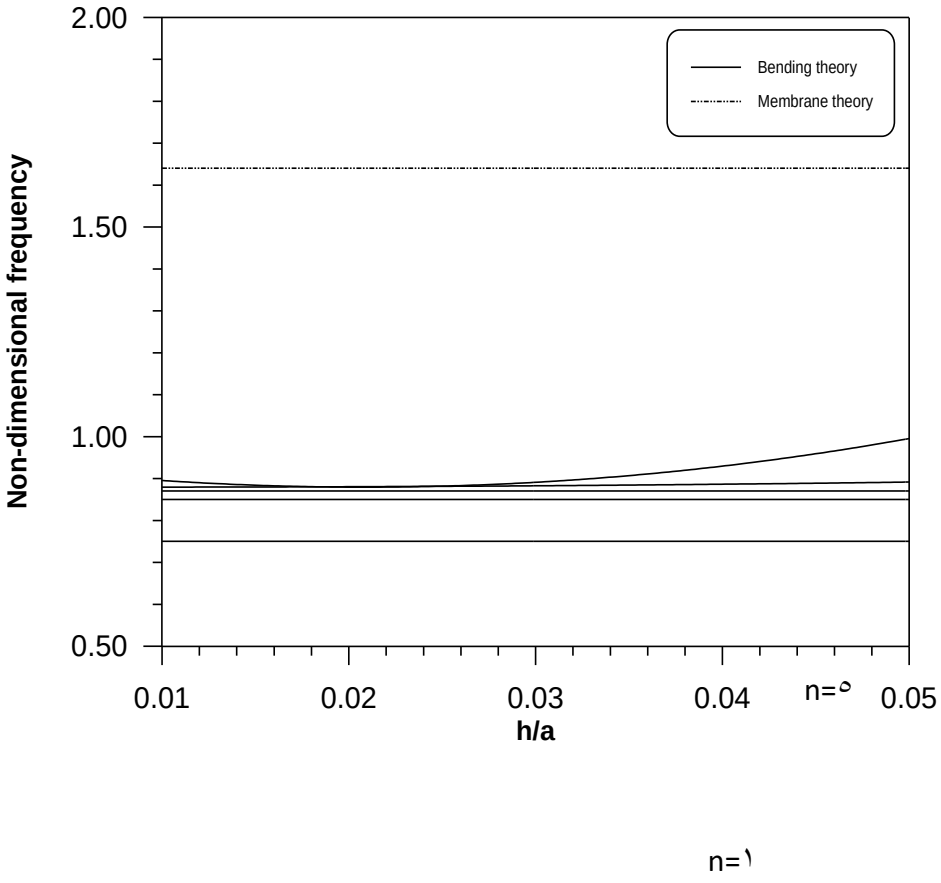

Fig. (٤-٦): Effect of the thickness to major axis ratio on the natural frequencies of a full sphere or a prolate spheroidal shell (e=٠) obtained by RRM

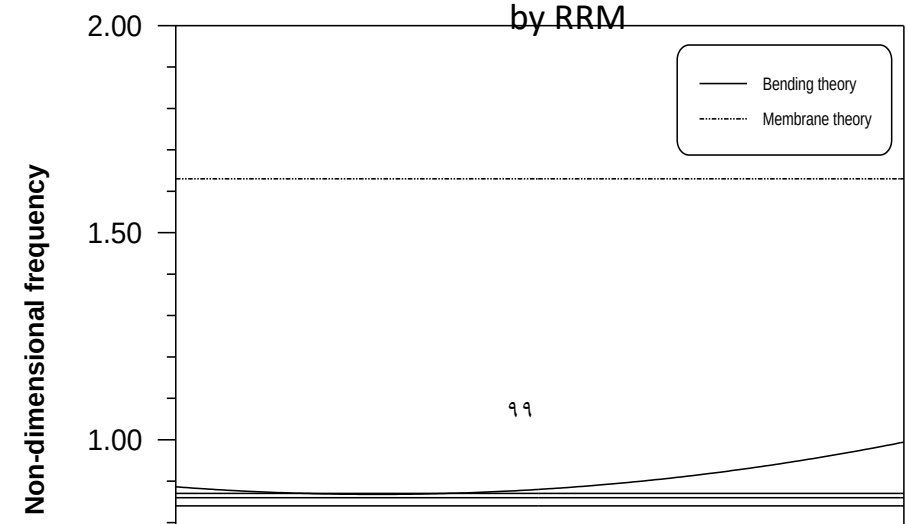

n=٥

n=١

Fig. (٤-٧): Effect of the thickness to major axis ratio on the natural frequencies of a full sphere or a prolate spheroidal shell (e=٠) obtained by BMM

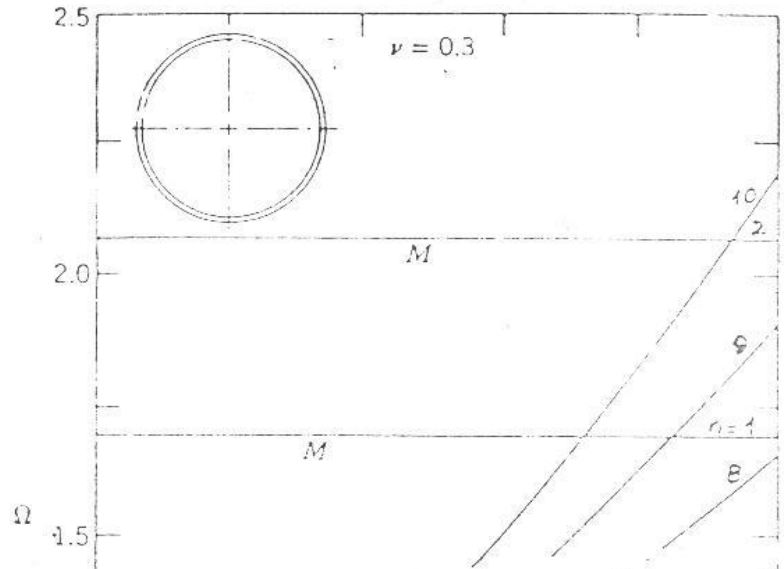

Fig. (٤- ٨): Effect of thickness to radius ratio on the natural frequencies of a full sphere extracted from ***[١٠]***

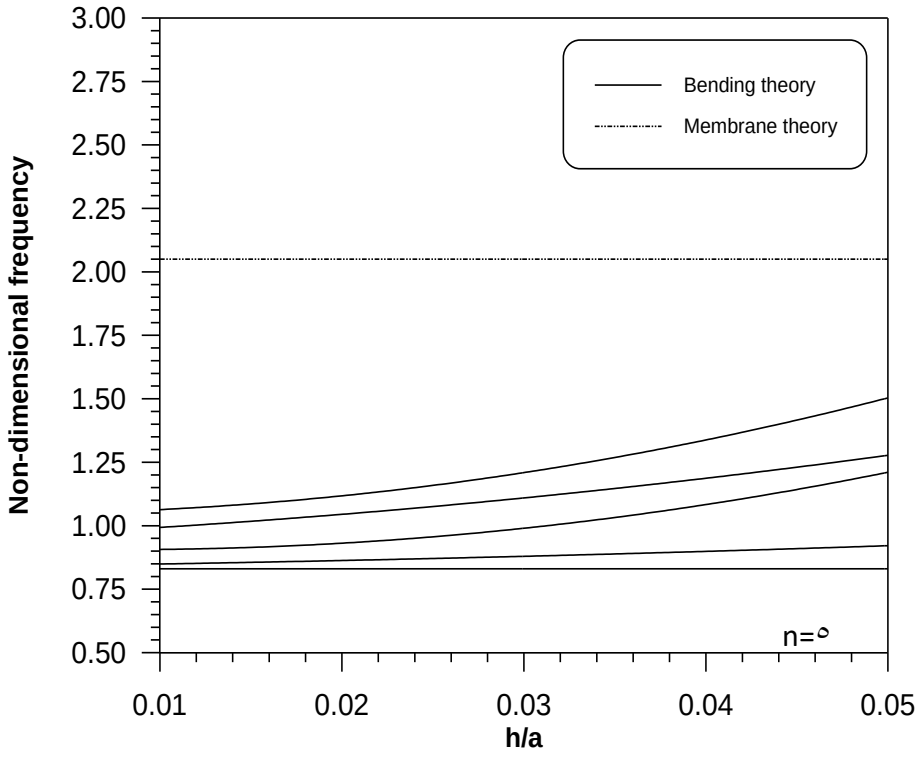

n=١

Fig. (٤- ٩): Effect of thickness to major axis ratio on the natural frequencies of a prolate spheroidal shell (e=٠.٣) obtained by RRM

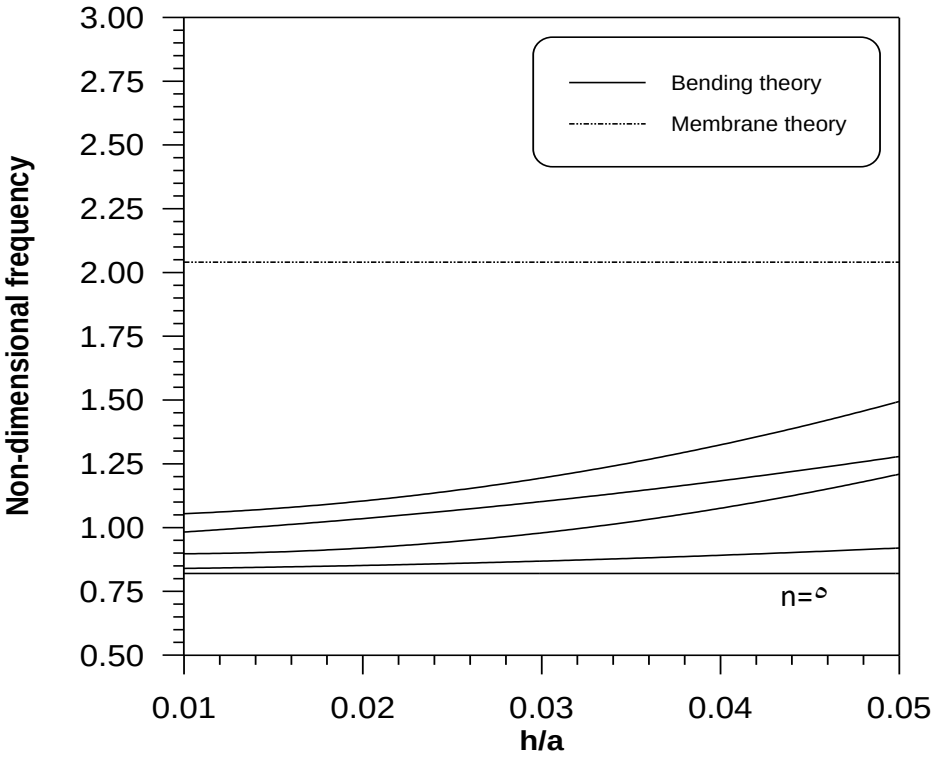

n=١

n=1

Fig. (٤-١٠): Effect of thickness to major axis ratio on the natural frequencies of a prolate spheroidal shell (e=٠.٣) obtained by BMM

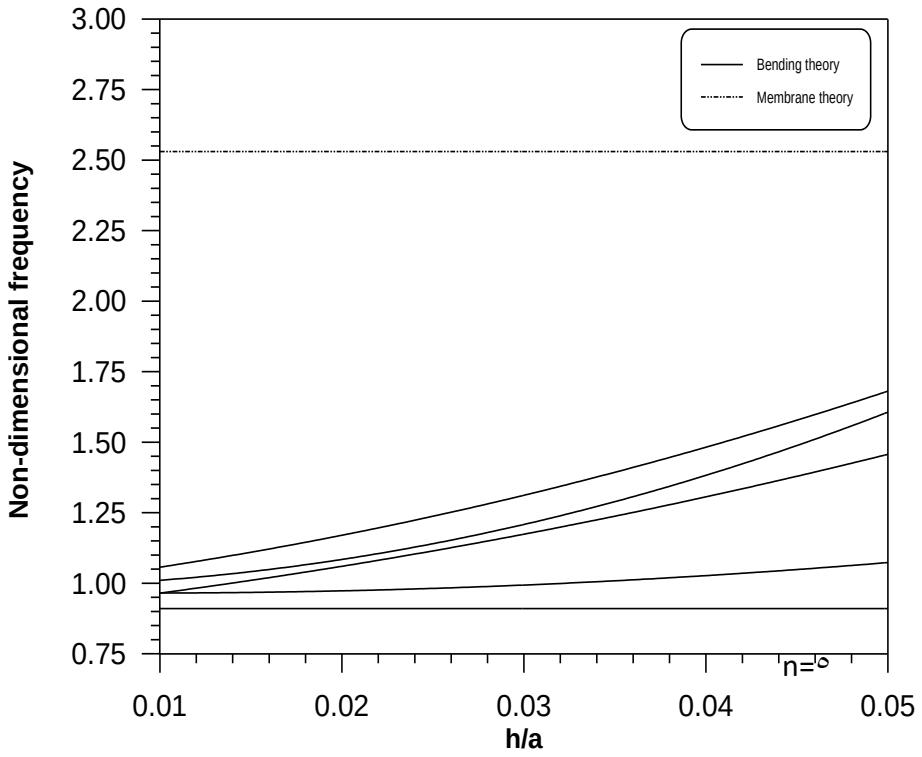

n=١

Fig. (٤-١١): Effect of thickness to major axis ratio on the natural frequencies of a prolate spheroidal shell (e=٠.٧) obtained by RRM

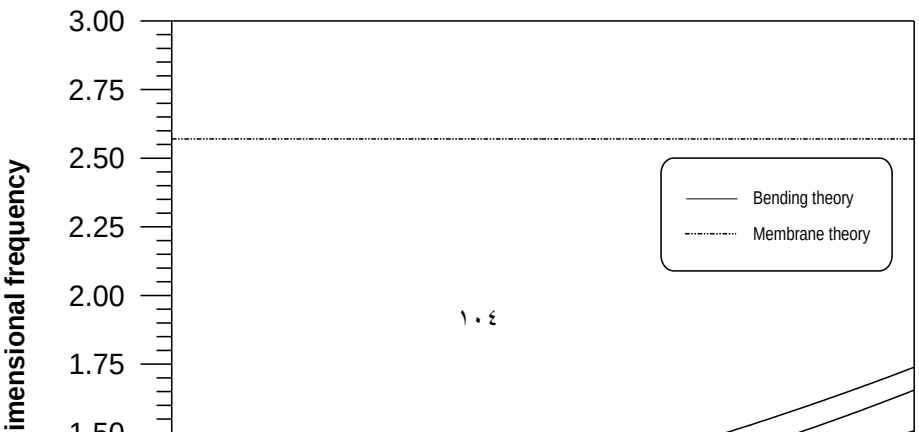

n=٥

n=١

Fig.(٤-١٢): Effect of thickness to major axis ratio on the natural frequencies of a prolate spheroidal shell (e=٠.٧) obtained by BMM

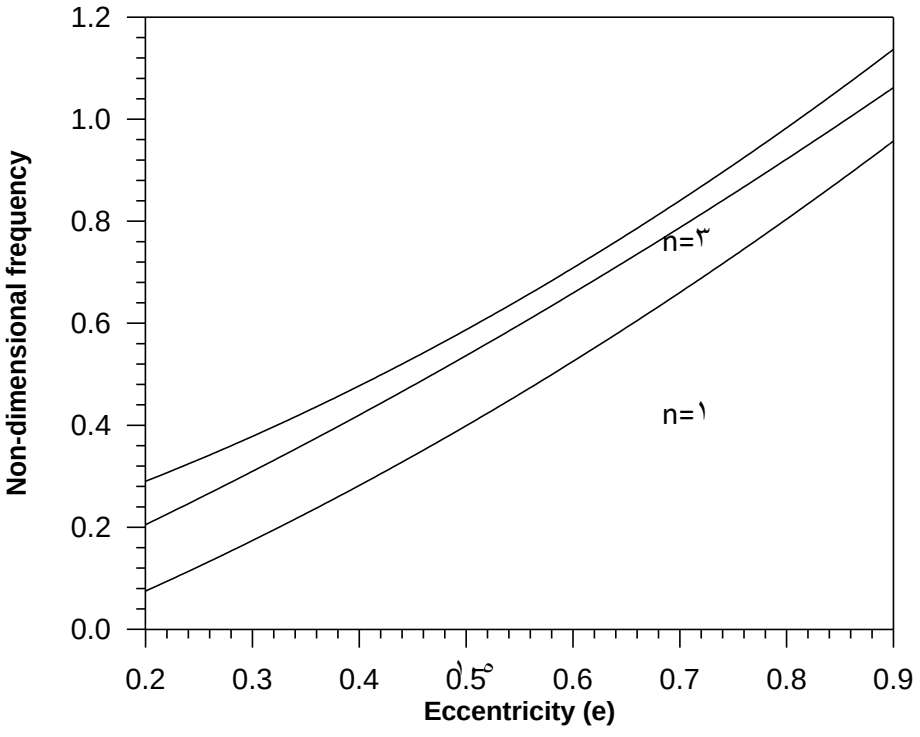

Fig. (٤-١٣): Effect of eccentricity on the three first bending modes obtained by RRM

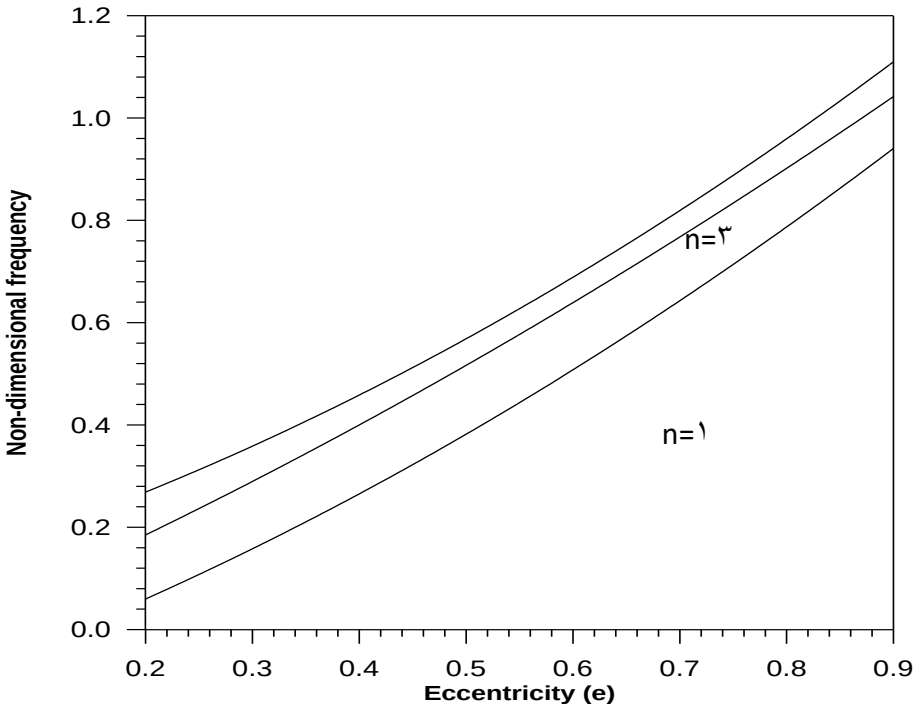

Fig. (٤-١٤): Effect of eccentricity on the three first bending modes obtained by BMM

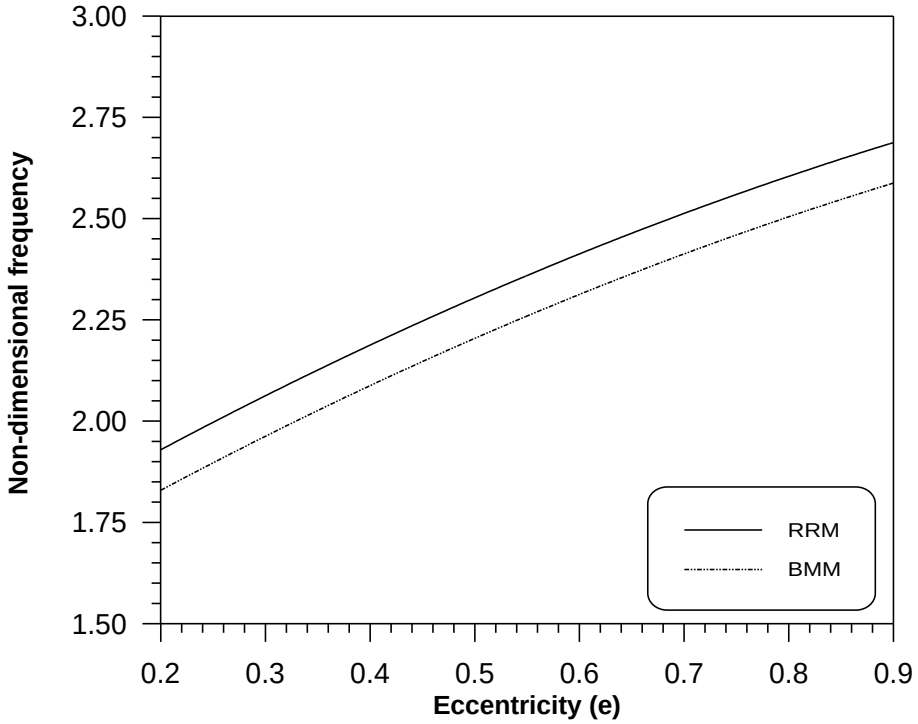

Fig. (٤-١٥): Effect of eccentricity on the first membrane modes

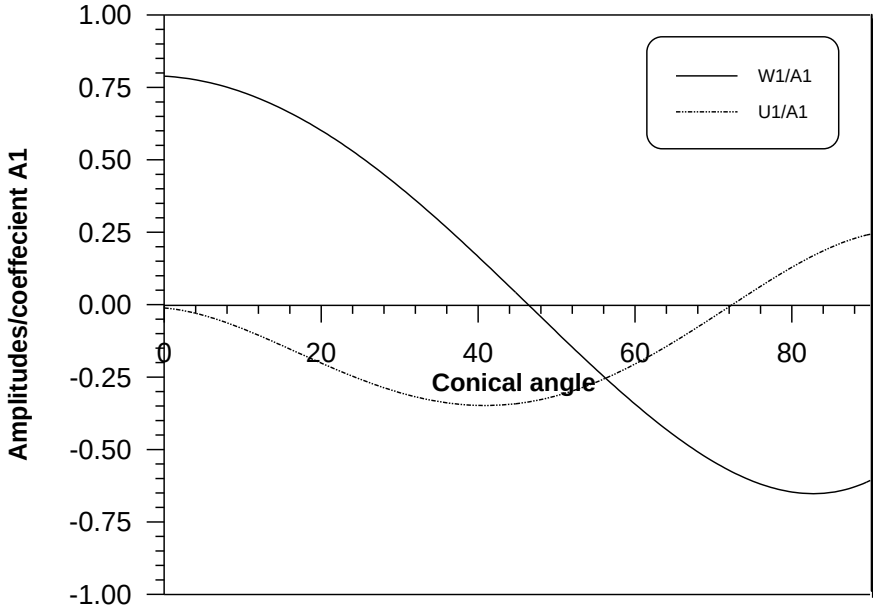

Fig. (٤-١٦): Mode shape associated with the first natural frequency of a prolate spheroidal shell (e=٠.٧) obtained by RRM

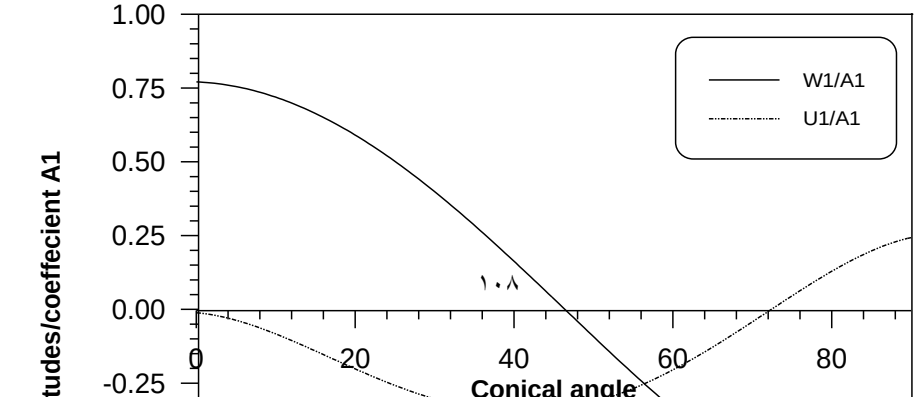

Fig. (٤-١٧): Mode shape associated with the first natural frequency of a prolate spheroidal shell (e=٠.٧) obtained by BMM

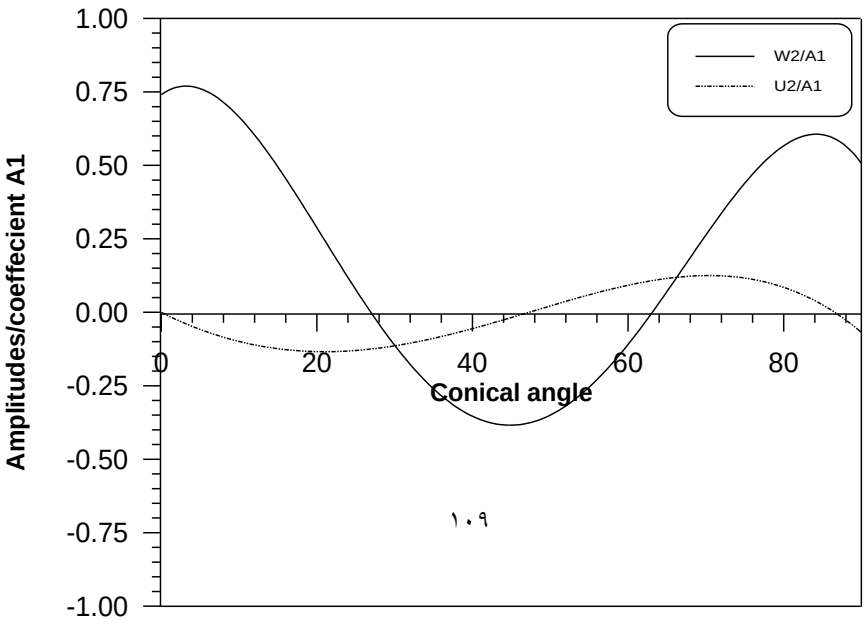

Fig. (٤-١٨): Mode shape associated with the second natural frequency of a prolate spheroidal shell (e=٠.٧) obtained by RRM

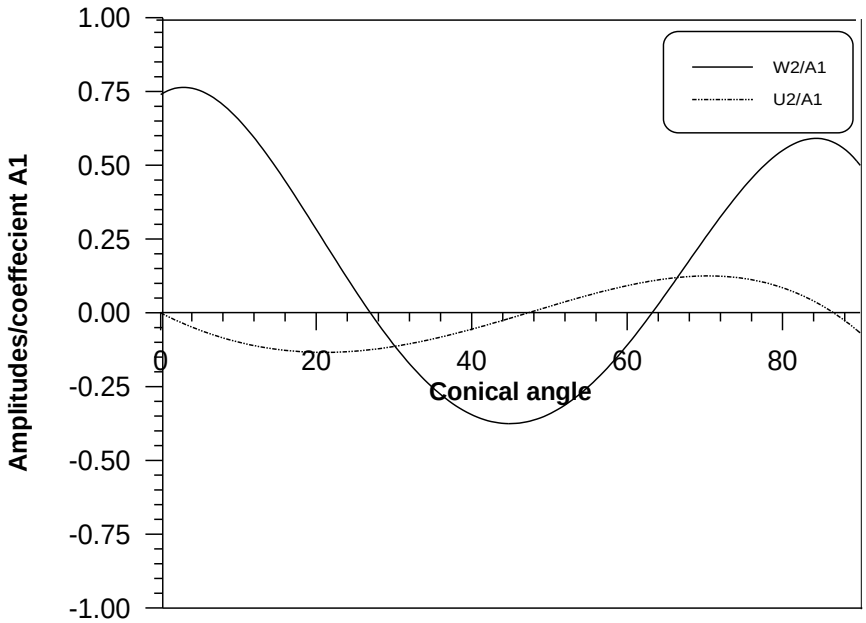

Fig. (٤-١٩): Mode shape associated with the second natural frequency of a prolate spheroidal shell (e=٠.٧) obtained by BMM

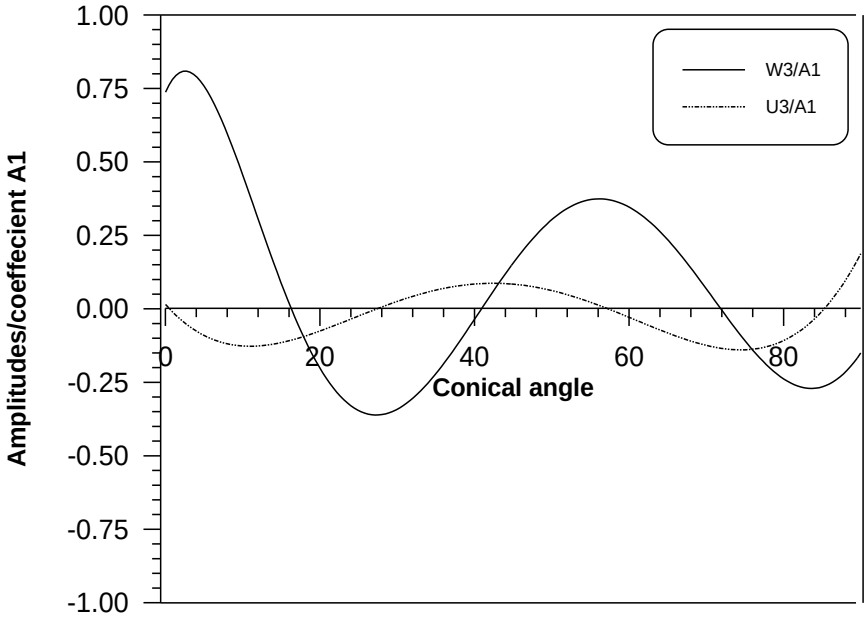

Fig. (٤-٢٠): Mode shape associated with the third natural frequency of a prolate spheroidal shell (e=٠.٧) obtained by RRM

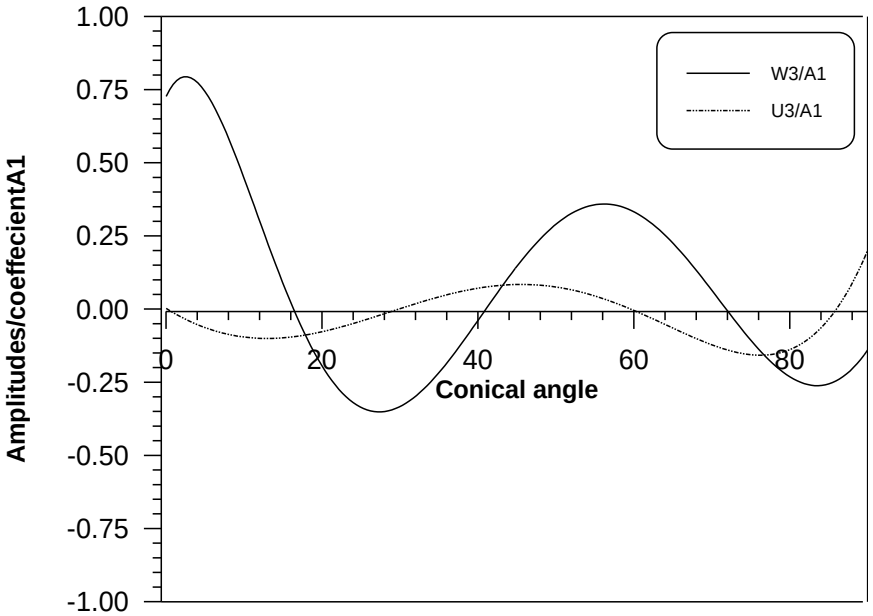

Fig. (٤-٢١): Mode shape associated with the third natural frequency of a prolate spheroidal shell (e=٠.٧) obtained by BMM

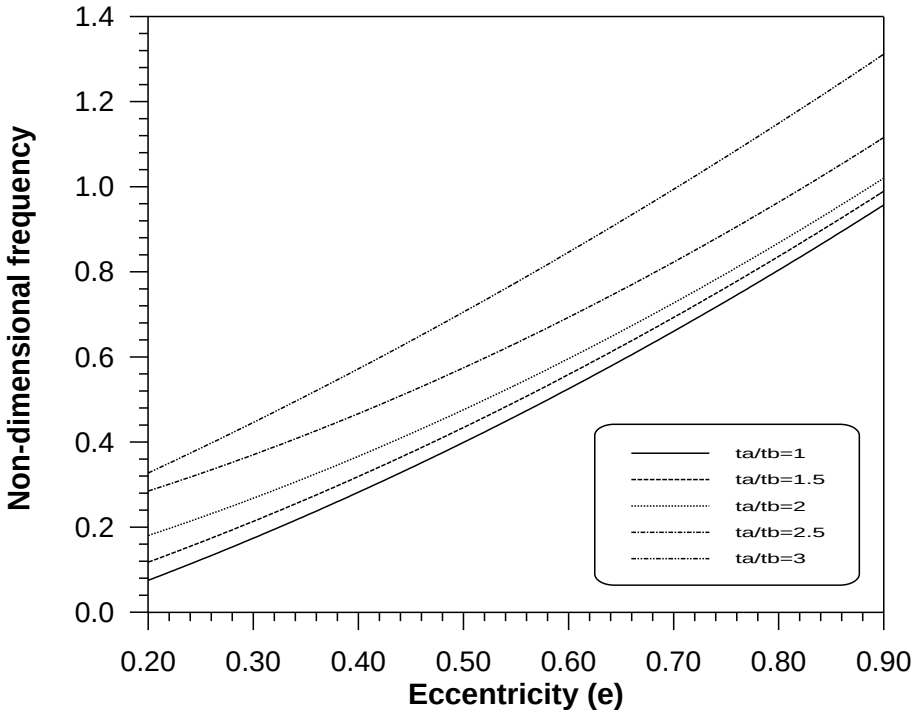

Fig. (٤-٢٢): Effect of eccentricity on the variable thickness ratio of a prolate spheroidal shell

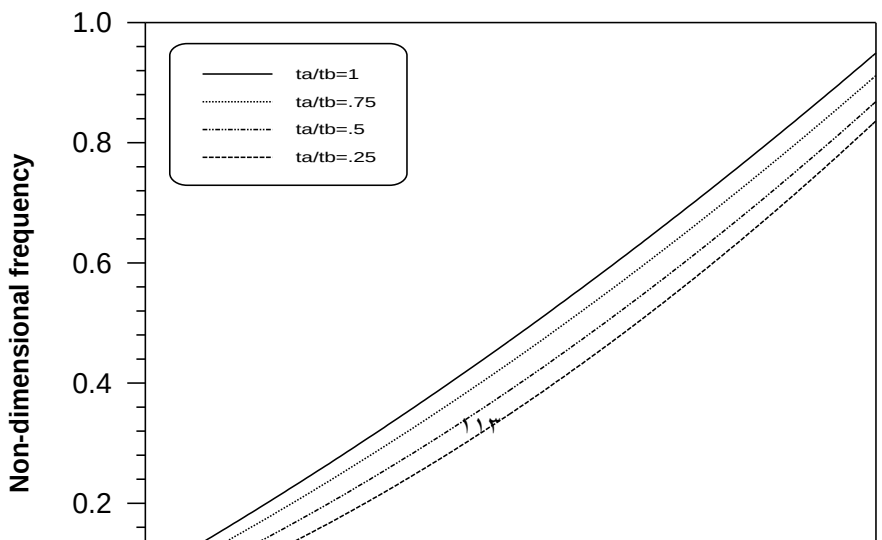

Fig. (٤-٢٣): Effect of eccentricity on the variable thickness ratio of a prolate spheroidal shell

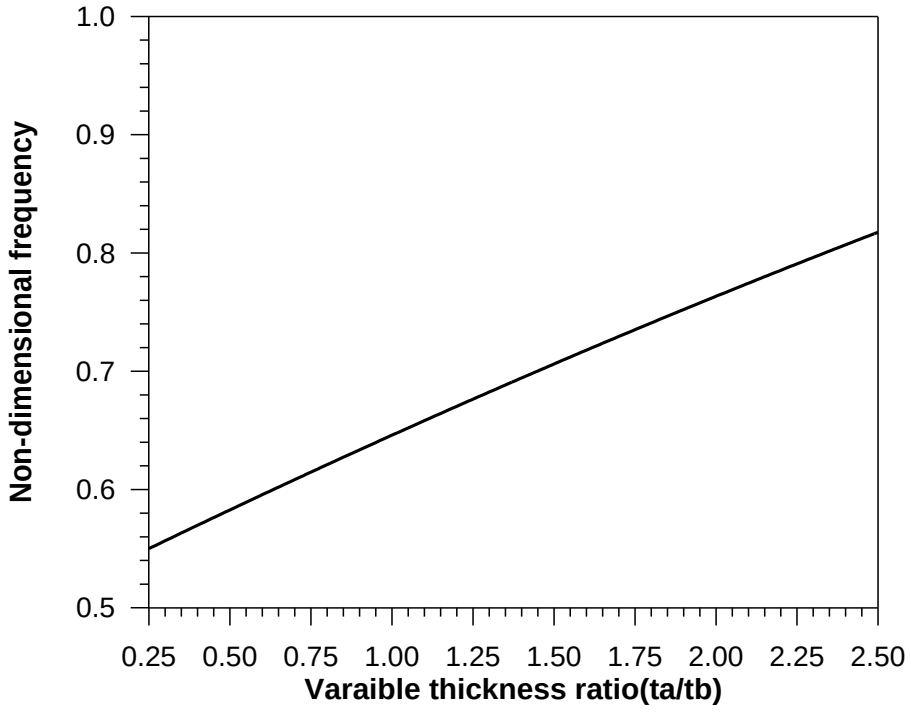

Fig. (٤-٢٤): Effect of the thickness ratio on the non-dimensional frequency for the eccentricity ratio (e=٠.٧)

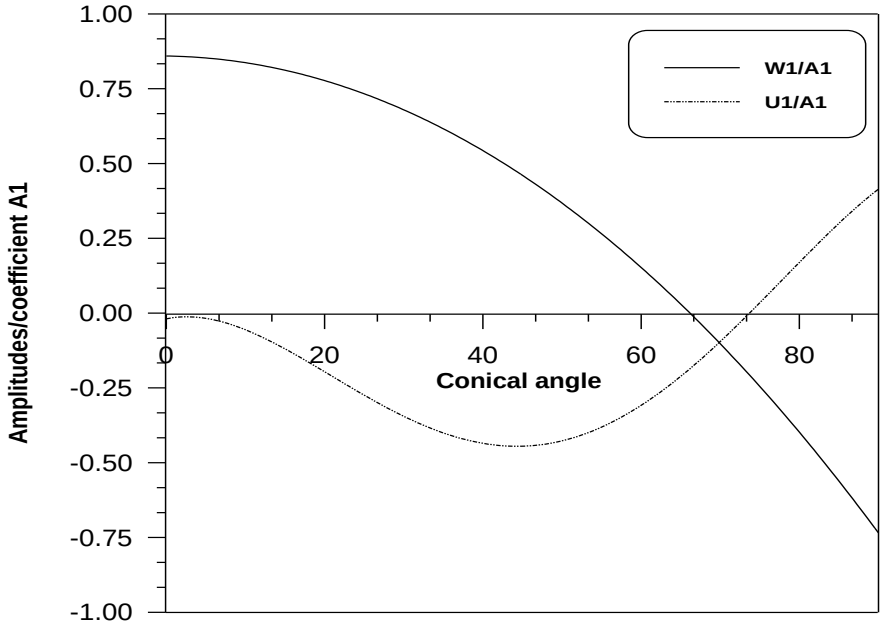

Fig. (٤-٢٥): Mode shape associated with the second natural frequency of a prolate spheroidal shell (e=٠.٧) for thickness ratio (ta/tb=٢)

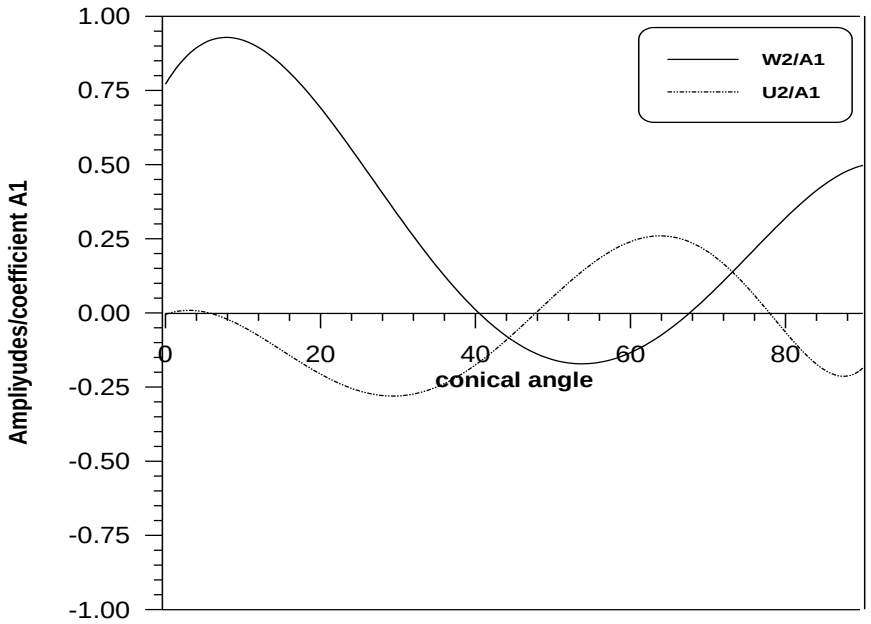

Fig. (٤-٢٦): Mode shape associated with the second natural frequency of a prolate spheroidal shell (e=٠.٧) for thickness ratio (ta/tb=٢)

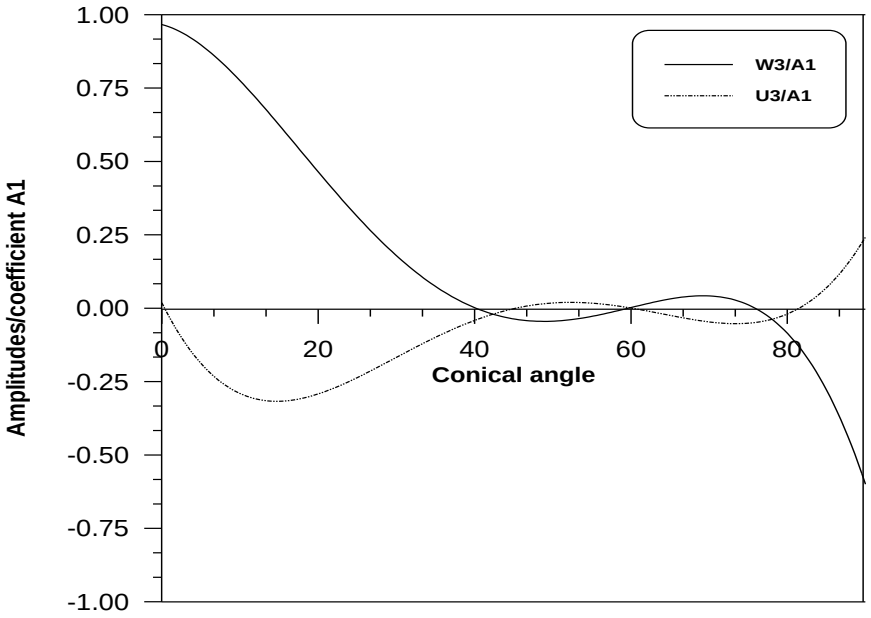

Fig. (٤-٢٧): Mode shape associated with the third natural frequency of a prolate spheroidal shell (e=٠.٧) for thickness ratio (ta/tb=٢)

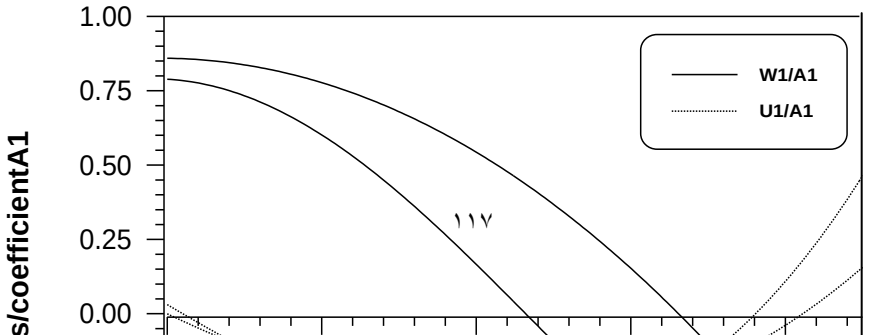

Fig. (٤-٢٨): Compare mode shape associated with the first natural frequency of a prolate spheroidal shell (e=٠.٧) for different thickness ratio

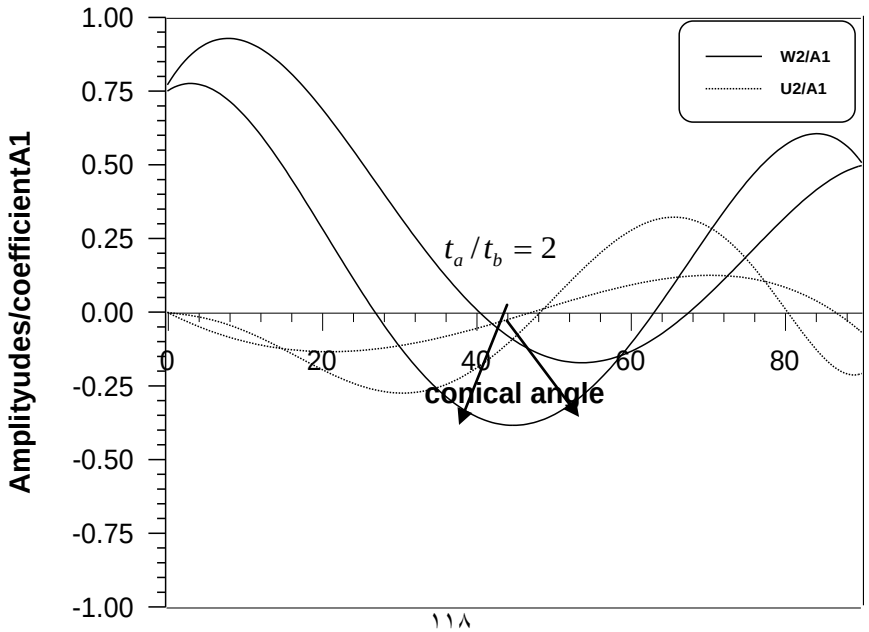

$t_a / t_b = 1$

Fig. (٤-٢٩): Compare mode shape associated with the second natural frequency of a prolate spheroidal shell (e=٠.٧) for different thickness ratio

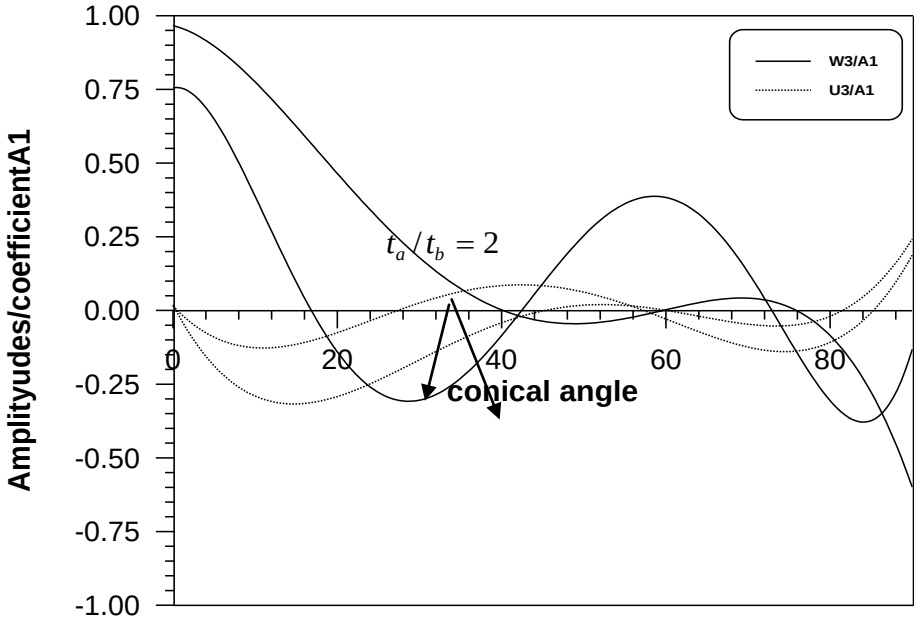

$$t_a / t_b = 1$$

Fig. (٤-٣٠): Compare mode shape associated with the third natural frequency of a prolate spheroidal shell (e=٠.٧) for different thickness ratio

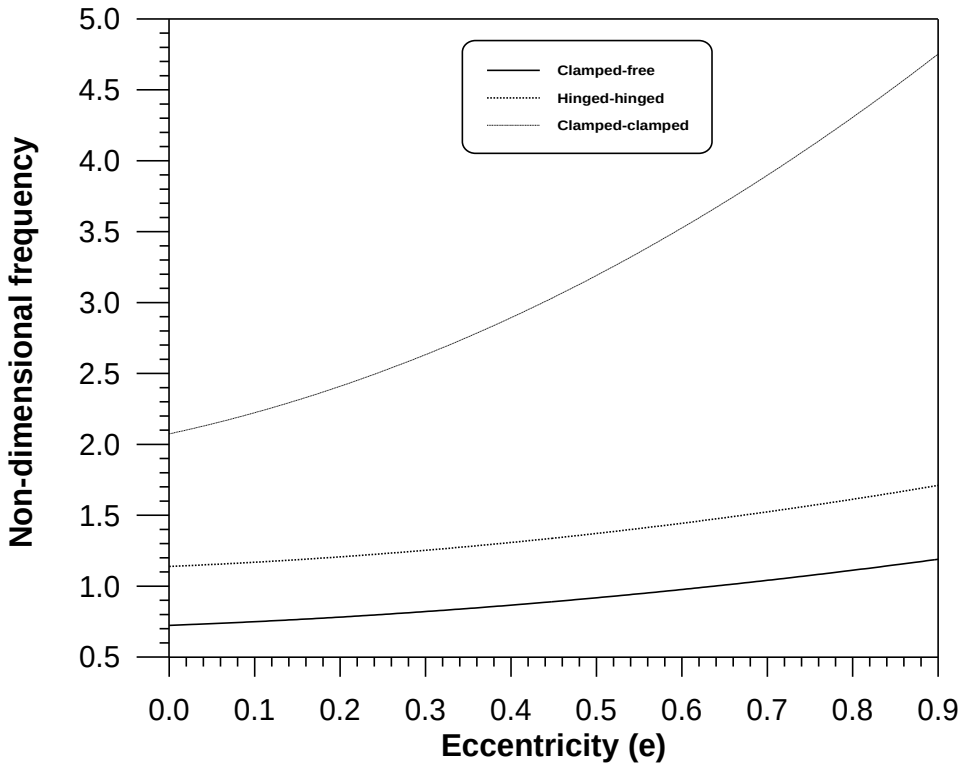

Fig. (٤- ٣١): Effect of eccentricity on the first bending mode for various boundary conditions

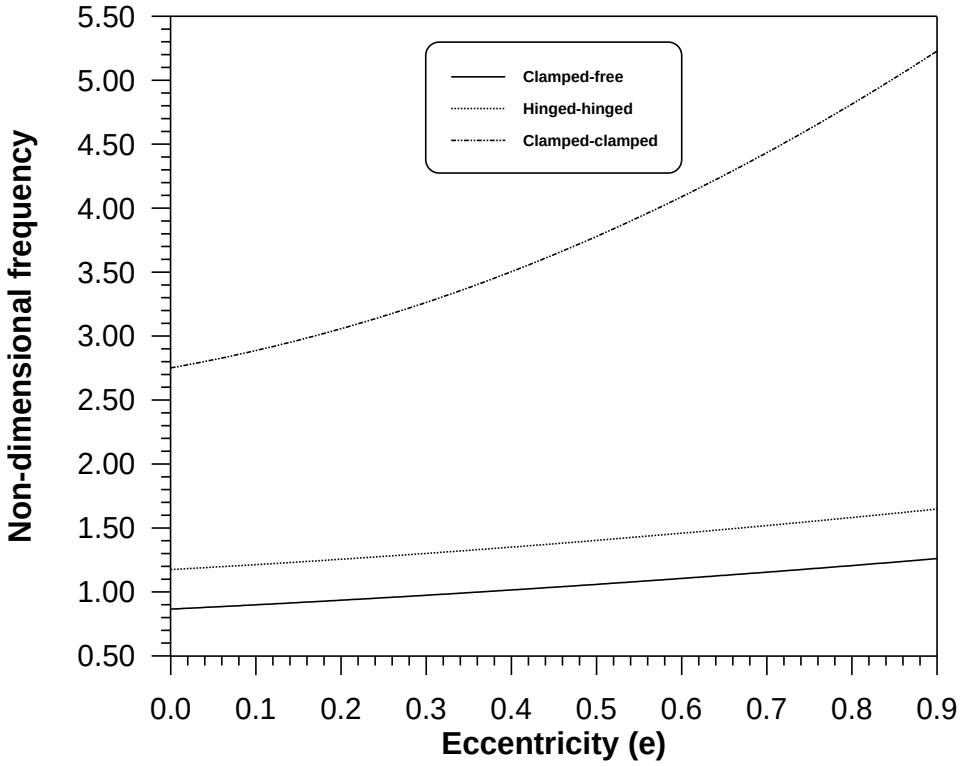

Fig. (٤- ٣٢): Effect of eccentricity on the second bending mode for various boundary conditions

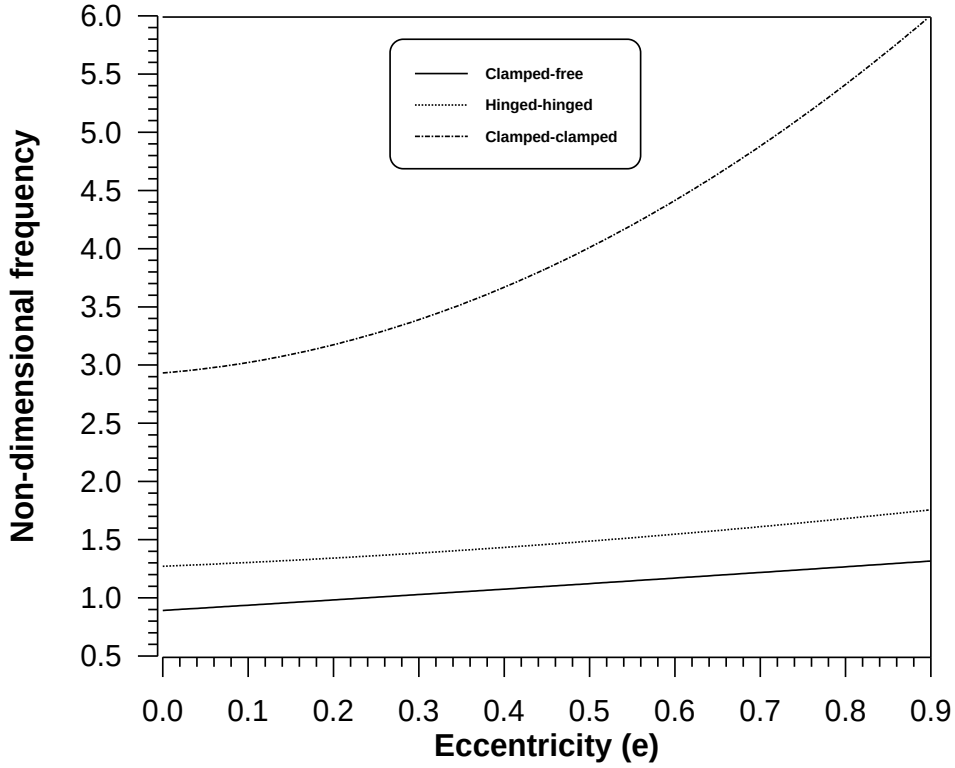

Fig. (٤-٣٣): Effect of eccentricity on the third bending mode for various boundary conditions [٢٢]

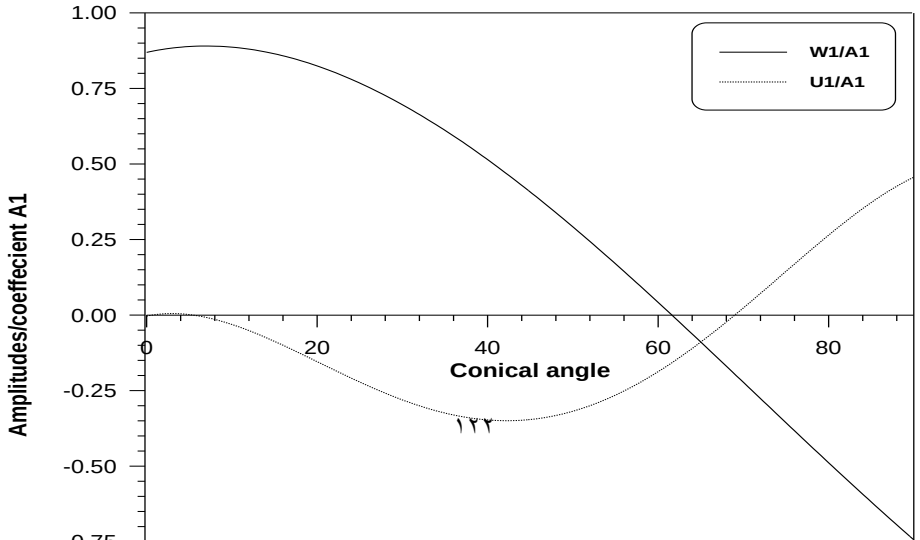

Fig. (٤-٣٤): Mode shape associated with the first natural frequency of a prolate spheroidal shell (e=٠.٧) for clamped –free boundary conditions.

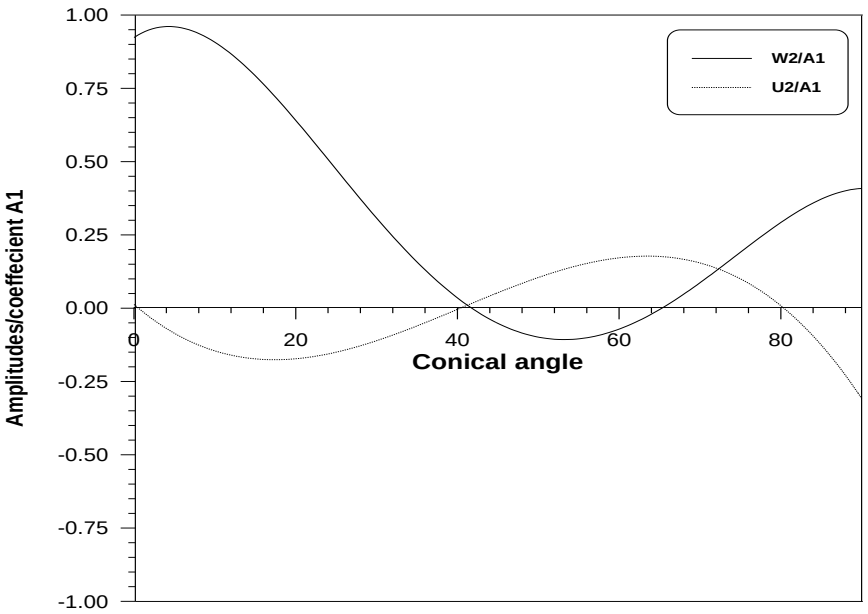

Fig. (٤-٣٥): Mode shape associated with the second natural frequency of a prolate spheroidal shell (e=٠.٧) for clamped –free boundary conditions.

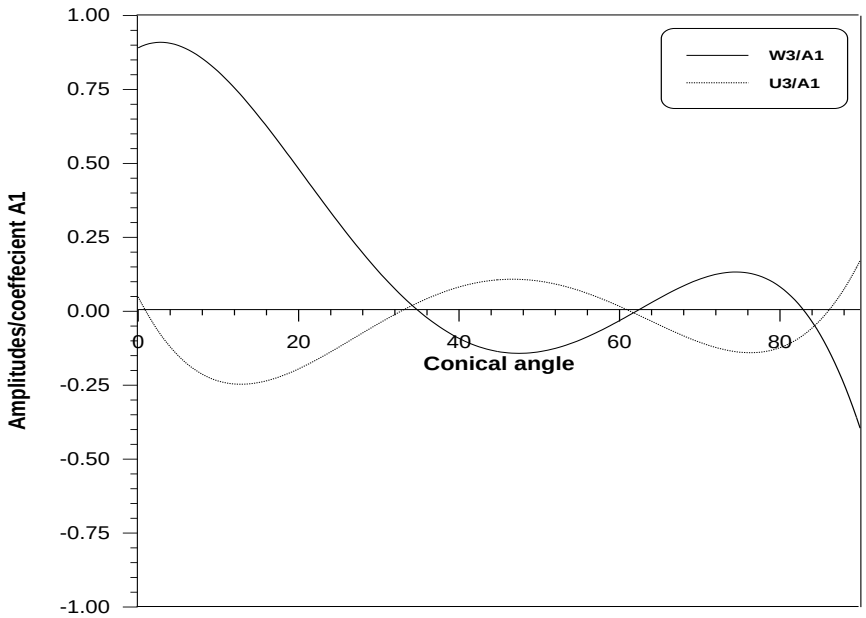

Fig. (٤-٣٦): Mode shape associated with the third natural frequency of a prolate spheroidal shell (e=٠.٧) for clamped –free boundary conditions.

CHAPTER FIVE

CONCLUSIONS AND RECOMMENDATIONS

٥.١ Conclusions

The main conclusions obtained from the present work can be summarized as follows:

١-The Boundary Matching Method and Rayleigh – Ritz Method used in this work predicts well the natural frequencies of a prolate spheroidal shell for all values of eccentricity ratio.

٢-Natural frequencies are seen to have two types of behavior against increasing the shell thickness to major radius ratio. One type, which is associated with the bending modes, which is tend to increase with the thickness, while the other type, which is associated with membrane modes, remains unaffected by the thickness variation.

٣-Both Bending and membrane modes natural frequencies tend to increase with increasing eccentricity ratio.

٤-Natural frequencies are seen to have a behavior against the shell thickness ratio. The natural frequency tends to increase with the increasing the ratio of thickness of the shell.

٥.٢ Recommendations for Further Work

The present work lays the foundation, for further study and through out the course of this investigation, further extension of the work on the undergoing problem. The following points are suggested as a future work:

١. In the present work a Boundary Matching Method model of two spherical caps and Rayleigh – Ritz Method were used to predict the natural frequencies of prolate spheroidal shells, it would be interesting model consisting of two spherical caps joined by a toroidal shell. Also, it is interesting to use other methods such as the Finite Element Method to the present problem.

٢. It is felt that the method used in this work might be extended to include other types of practical boundary conditions such as a prolate spheroid with middle support.

٣. Experimentally Investigation to several prolate spheroidal shells with various eccentricities ratio and thickness ratios.

REFERENCES

١-**Sitzurgsber, A.,** "On the Small Free Vibration and Deformation of a Thin Elastic Shell", J. App.Math., Vol., ١٤٦, PP.٥٠٥- ٤١٥, ١٩٣٧.

٢-**Reissner, E.,** "Vibration of Shallow Shell", J. App.Math., Vol. ١٣, PP. ١٦٩- ١٧٦, ١٩٥٥.

٣-**Johnson, M. W. and Reissner, E.,** " On Vibration of Shallow Spherical Shell", J. App.Math., Vol., ١٥, PP.٣٦٧- ٣٨٠, ١٩

٤-**Kalnins, A. and Naghdi, P. M.,** "Axisymmetric Vibration of Shallow Elastic Spherical Shells", J.Acoust. Soc. Amer., Vol.٣٢, PP.٣٤٢-٣٤٧, ١٩٦٠.

٥-**Dimmagio, F. L. and Silibiger, A.,** "Free Extensional Torsional Vibrations of a Prolate Spheroidal Shell", J. Acoust. Amer., Vol. ٣٣, PP.٥٦, ١٩٦١.

٦-**Silibiger, A. and Dimaggio, F.**L., "Extensional Axisymmetric Second Class Vibration of a Prolate Spheroidal Shell", Columbia University Technical Report No.٣, ١٩٦١.

٧-**Wilfred, E.,** "Axisymmetric Modes of Vibration of Thin Spherical Shell", J.Acoust. Soc. Amer.,Vol.٣٣, PP. ١٧٤٩-١٧٨٥, ١٩٦١.

٨-**Shiraishi, N. and Dimaggio, F.L.,** ”Perturbation Solutions of a Prolate Spheroidal Shells” J. Acoust. Soc. Amer.,Vol.٣٤, PP. ١٧٢٥-١٧٣١, ١٩٦٢.

٩-**Kalnins, A,** “Free Nonsymmetric Vibrations of Shallow Spherical Shells” ,J. App. Mech., PP. ٢٢٥-٢٣٣, ١٩٦٣.

١٠-**Kalnins, A,** “Effect of Bending on Vibrations of Sphercal Shells”, J. Acoust. Soc. Amer., Vol. ٣٦, PP., ٧٤- ٨١, ١٩٦٤.

١١-**Numergut, P. J. and Brand, R.S.,** “Axisymmetric Vibrations of a Prolate Spheroidal Shell”, J. Acoust. Soc. Amer., Vol. ٣٨, PP.٢٦٢-٢٦٥, ١٩٦٥.

١٢-**Penzes, L. and Burgin, G.,** ”Free Vibration of Thin Isotropic Oblate Spheroidal Shells”, General Dynamic Report No.GD/C-BTD , ٦٥-١١٣, ١٩٦٥.

١٣-**Kalnins, A. and Wilkinson, F.P.,** ”Natural Frequencies of Closed

Spherical Shells”, J. App. Mech. Vol. ٩, PP.٦٥, ١٩٦٥.

١٤-**Dimaggio, F.L. and Rand, R.,** "Axisymetrical Vibrations of Prolate Spheroidal Shells", J. Acoust. Soc. Amer. Vol. ٤٠, PP.١٧٩-١٨٩, ١٩٦٦.

١٥-**Yen, T. and Dimaggio, F.L.,** ”Forced Vibrations of Submerged Spheroidal Shells”, J. Acoust. Soc. Amer. Vol.٤١, PP. ٦١٨-٦٢٦, ١٩٦٧.

١٦-**Rand, R. and Dimaggio, F.L.,** ”Vibrations of Fluid- Filled Spherical and Spheroidal Shells”, J.Acoust. Soc. Amer.,Vol.٤٢, PP. ١٢٧٨-١٢٨٦, ١٩٦٧.

١٧-**Penzes, L.,** "Free Vibrations of Thin Orthotropic Oblate Spheroidal Shells”, J. Acoust. Soc. Amer. Vol.٤٥, PP.٥٠٠-٥٠٥, ١٩٦٩.

١٨-**Huang H.,** "Transient Interaction of Plane Acoustic Waves with Spherical Elastic Shell”, J. Acoust. Soc. Amer., Vol.٤٥ (٣), PP.٦٦١-٦٧٠, ١٩٦٩.

١٩-**Hayek, S. and Dimaggio, F.L.,** ” Complex Natural Frequencies of Vibration Submerged Spheroidal Shells”, J. of Sound and structures Vol.٦, PP. ٣٣٣-٣٥١, ١٩٧٠.

٢٠-**S., Timoshenko,** “Theory of Plates and Shells” New York, ١٩٧٠.

٢١-**Bedrosian, B. and Dimaggio, F.L.,** ” Transient Response of Submerged Spheroidal Shells”, J. of Solids and Structures Vol. ٨, PP.١١-١٢٩, ١٩٧٢.

٢٢-**Berger, B. S.,** “The Dynamic Response of a Prolate Spheroidal Shell Submerged in an Acoustical Medium”, J. App. Mech., Vol.٤١, PP. ٩٢٥-٩٢٩, ١٩٧٤.

٢٣-**L., Meirovitch,** “Elements of Vibration Analysis” New York, ١٩٧٧

٢٤-**Burroughs, C.B. and Magrab, E. B.,** “Natural Frequencies of Prolate Spheroidal Shells of Constant Thickness”, J. of Sounds and Vibration, Vol. ٥٧, PP. ٥٧١-٥٨١, ١٩٧٨.

٢٥**Irie, T., Yamada, G. and Muramoto, Y.,** “Free Vibration of Point-Supported Spherical Shell”, Transactions of ASME Vol. ٥٢, PP. ٨٩٠-٨٩٦, ١٩٨٥.

٢٦-**Tavakoli, M. S. and Singh, R.,** “Einensolutions of Ioined / Hermetic Shell Structures using the State Space Method”, J. Sound and Vibration Vol. ١٠٠, PP. ٩٧-١٢٣, ١٩٨٩.

٢٧-**Okakzaki, A., Urata, Y. and Tatemichi, A.,** “Damping Properties of Three-Layered Shallow Spherical Shells with a Constrained Viscoelastic Layers”, JSME Intern. J., Series I., Vol. ٣٣, PP. ١٤٥-١٥١, ١٩٩٠.

٢٨-**Zhang, P. and Geer, T. L.,** "Excitation of Fluid – Fluid, Submerged Spherical Shell by a Transient Acoustic Waves" J, Acoust. Soc. Amer. Vol. ٩٣(٢), PP. ٦٩٦-٧٠٥, ١٩٩٣.

٢٩-**Zhu, F.,** "Rayleigh – Ritz Method in Coupled Fluid – Structure Interaction Systems and Its Applications", J. Sound and Vibration Vol. ١٨٦(٤), PP. ٥٤٣-٥٥٠, ١٩٩٥.

٣٠-**Wasmi, H. R, Ph.D. Thesis,** "Static and Dynamic Numerical and Experimental Investigation of Oblate and Prolate Spheroidal Shells with and without Framed Structure" University of Baghdad, ١٩٩٧.

٣١-**Michael, A. Spague and Thomas L. Geers,** "Response of Empty and Fluid – Fluid, Submerged Spherical Shells to Plane and Spherical, Step – Exponential Acoustic Waves" J. of shock and Vibration, Vol. ٦, PP. ١٤٧-١٥٧, ١٩٩٩.

٣٢- **Aleksandr, Korjanik, Rolands, R., Holmalte, B., and Andris, C.,** "Free Damped Vibrations of Sandwich Shells of Revolution", J. of Sandwich Structures and Materials, Vol.(٣), PP. ١٧١-١٩٦, ٢٠٠١.

٣٣-**Antoine, C., Mathieu, F., Oliver T., Michel F., and Cyril T.,** "Vibrations of Shallow Spherical Shells and Gongs", J. of sound and Vibration, ٢٠٠٢.

٣٤-**Nawal H., M.Sc. Thesis,** " ", University of Babylon, ٢٠٠٥.